AD-A228 756

APPLICATIONS RESEARCH STUDIES ON MICROTUBULES

J. David Margerum, K.C. Lim, Anna M. Lackner, Leroy J. Miller, Elena Sherman, Willis H. Smith, Jr., and Camille I. van Ast

Hughes Aircraft Research Laboratories

3011 Malibu Canyon Road

Malibu, California 90265

DTIC
ELECTE
NOV 05 1990
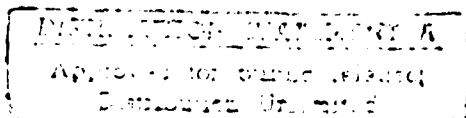S D

September 1990

N00014-87-C-2354

Final Report

August 1987 through July 1990

Prepared for

NAVAL RESEARCH LABORATORIES

WASHINGTON, DC 20375-5000

Sponsor

DARPA/DEFENSE SCIENCE OFFICE

Arlington, VA 22209-2308

REPORT DOCUMENTATION PAGE		Form Approved OMB No. 0704-0188

1a. REPORT SECURITY CLASSIFICATION Unclassified	1b. RESTRICTIVE MARKINGS

2a. SECURITY CLASSIFICATION AUTHORITY	3. DISTRIBUTION / AVAILABILITY OF REPORT
2b. DECLASSIFICATION / DOWNGRADING SCHEDULE	

4. PERFORMING ORGANIZATION REPORT NUMBER(S)	5. MONITORING ORGANIZATION REPORT NUMBER(S)

6a. NAME OF PERFORMING ORGANIZATION Hughes Research Laboratories	6b. OFFICE SYMBOL (If applicable)	7a. NAME OF MONITORING ORGANIZATION

6c. ADDRESS (City, State, and ZIP Code) 3011 Malibu Canyon Road Malibu, CA 90265	7b. ADDRESS (City, State, and ZIP Code)

8a. NAME OF FUNDING / SPONSORING ORGANIZATION Naval Research Laboratories	8b. OFFICE SYMBOL (If applicable) Code 6190	9. PROCUREMENT INSTRUMENT IDENTIFICATION NUMBER N00014-87-C-2354

8c. ADDRESS (City, State, and ZIP Code) 4555 Overlook Ave. SW Washington, DC 20375-5000	10. SOURCE OF FUNDING NUMBERS			
	PROGRAM ELEMENT NO.	PROJECT NO.	TASK NO.	WORK UNIT ACCESSION NO.

11. TITLE (Include Security Classification)

Applications Research Studies on Microtubules

12. PERSONAL AUTHOR(S)
Margerum, J.D., Lim, K.C., Lackner, A. M., Miller, L.J., Sherman, E., Smith, Jr., W.H., van Ast, C.I.

13a. TYPE OF REPORT Final	13b. TIME COVERED FROM 8/12/87 TO 7/11/90	14. DATE OF REPORT (Year, Month, Day) 1990 September 28	15. PAGE COUNT 84

16. SUPPLEMENTARY NOTATION

17.	COSATI CODES		18. SUBJECT TERMS (Continue on reverse if necessary and identify by block number)
FIELD	GROUP	SUB-GROUP	

19. ABSTRACT (Continue on reverse if necessary and identify by block number)

This final report describes progress completed on two of three phases of work aimed at defining new applications areas for microtubules formed as self-organizing microstructures from lipids with diacetylenic lecithin structures. The emphasis in the first phase was on the suspension, orientation, and electro-optical properties of metalized microtubule dispersions in fluids, liquid crystals, and polymers, and on techniques for controlling the orientation and attachment of microtubules to surfaces. The emphasis in the second phase was on phase shift effects in the millimeter wave region with field effects on metalized microtubule dispersions, in regard to potential applications such as scanning radar antennas and radar lenses. In these studies it was discovered that composite fluids consisting of metalized microtubules dispersed in liquid crystals have the highest birefringence values ($\Delta n = 0.3$) which have been reported in the millimeter wave region and that these composite fluids are readily aligned by applied electrical and magnetic fields.

20. DISTRIBUTION / AVAILABILITY OF ABSTRACT ☐ UNCLASSIFIED / UNLIMITED ☒ SAME AS RPT. ☐ DTIC USERS	21. ABSTRACT SECURITY CLASSIFICATION
22a. NAME OF RESPONSIBLE INDIVIDUAL	22b. TELEPHONE (Include Area Code)	22c. OFFICE SYMBOL

DD Form 1473, JUN 86   Previous editions are obsolete

19. (Con't)

Exploratory studies on potential applications of microtubules in the electro-optical arena showed that although the transmission and scattering of visible light could be modulated by applying fields to control the alignment direction of metalized microtubules in dispersions, their birefringence and phase shift effects in the microwave (millimeter wave) region were the most promising areas for new device development. Microtubules coated with permalloy or nickel could be aligned by application of either electric or magnetic fields. Metalized microtubules could be dispersed well in liquid crystals, with more stable suspensions than those in isotropic fluids of comparable viscosity, and that the microtubule/liquid-crystal composites showed high birefringence at relatively low microtubule concentrations, which is important because lower concentrations are much more stable than higher concentrations.

Alignment switching of metalized microtubule dispersions between orthogonal field (magnetic or electric) directions induced substantial birefringent phase shift changes (up to 100° per cm pathlength at 30 GHz) in the millimeter wave region. Relatively short path lengths of microtubule dispersions can thus provide ample field-induced phase changes for radar phase shift modulators, traveling wave slot array antennas, and beam steering devices. However, metalized microtubules of the size presently available settle out of their dispersions (under a gravitational field) and also show irreversible filamentation and clustering effects under applied fields, unless mechanical agitation is applied. The only practical dynamic phase shift devices at present are flow cell types of modulators in which the media (such as microtubules in liquid crystals) is pumped through a cell or slot antenna and is modulated by an applied electrical field. Such flow cell radar phase modulators should be much less expensive than the presently used ferrite phase shifters. The availability of smaller metalized microtubules (*e.g.,* about 1 to 2 µm long and 0.1 µm in diameter) and improved organic coatings would probably provide dispersions which would be stabilized against both settling and field clustering effects, and which could be used a wide range of low cost radar phase shift modulators and scanning antennas.

Solid polymer layers and free-standing films were made containing well-aligned patterns of metalized microtubules in the 0.5 to 1.0% range, using optical cement host dispersions that were slowly cured by ultraviolet exposure in the presence of an aligning magnetic field. We showed that this technique could be used to prepare a microwave gradient index lens for a 94 GHz radar beam. It should be feasible to align higher concentrations (*e.g.,* 1 to 4%) of the presently available metalized microtubules in polymeric layers, using polymeric coatings on the metal and using hosts such as polymer solutions (solidified by solvent evaporation), thermoplastics, or prepolymers which are slowly cured thermally. Thus, a wide variety of inexpensive radar lenses and phase waveplates should be feasible for a various applications, such as the polarization splitting of in-coming and out-going radar signals.

ACKNOWLEDGMENTS

per AD-A 225694

Dist

A-1

TABLE OF CONTENTS

LIST OF FIGURES

LIST OF FIGURES

LIST OF FIGURES

LIST OF FIGURES

LIST OF TABLES

SECTION 1

INTRODUCTION

The microtubules used in this study are self-organizing microstructures formed from lipids with diacetylenic lecithin structures. The formation and properties of these microtubules were discovered in pioneering work by a group of researchers working in the Bio/Molecular Engineering Branch of the Naval Research Laboratories.[1-5] They also discovered that much greater stability and many other important properties were obtained by coating these microstructures with metal.[6-7] The studies in this contract were made using material supplied by the NRL group, either as bulk lipid material, microtubules, or metalized microtubules. Most of our studies were made on metalized microtubules, which are often referred to simply as microtubules (or abbreviated as μTs) in this report when it is clear from the context that metalized microtubules were used.

The Hughes Research Laboratories participated in the NRL/DARPA Workshop on "Novel Lipid Structures" on 12 to 16 May 1986, in which many potential applications of microtubules were discussed by the participants. Subsequently, on 1 April 1987, the Hughes Research Laboratories submitted a proposal to DARPA entitled "Applications Research Studies of Microtubules." This resulted in the present contract, which was originally planned as a three phase study of one year each with the general goal being to investigate techniques basic to novel applications of lipid microtubules for electro-optical, optical, and sensor devices, and to study the feasibility of such device applications. Initially, the overall program had two main areas: (1) to study ordered microtubules in fluids and films, for applications such as variable transmission windows, IR polarizers, and dichroic filters; (2) to study the ordered attachment of microtubules to surfaces, for applications such as nonlinear optical devices and acoustic detectors. The emphasis in the first phase was on the suspension, orientation, and electro-optical properties of metalized microtubule dispersions in fluids, liquid crystals, and polymers, and on techniques for controlling the orientation and attachment of microtubules to surfaces. The emphasis in the second phase was on phase shift effects in the millimeter wave region with field effects on metalized microtubule dispersions, in regard to potential applications such as scanning radar antennas and radar lenses. In the course of these studies we discovered that composite fluids consisting of metalized microtubules dispersed in liquid crystals have the highest birefringence values which have been reported in the millimeter wave region (*e.g.*, 30 GHz), and that these composite fluids are readily aligned by applied electrical and magnetic fields. The first two phases were completed over a three-year period, and the third phase (on more detailed device feasibility studies) has not yet been funded.

SECTION 2

GROWTH AND ALIGNMENT OF NON-METALIZED MICROTUBULES

2.1 GROWTH OF MICROTUBLES

We used a sample of the diacetylenic lecithin 1,2-bis(10,12-tricosadiynoyl)-*sn*-glycero-3-phosphocholine, whose chemical structure is shown in Figure 2-1, to grow microtubules for our studies. This small sample of the bulk lipid was provided to us by Barbara Herendeen of NRL, where it was initially abbreviated as $DC_{8,9}PC$ and subsequently abbreviated as $DC_{23}PC$.

9029-04-25

$$CH_2-O-\underset{\underset{O}{\|}}{C}-(CH_2)_8-C\equiv C-C\equiv C-(CH_2)_9-CH_3$$

$$CH-O-\underset{\underset{O}{\|}}{C}-(CH_2)_8-C\equiv C-C\equiv C-(CH_2)_9-CH_3$$

$$CH_2-O-\underset{\underset{O-}{|}}{\overset{\overset{O}{\|}}{P}}-O-CH_2CH_2N^+(CH_3)_3$$
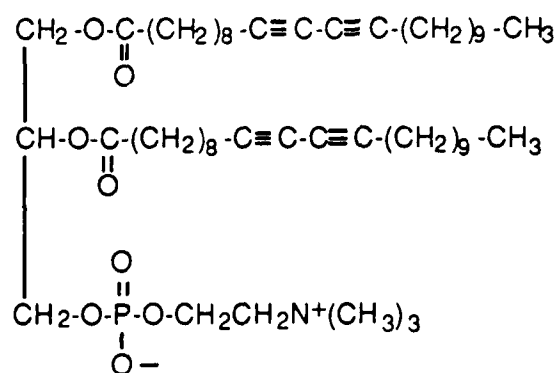
1,2-bis(10,12-tricosadiynoyl)-sn-glycero-3-phosphocholine

Figure 2-1. Chemical structure of microtubule lipid material, $DC_{8,9}PC$ (or, $DC_{23}PC$).

We explored several of the microtubule growth techniques discovered by the NRL group. We generally used either the technique of microtubule crystallization from a homogeneous ethanol/water solution upon the addition of excess water by direct addition while stirring the solution,[3] or by the "isopiestic method" in which water vapor is picked up slowly by an alcohol solution of the lipid in a controlled relative humidity chamber.[8] Formation by the isopiestic method was studied with variations in $D_{8,9}PC$ concentration, stirring, and the addition of acid or base. We found that stirring interfered with the formation of tubular structures, and basic solutions resulted in amorphous clumps. Microtubules were formed with less aggregation from the more dilute solutions (1 mg/ml) which were either neutral or acidic. We also found that the quality of the microtubules grown by the isopiestic method could be improved by initially adding a surfactant to the alcohol solution of the lipid. In particular, the addition of one part of cetyltrimethyl-ammonium bromide (CTAB) to six parts (by weight) of the lipid in the solution

2

resulted in the growth of more uniform microtubules which were considerably less subject to clumping problems. These advantageous effects of using CTAB are illustrated by the microscope pictures in Figure 2-2 of microtubule dispersions in water.

WITHOUT CTAB

WITH CTAB
(6:1, LIPID: CTAB)

100 μm
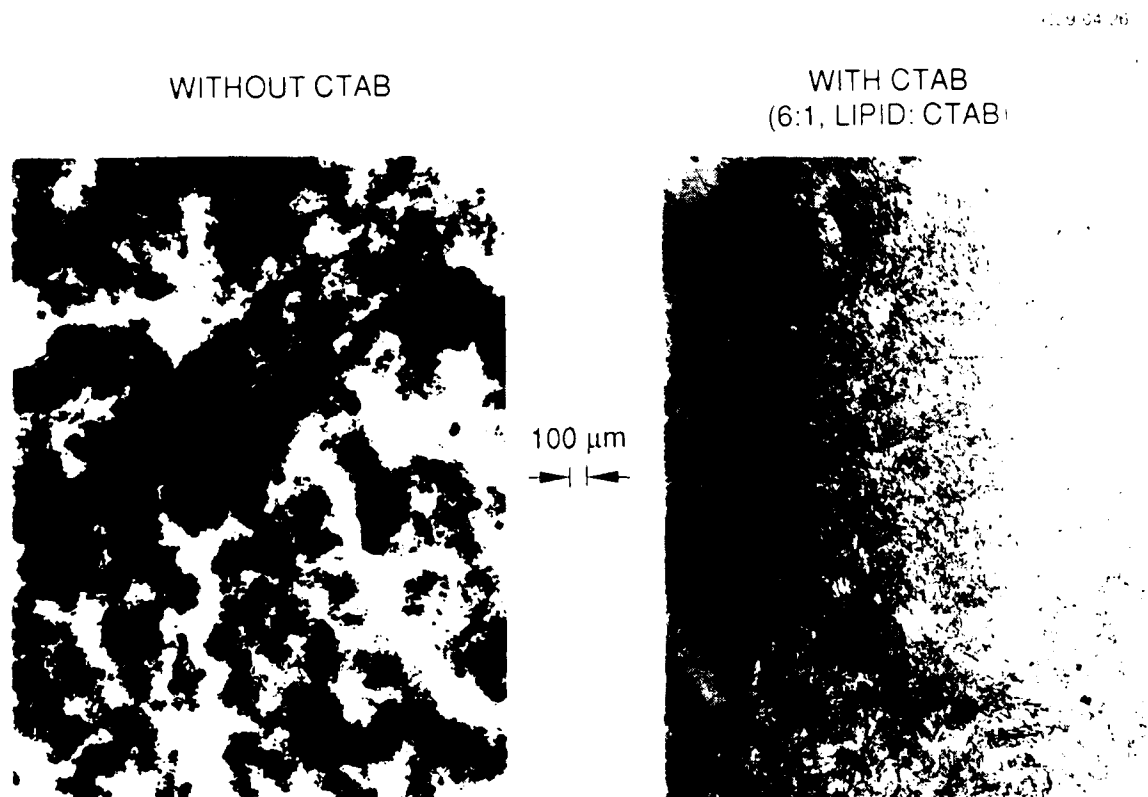
Figure 2-2. Effect of CTAB surfactant on microtubules grown by the isopiestic method.

2.2 SURFACE ALIGNMENT OF NON-METALIZED MICROTUBLES

In a series of experiments, we attempted to obtain controlled directionality of surface-parallel alignment of microtubules. At higher concentrations (3% by weight), the microtubules themselves showed liquid-crystal-like self ordering, as shown in Figure 2-3. However, surface treatment methods (such as directional rubbing, angle deposited SiO_2, etc.) which are used for the alignment of liquid crystal molecules had no significant effect on the much larger microtubules. We experimented particularly on the use of surface gratings etched into surfaces as a potential method of aligning the microtubules along the groove direction of the gratings. We produced these gratings by various holographic/lithographic processes, resulting in surface grating such as those shown in Figure 2-3. This grating had a 6.6 μm periodicity and a 0.5 μm

3

depth, etched in a SiO_2 coating on glass. In both pictures of Figure 2-3, the surface grating grooves (which run from left to right at a tilt of about 45°) had no effect on the microtubule alignment, whether a concentrated or a dilute concentration of the microtubules was used. (These microtubules had been grown in the presence of CTAB, as described above.) This lack of effect was typical of our results with surface gratings, even when the microtubule dispersion was flowed across the surface in the same direction as the grooves. Surface alignment was studied with unpolymerized, UV-polymerized,[2,3] and metal coated microtubules in aqueous suspension with various additives such as alcohol or surfactant (CTAB). These experiment were mainly with dilute microtubule dispersions (about 1%). Although flow alignment was often observed, only weak directional surface-attached alignment in the grating direction was obtained.

CONCENTRATED μTs   DILUTED μTs

⊢—▶| |◀—— 100 μm
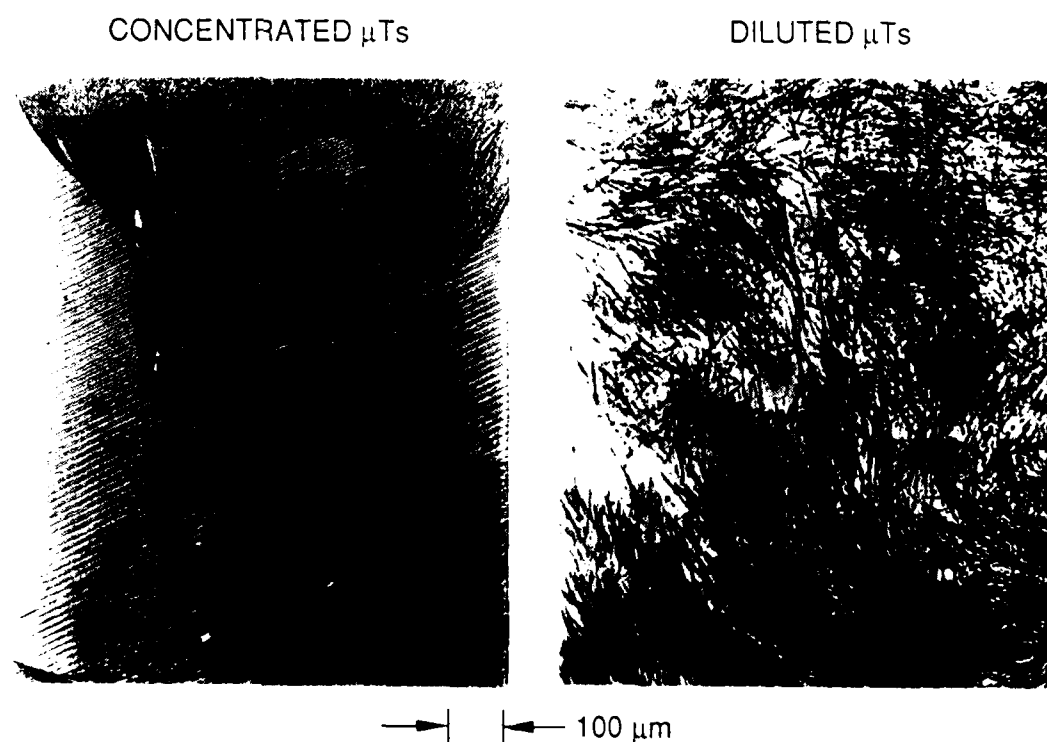
Figure 2-3. Liquid-crystal-like ordering of microtubule dispersions, without alignment by surface gratings (6.6 μm period, 0.5 μm deep) in silica-coated glass.

We studied surface-perpendicular alignment of microtubules grown by the isopiestic method from a solution in the presence of a hydrophobic surface. The microtubules grew on this surface in rosette clusters which remained attached when the surface was removed from the solution. Each cluster consisted of microtubules which appeared to have grown outward into the solution in all directions from a nucleating site on the surface. A comparison of microtubule growth on treated and untreated surfaces is shown in Figure 2-4. The hydrophobic surface was prepared by treating a SiO_2-coated glass (or conductive glass) with hot octadecyl alcohol. (This is a patented Hughes technique for bonding alkoxy groups to surfaces for obtaining surface-perpendicular liquid crystal alignment.[9,10]) We found that the rosette cluster growth of microtubules occurred preferentially on the silica surface in an area with the surface-bonded alkoxy groups, whereas at the same time very few microtubules grew in an area where th ...koxy groups had been removed by reactive ion etching of the same substrate with oxygen. The ratio of rosettes in these two areas was 16:1. This is an indication that a hydrophobic treatment could probably be used to control the initiation and perhaps the directionality of microtubule surface growth.

SILICA BONDED WITH
OCTADECYL ALCOHOL

UNTREATED
GLASS SURFACE

|◄—— 100 μm
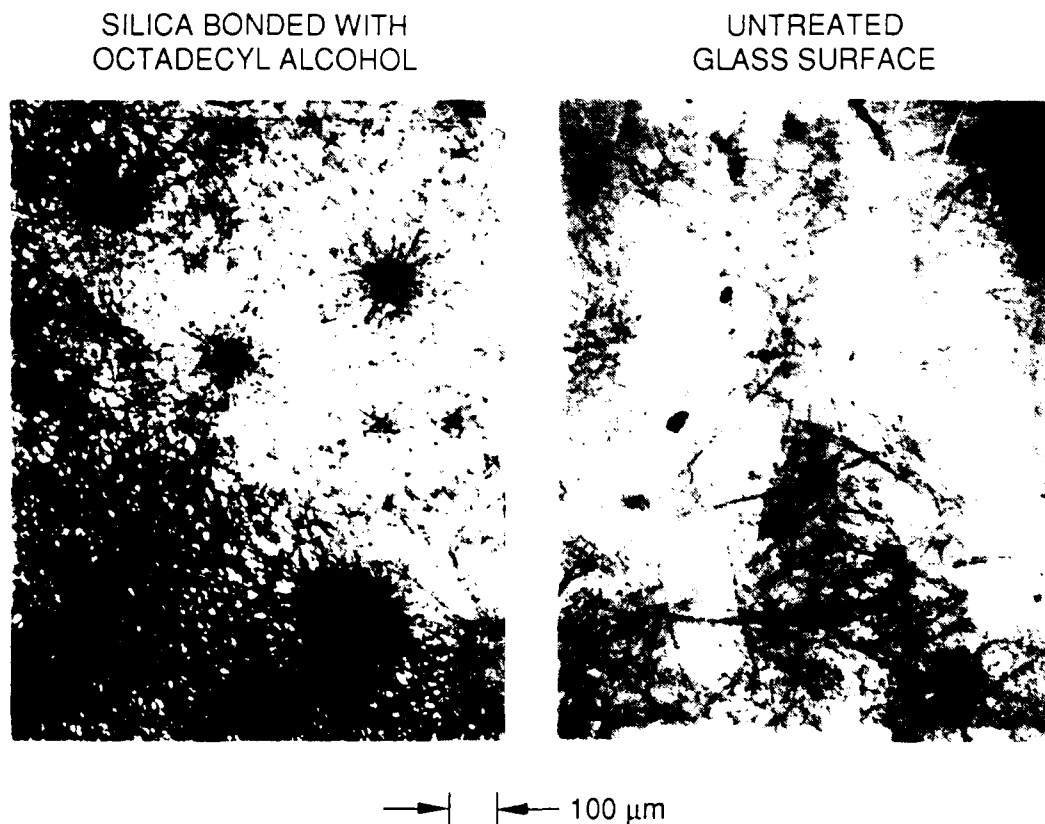
Figure 2-4. Comparison of microtubules grown on hydrophobic (octadecanol treated) and untreated silica surfaces.

5

SECTION 3

CHARACTERIZATIONS OF METALIZED MICROTUBULES

The metal-coated microtubules used in these studies were obtained either (1) metalized by NRL and sent to us (dry, or with a supernatent fluid), or (2) were metal-coated by us after receiving catalyzed microtubule samples from NRL, which were ready for plating. The metal plating techniques used were variations of those which have been described by the NRL group.[6,7] When we did the metal plating in our laboratories, it was primarily for the purpose of being able to proceed with surface treatment reactions immediately after plating rather than after the samples were aged and partially oxidized. We began our studies with copper-coated microtubules, and then used mainly ones which were coated with permalloy or nickel because these were both ferromagnetic and readily aligned by magnetic fields as well as electrical fields.

Metalized microtubules usually have the shape of a hollow cylinder, and have fairly uniform diameter (from a given batch) which is often about 0.6 μm. Their length (after metalization) was usually in the range of 5 to 100 μm, depending upon the starting microtubule sample and the handling procedures in metalization and separation. The median length of most of the microtubule samples used in our experiments was usually in the range of about 10 to 30 μm. Figure 3-1 shows an optical microscope picture of a diluted dispersion of randomly-aligned Ni-coated microtubules. In this picture some of the microtubules are seen in a full length view, while others appear only as short lines or dots because they are pointed downward. Figure 3-2 shows SEM pictures of individual permalloy-coated microtubules. These two pictures were selected from the same batch to illustrate the variation that occurs in the thickness of the metalization. Both microtubules were about 0.6 μm in diameter, but the metal coating thickness was 0.03 μm for one and 0.15 μm for the other. The metal coating is on the inside as well as the outside of the microtubule, with a thin layer of lipid structure in between. The thickness of the metal coating was usually more uniform in the Ni-coated microtubules, particularly when polyvinylpyrrolidone (PVP) was used in the plating solution. Figure 3-3 shows a typical length distribution curve of a sample of Ni-coated microtubules. The lengths were measured from microscope picture. The arithmetic mean of the distribution curve is a length of 10 μm, corresponding to the average length of this sample of microtubules. The average length of microtubules in a dispersion depend on the history of the sample, including how much agitation, stirring, and sonication was used to help disperse the sample. All of these techniques, which were used to help disperse the sample, tend to break the microtubules and shorten their average length. We also measured the apparent optical density, due to light absorption and scattering, of microtubule dispersions as a function of concentration. Such results

for randomly-aligned dispersions of permalloy-coated microtubules in paraffin wax oil are shown in Figure 3-4 for samples with two different average lengths. These calibrations were used to estimate the concentration of some arbitrarily diluted dispersions.

|←—— 100 μm ——→|

Figure 3-1.   Optical microscope picture of Ni-coated microtubules in paraffin oil.

| 0.03 μm | METAL COATING THICKNESS | 0.15 μm |
| 0.6 μm | μTs DIAMETER (o.d.) | 0.6 μm |

Figure 3-2.   SEM pictures of permalloy-coated microtubules.

9029-04-29
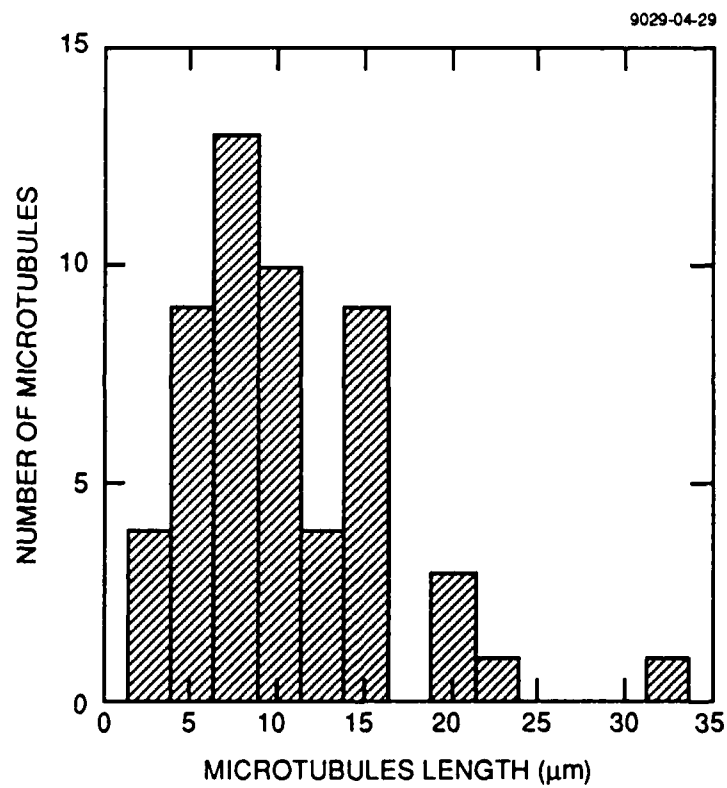
Figure 3-3.   Length distribution of Ni-coated microtubules in a dispersion.

8
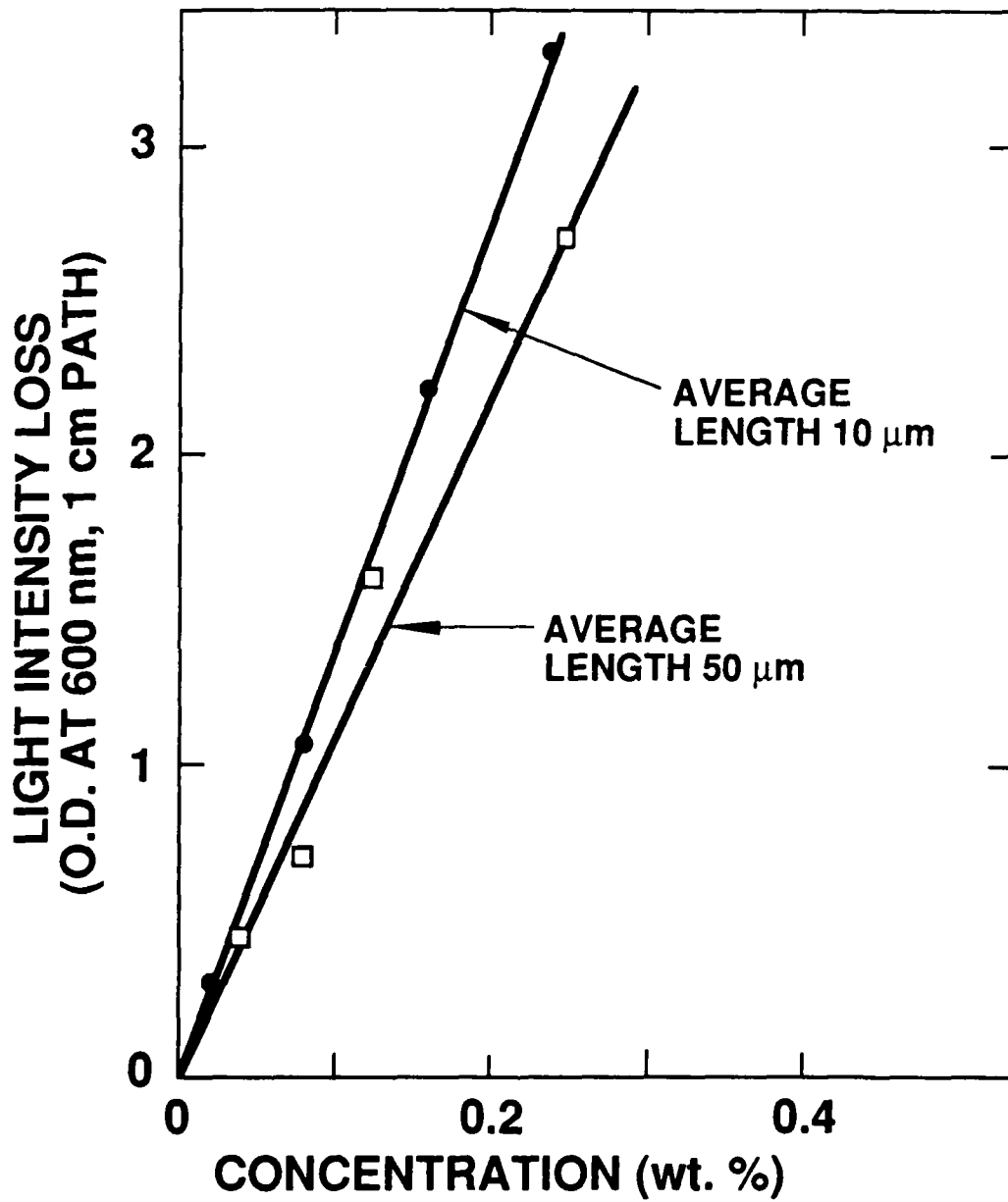
Figure 3-4. Visible optical density of permalloy-coated microtubules in paraffin wax oil.

SECTION 4

SURFACE TREATMENT OF METALIZED MICROTUBULES

The surfactants listed in Table 4-1 were among those we studied as a potential means of improving the dispersion of the microtubules in host fluids. The first five surfactants listed were used mainly on a batch of permalloy-coated microtubules which had not been surface treated after metalization. (This particular batch contained many clumps and was not responsive to a magnetic field.) These surfactants did not give any significant improvement on the dispersion of the batch of microtubules in optical cements (Norland NOA-65 or Merck Optistick 2060). The next seven surfactants in Table 4-1 were used on batch NEM1 of permalloy-coated microtubules, which had been surface treated by NRL with 2-(3,4-epoxycyclohexyl)-ethyltrimethoxysilane [EHEMS]. This batch of microtubules (without surfactants) had good dispersion in acetone, but poor dispersion in hexane, which was of interest because it is a nonpolar host that is miscible in paraffin wax oil (Fluke 76234) which was used for microwave measurements of microtubule dispersions. These surfactants did not improve the quality of the dispersions in either acetone or hexane.

TABLE 4-1. Surfactants Used in Studies of Dispersing Metalized Microtubules.

Dispersions in Optical Cement Fluids of Untreated Permalloy-coated Microtubules
Modaflow
Hexadecyltrimethylammonium bromide
Hexadecyltrimethylammonium stearate
Tween 20 [Polyoxyethylene(20)sorbitan monolaurate]
Dodecyl sodium sulfate
Dispersions in Acetone or Hexane of EHEMS-Treated Permalloy-coated Microtubules
XD Tergitol
TMN-6 Tergitol
NP-4 Tergitol
15-S-7 Tergitol
7500 Silwet
7607 Silwet
L77 Silwet

The surface active agents listed in Table 4-2 were used to treat metalized microtubules to improve their dispersion in host fluids such as hexane, paraffin wax oil, or liquid crystals. The initial clumpy batch of permalloy-coated microtubules could not be redispersed after surface treatment with the silanes. However, much better results were obtained when we used freshly Ni-coated microtubules, which were metalized at HRL just prior to the treatment with the surface active agents. In these studies, we found that the three silanes which were most effective for surface treatment of the metalized microtubules were those whose structures, names, and abbreviations are shown in Figure 4-1. Use of the MAP silane, in particular, gave significant dispersion improvements as indicated by slower settling rates. For example, the settling rate in ethanol was two times better (slower) for MAP-treated as compared to untreated Ni-coated microtubules. These surface-treated microtubules settled very slowly in the much more viscous paraffin wax oil, in which up to 1% by weight remained well dispersed for several hours. Subsequent to these studies, we adopted the use of polyvinylpyrrolidone (PVP) as an additive in the plating process, as recommended by the NRL group, to keep the microtubules better dispersed during plating. The plating conditions are summarized in Table 4-3. The use of PVP during plating reduced the microtubule clustering and the presence of small particles stuck on their surface. Such batches of metalized microtubules could probably be further improved by silane surface treatment.

TABLE 4-2. Silanes Used for μT Surface Treatment Studies.

3-Glycidoxypropyltrimethoxysilane
2-(3,4-Epoxycyclohexyl)-ethyltrimethoxysilane
3-(Mercaptopropyl)-trimethoxysilane
N-Trimethoxysilylpropyl N,N,N-trimethylammonium chloride
N-Methylaminopropyltrimethoxysilane
Phenyltrimethoxysilane
Diphenyldichlorosilane
Octadecyltrimethoxysilane

N - Methylaminopropyltrimethoxysilane (MAP)

$$H_3C-\underset{\underset{H}{|}}{N}-(CH_2)_3-Si\overset{\diagup OCH_3}{\underset{\diagdown OCH_3}{-OCH_3}}$$

2 - (3,4-Epoxycyclohexyl)-ethyltrimethoxysilane (EHEMS)

$$-(CH_2)_2-Si\overset{\diagup OCH_3}{\underset{\diagdown OCH_3}{-OCH_3}}$$
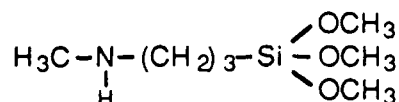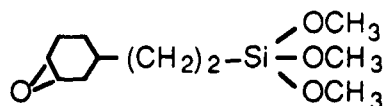
Octadecyltrimethoxysilane (ODTMS)

$$C_{18}H_{37}Si\overset{\diagup OCH_3}{\underset{\diagdown OCH_3}{-OCH_3}}$$
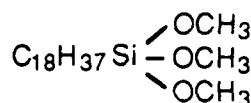
Figure 4-1. Structure of silanes most effective as surface treatment agents.

TABLE 4-3. Plating Mixture for Microtubules, With and Without PVP.

With PVP	Without PVP
1 ml catalyzed microtubule dispersion	1 ml catalyzed microtubule dispersion
10 ml water + 0.025% PVP	10 ml water
1 ml Ni plating bath	1 ml Ni plating bath

Another surface treatment was based on building a block copolymer, modified epoxy resin on the surface of the microtubules. The purpose of this surface treatment was to reduce interaction between microtubules, particularly in the presence of applied electrical or magnetic fields. Poly-dimethylsiloxane, aminopropyldimethyl terminated (molecular weight = 25,000) was used on permalloy-coated microtubules which had previously been treated with EHEMS. The reaction at the microtubule surface is diagrammed in Figure 4-2, where n = 37 (approximately). After this treatment, the microtubule dispersion was worse in acetone and ethanol, but better in toluene and in xylene, which are less polar hosts. However, little improvement was observed in applied fields, where electrical fields particularly caused flocculation of the microtubules which was essentially irreversible.

12

9029-04-31
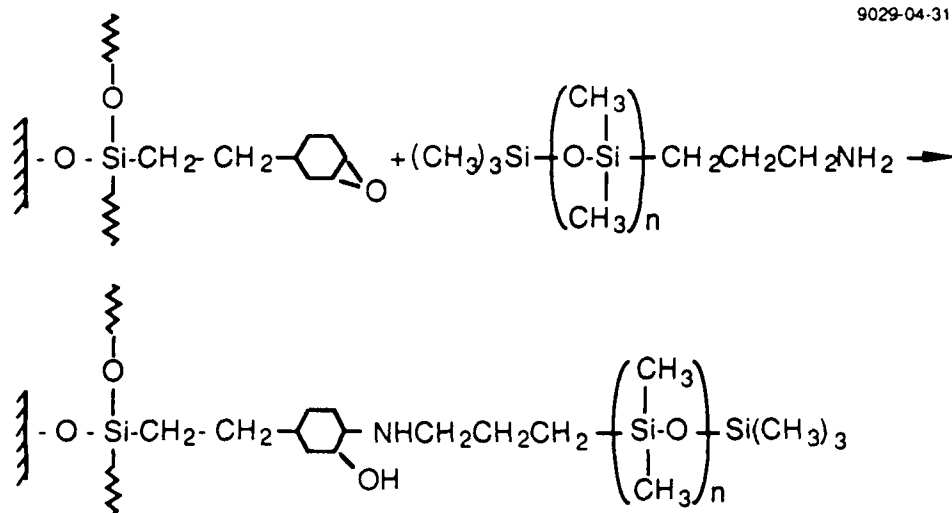
Figure 4-2. Diagram of block copolymer surface treatment of metalized microtubules.

13

SECTION 5

SETTLING RATES OF MICROTUBULE SUSPENSIONS

5.1 DISPERSIONS IN FLUIDS

Small particles often disperse poorly in liquid media. In low viscosity media, both a highly polar fluid such as water and a non-polar fluid such as FC-77 fluorocarbon (from 3M), the metalized microtubules tend to aggregate loosely. However, both permalloy and nickel coated microtubules dispersed well in many viscous liquid media without the undesirable effect of aggregations, particularly when the microtubules had been surface treated. Our experiments utilized the following liquid media to disperse and suspend metalized microtubules:

> Glycerol/water mixture,
> Paraffin wax oil (Fluka PW76234),
> Molten paraffin wax,
> Liquid crystals (e.g. ROTN-404),
> NOA-65 optical epoxy (uncured).

5.2 SETTLING RATE OF MICROTUBULE SUSPENSIONS

Because the metalized microtubules have a high specific density of about 4, they settle out in nearly all common fluids. When dispersed in a high viscosity (>100 cP) media, their suspension time can be increased to the order of hours. Our experiments on settling rates demonstrated that a uniformly distributed suspension of metalized microtubules in paraffin oil has at least two order of magnitude longer settling time than calculated for a layer of microtubules in this media.

Figure 5-1 shows the experimental system used to study the settling rate of suspensions. The settling rate was characterized by monitoring the transmission intensity of a He-Ne laser beam scanning between the top and bottom of a vertical column of the suspension contained in a optical cuvette. Two different types of settling experiments were performed on Ni-coated microtubules (average length about 20 μm) suspended in Fluka PW76234 paraffin oil: the settling rate was measured for a layer of microtubules and for a uniform dispersion of microtubules, and these were compared to calculations using the Stoke's equation.

The settling rate of a drop of microtubules dispersed in paraffin oil, at 0.01 wt.% concentration, was measured after it was introduced as a layer at about 3/4 of the height of a column of pure paraffin oil. The results are shown in Figure 5-2. The layer reformed as a suspended droplet of microtubules, and an average settling rate of 3×10^{-4} cm/sec was obtained.

According to the Stoke's Eq. (1), the viscous drag F_v of a prolate particle settling through a liquid medium is given by:

$$F_v = 6 \pi \eta R v, \qquad\qquad (1)$$
$$\text{where } R = [8/3] [ab^2/(\chi_\phi + \alpha_\phi a^2)].$$

and where η is the viscosity of the liquid medium, a and b are the semi-major and semi-minor axis of the prolate, χ_ϕ and α_ϕ are geometric constants, and v is the velocity of the settling prolate particle. The settling rate of a drop of microtubules was calculated using the Stokes' equation and assuming a Gaussian distribution in the semi-major axis a (average a = 10 μm, with a standard deviation of 10 μm) and with a constant semi-minor axis b = 0.5 μm. The calculated density profiles of a settling drop of such microtubules in paraffin wax oil is shown in Figure 5-3 at settling distances of 0.08, 0.16, and 0.24 cm. The calculated settling rate was 2.7×10^{-4} cm/sec, which was similar to the experimental value, as indicated in Figure 5-2.

9029-23-2'
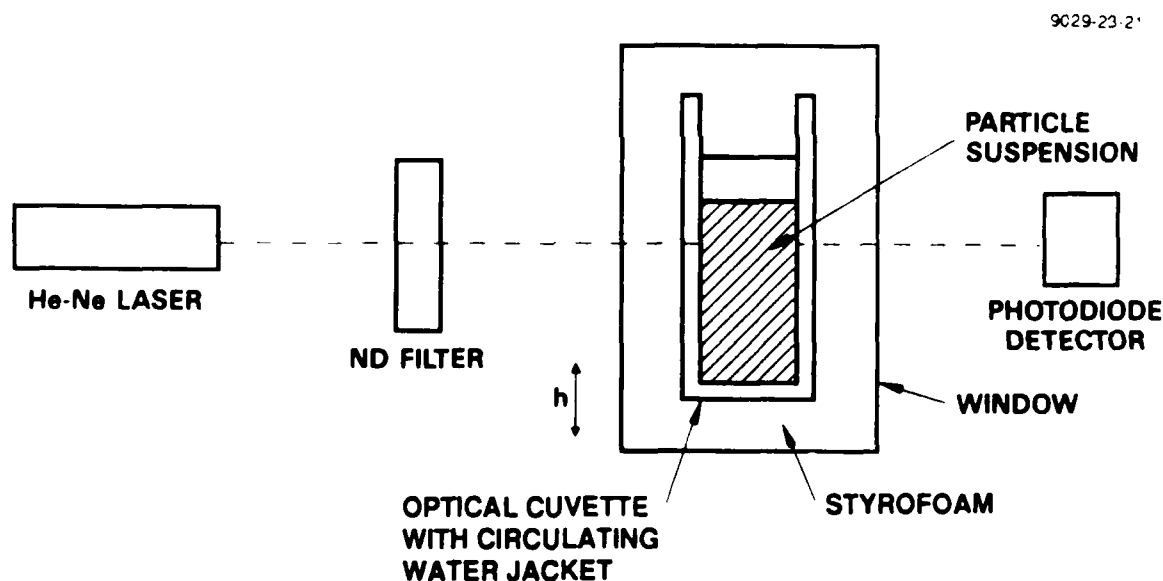
Figure 5-1.   Apparatus for microtubule settling rate studies.

The settling rates of a volume of homogeneously mixed microtubules suspended in PW76234, at the same 0.01 wt.%, are shown in Figure 5-4. These were unexpectedly different from the first experiment, with much slower settling rates. The curves for the intensity of transmitted light

15

were scanned at times up to 384 hours after the beginning of experiment. It is apparent that a uniformly distributed suspension settles at a much slower rate than expected from the Stokes equation. Further experiments are needed to understand this phenom na and to exploit such effects for obtaining stable suspensions of particles.
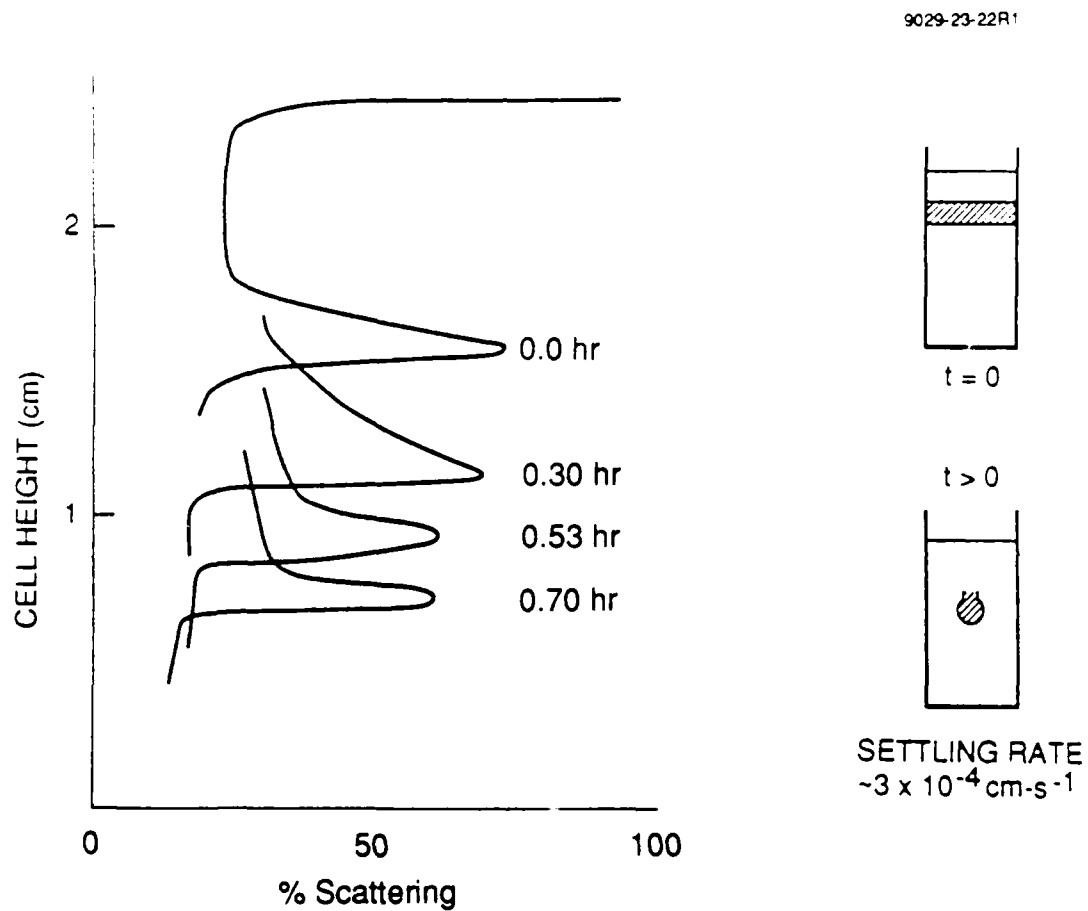
Figure 5-2.   Settling rate of a Ni-coated microtubule layer in paraffin wax oil.

16
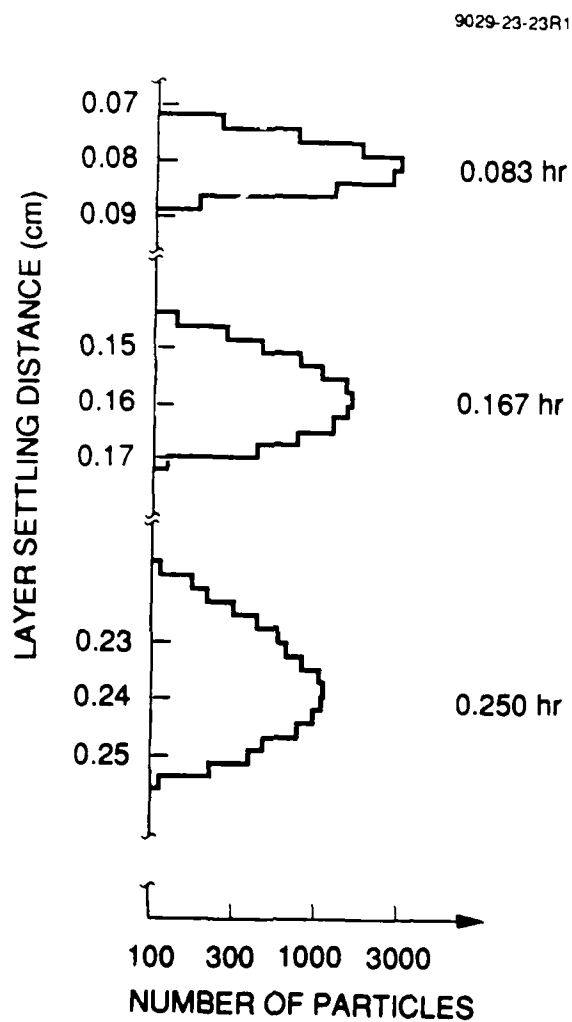
Figure 5-3.   Computer simulation of the settling rate of a microtubule layer.

17
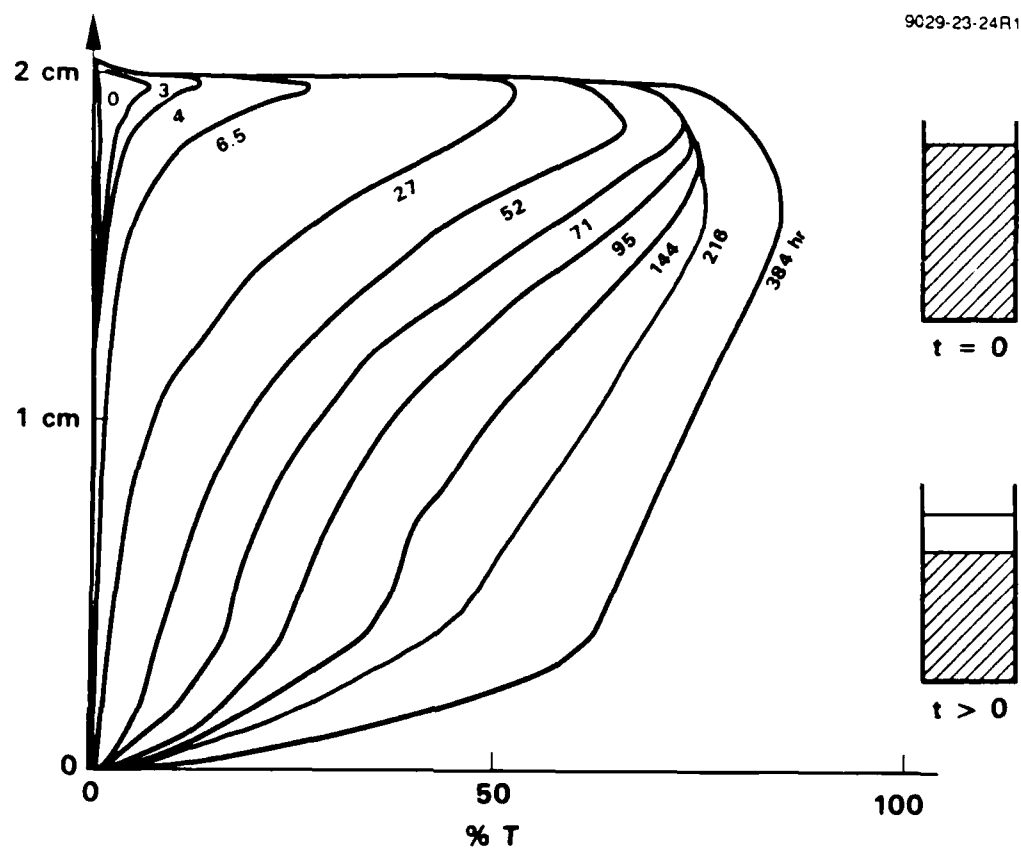
Figure 5-4.   Settling rate for a uniform dispersion of Ni-coated microtubules in PW76234.

SECTION 6

DYNAMIC RESPONSE OF INDIVIDUAL MICROTUBULES IN E-FIELDS

The switching processes and behavior of an active liquid dielectric composite media, such as metalized microtubules dispersed in an isotropic fluid, depend on the dynamic response of the suspended particles to an applied field. We experimentally measured the transient dynamic responses of individual microtubules to applied external electric fields. The dynamic responses of similarly shaped particles was calculated theoretically, and we showed good agreement between the experimental and theoretical dynamic responses for particles of the microtubule sizes.

The transient dynamic responses to an electric field of a single metalized microtubule suspended in paraffin wax oil was observed and measured with a system which included a microscope hooked up to a video recorder (30 frames per second), as indicated in Figure 6-1. The motion of a microtubule was observed and recorded. The time response was determined by replaying the video recorder one frame at a time. The number of frames, N, taken by a microtubule in rotating through an angle $\Delta\theta$ was recorded, where $\Delta\theta = \theta_1 - \theta_2$, with $35° < \theta_1$, $\theta_2 < 65°$, and θ_i was the angle between the external field and the microtubule. The response time was calculated using Eq. (2),

$$\tau = (N \times 90) / (\Delta\theta \times 30). \tag{2}$$

A log-log plot of the measured response times for an estimated 90° rotation of a microtubule, as determined by Eq. (2), is shown as a function of electric field strength in Figure 6-2 for different lengths of microtubules. Various length microtubules responded similarly, at least within the experimental error of our measurement system, where the field strength is uncertain and the microtubule lengths are estimated for each microtubule. These metalized microtubules were about 0.6 μm in diameter, and the Fluka 76234 oil had a viscosity of 180 cP at 22 °C.

In our theoretical calculation, we approximated the metalized microtubules as a long thin cylinder hydrodynamically, and a metallic prolate electrically, respectively. The size and bulk of the particle were large enough to preclude the use of Smoluchowski equation, instead the equation of angular rotation of a particle with a moment of inertia I subject to an external torque Γ was written as Eq. (3),

$$\Gamma = I\ddot{\theta} + f(\dot{\theta}) \tag{3}$$

where f(θ) was a function of angular velocity θ̇. Using the viscous drag expression of two dimensional flow pass a cylinder, $f(\dot\theta)$, for a cylindrical object rotating about an axis perpendicular and at midpoint to its axis of symmetry, was,

$$f(\dot\theta) = 8\pi\eta \int [\dot\theta \ 1^2 \, dl] / [0.5 - G - \log(R/4)] \tag{4}$$

where the Reynolds number R was defined as ub/υ. In the above equations, η was the viscosity, G the Gamma function, b the radius of the cylinder, 2a the length of the cylinder, l the distance along the axis of symmetry from the center of the cylinder, u = lθ̇ the speed of the flow, ρ the density of the solvent, υ = η/ρ the specific viscosity, and θ the angle between the axis of symmetry and the field direction. The above expression for f(θ) was valid for small Reynolds number, R <<1, and the compatible condition that the radial component of flow had been neglected.

C8929-23-04
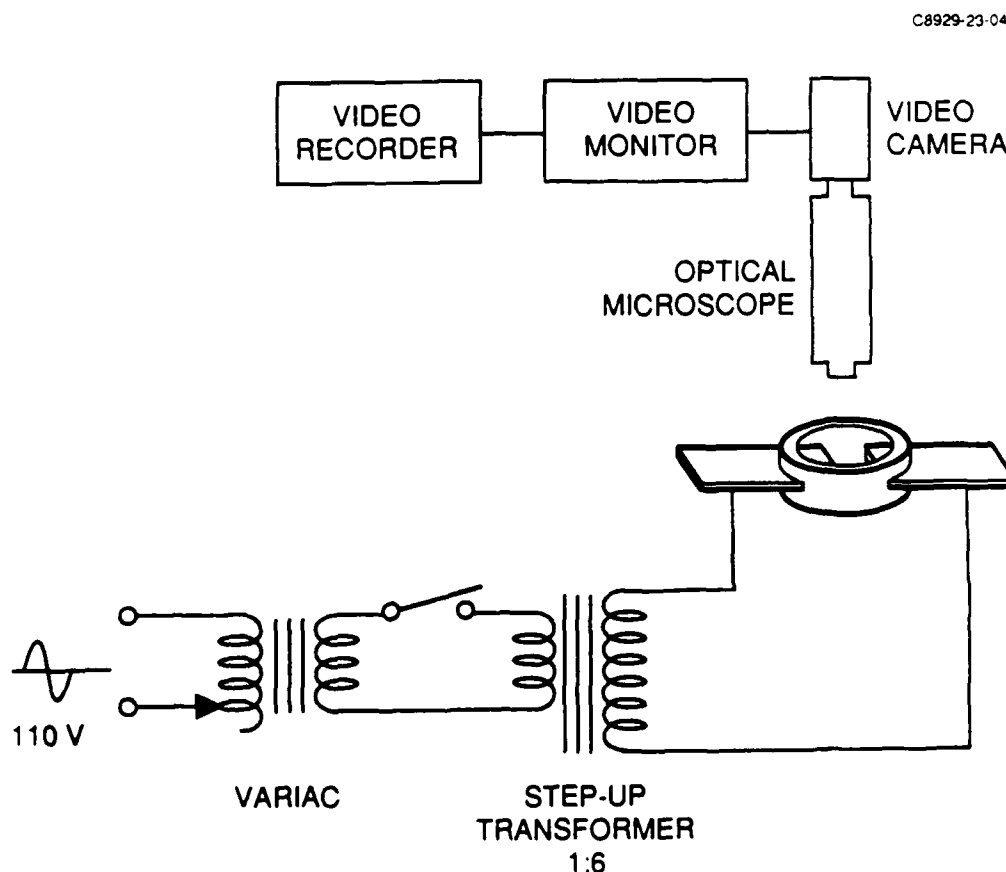
Figure 6-1.   Diagram of experimental system for observing response time of individual microtubules in an applied electrical field.
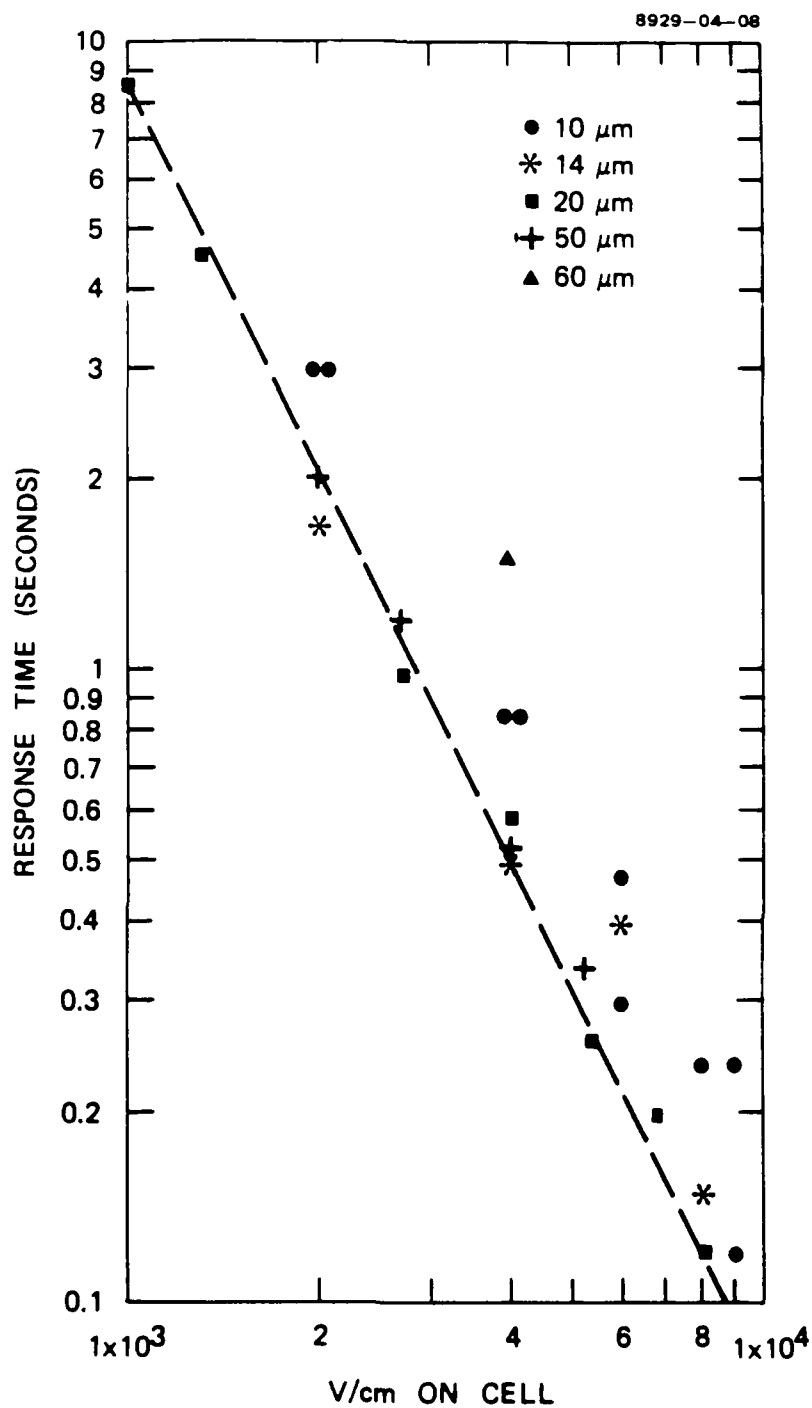
Figure 6-2. Response time of individual permalloy-coated microtubules as a function of applied field, in Fluka PW76234 oil.

For metalic particles, the induced dipole moments are far stronger than the permanent dipole moments, which could be neglected. The torque acted on a cylindrical metallic body due to its induced dipole moments, whose polarizabilities along and perpendicular to its axis of symmetry were respectively α_a and α_b, is given by Eq. (5),

$$\Gamma = \alpha_a E^2 \sin(\theta) \cos(\theta) - \alpha_b E^2 \cos^2(\theta). \qquad (5)$$

Since most of the metalized microtubules were long thin cylinders with eccentricity ($e^2 = 1-b^2/a^2$) close to unity, α_b could be neglected since $\alpha_a >> \alpha_b$. To further simplify the calculations without losing sight of the essential physical principles, α_a could be approximated by using that of a prolate in terms of its volume V and depolarization ratio L_a, where Eq. (6), (7), and (8) apply:

$$\alpha_a = V/(4\pi L_a) , \qquad (6)$$

$$V = 4\pi ab^2/3 , \qquad (7)$$

$$L_a = [(1-e^2) / e^2] [-1 + (1/2e) \ln [(1+ e) / (1-e)]. \qquad (8)$$

In the limit of high viscous drag and negligible moment of inertia, the equation of motion can be written as Eq. (9),

$$(V / 4\pi f L_a) E^2 \sin(\theta) \cos(\theta) = f\left(\dot{\theta}\right) \qquad (9)$$

The above equations were integrated numerically, without any fitting parameters, using the experimental parameters, η = 180 cP, ρ = 0.86 gm/cm3, a = 10 x 10^{-4} cm, b = 0.5 x 10^{-4} cm to obtain the response time at field strength E up to 109 V/cm. The calculated response times as a function of the applied field are shown as the main curve in Figure 6-3 for six orders of magnitude variation in the applied field. (The points shown in the main curve indicate where the calculations were made, and are not experimental points.) As indicated by the insert curves in Figure 6-3, there was general agreement between our experimental results and our calculated results, although the actual response times were shorter than the calculated values. The theoretical limit of response time, set by hydrodynamic drag, at high electric field strength (E >109 V/cm) were shown to be 10^{-9} sec, as indicated in Figure 6-3.

The calculated rotation angle for metal prolates was also compared with the experimentally observed rotation of metalized microtubules, as shown in Figure 6-4 for 20-μm-long microtubules. Just by fitting the curves only at their $\pi/4$ values, excellent agreement in the shape of the rotation curve was obtained when a higher field strength (4000 V/cm) was used for the calculated curve (solid line) than for the actual experimental points (2700 V/cm). In

general, the calculated response times in Figure 6-3 required higher fields to match the experimental response times, perhaps due to an oversimplification in our calculations for metal prolates versus hollow microtubules, or perhaps due to some experimental uncertainty in the field strengths.
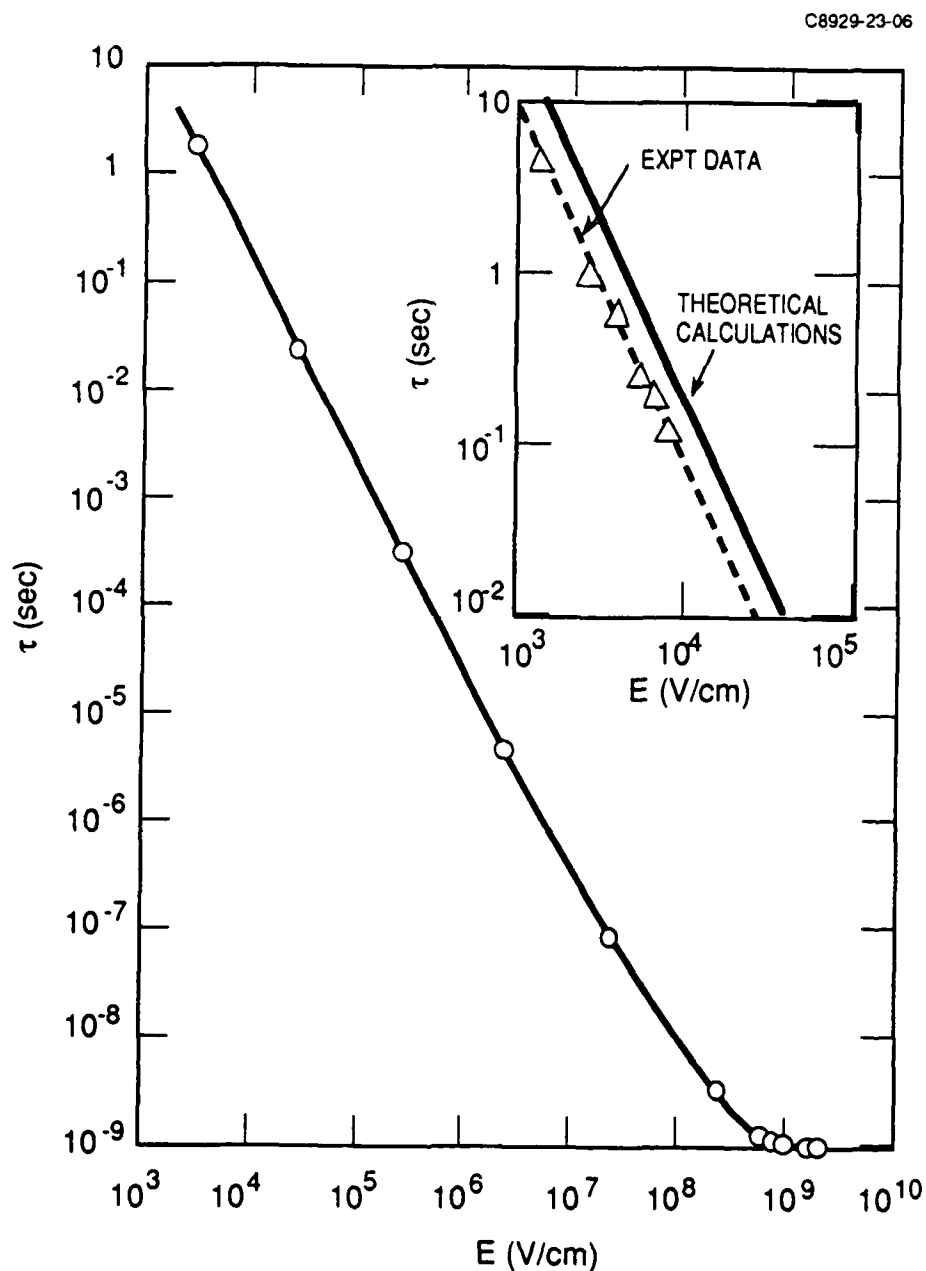
Figure 6-3.   Calculated microtubule response times as a function of applied field.
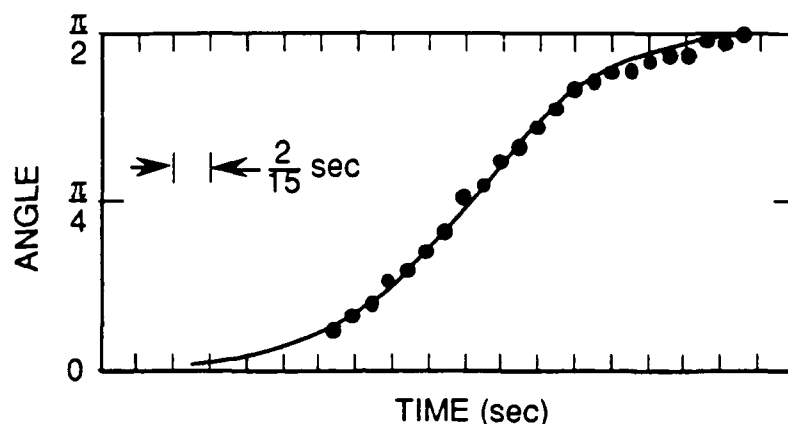
Figure 6-4. Time response for rotation angle of microtubules under an applied field.
(Experimental points at E = 2700 V/cm. Calculated curve at E = 4000 V/cm).

The effect of the length on the calculated response time of microtubules (as metal prolates) is shown in Figure 6-5 for the indicated semi-axis of the prolate at a field strength of 3000 V/cm in a fluid with a viscosity of 180 cP. These calculations indicate that the response time is only a factor of two times slower for a = 30 as compared to a = 5, which corresponds to the microtubule length range of 60 to 10 μm in Figure 6-2. Our experimental reproducibility for the various lengths in Figure 6-2 is probably greater than a factor than two, which may be why we observed no consistent length effect on these experimental response times.

To show the possible performance of future active composite media, the dynamic responses of an idealized active composite of suspension of metal particles in a low viscosity fluid was calculated. This is shown in Figure 6-6 as a theoretical calculated response time versus applied electric field of a liquid composite medium consisting of 1 μm x 10 μm metal particles suspended in a η = 1 cP liquid. Since the maximum field strength that is usually obtainable without dielectric breakdown in is fluid is about 10^5 V/cm, the characteristic *performance envelope* obtainable with this composite media is shown in the shaded area of Figure 6-6. This indicates that a response time as fast as 10^{-6} seconds could theoretically be reached with an applied field of 10^5 V/cm. (In comparison, note that liquid crystal optical devices operate in the 10^3 to 10^6 V/cm range.) This shows that liquid active composite dielectric media could, in principle, be made to operate at microsecond response times.

24

C8929-23-07R1

$b = 0.5 \times 10^{-4}$ cm
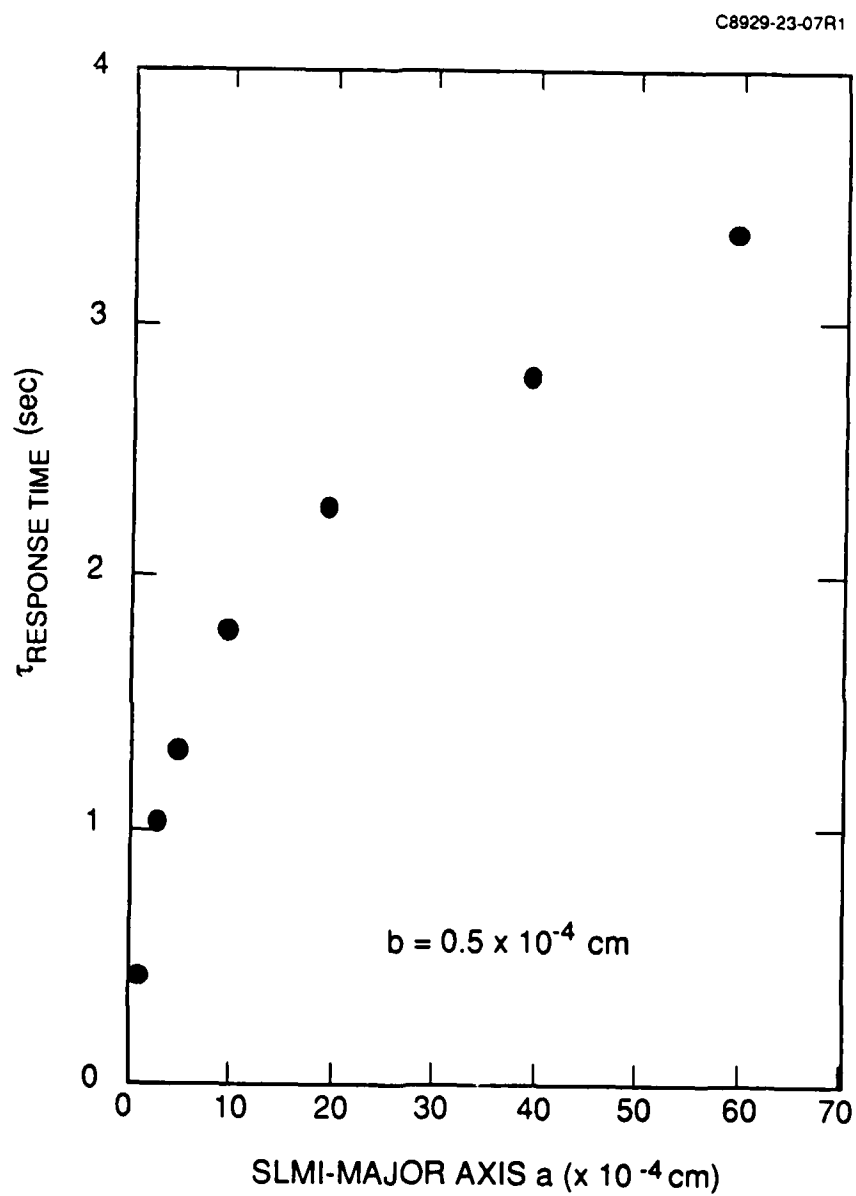
Figure 6-5. Calculated microtubule E-field response time as a function of length.

25
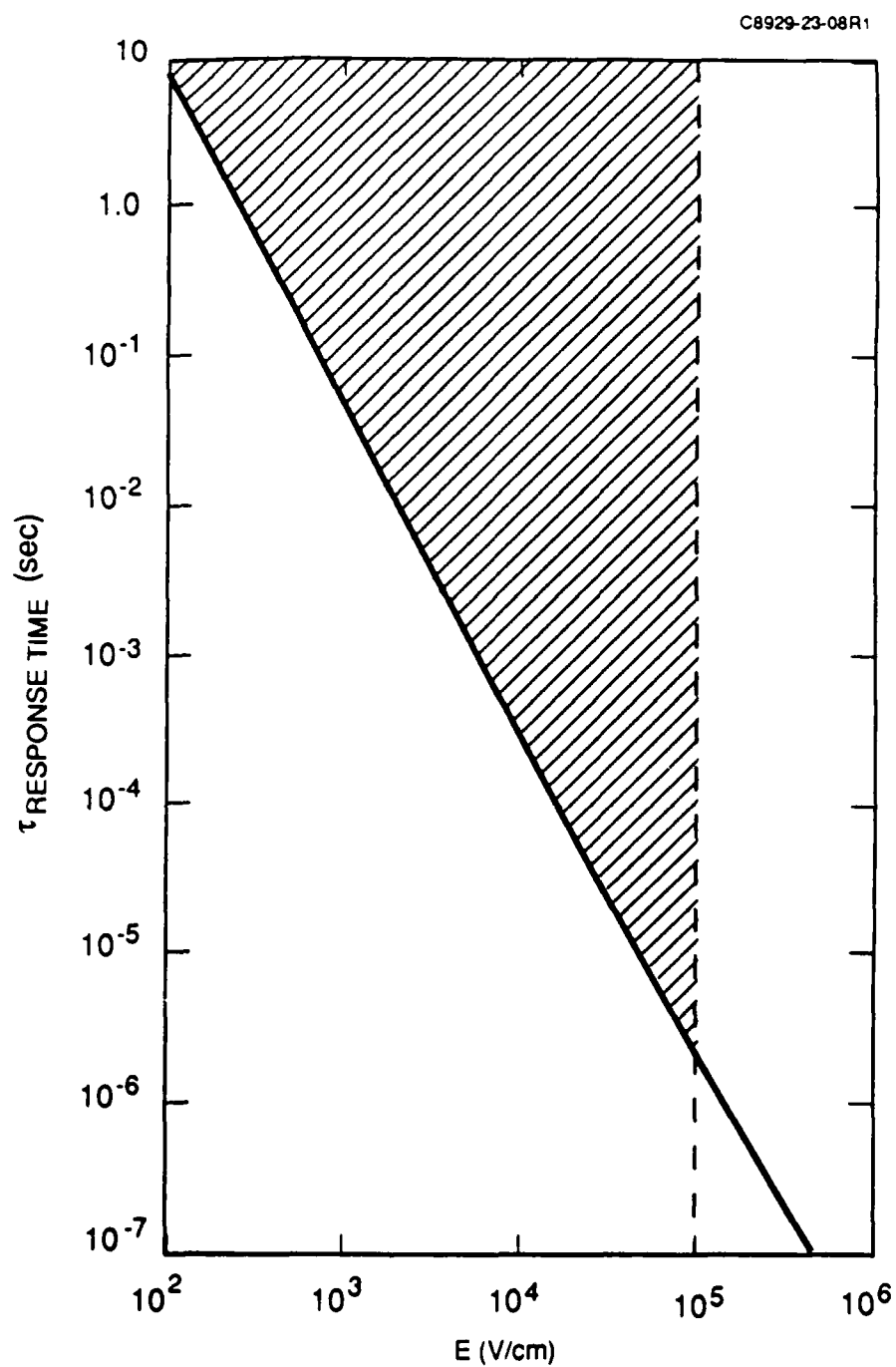
Figure 6-6.   Calculated performance envelope for E-field activation of microtubules.

SECTION 7

FIELD EFFECTS IN THIN LAYER FLUID DISPERSIONS

7.1 MICROTUBLES IN ISOTROPIC FLUIDS AND POLYMERS

Electrical fields alignment of metalized microtubules in fluid dispersions is readily observed in thin cells under a microscope. For example, Cu-coated microtubules (about 10 to 60 μm in length) dispersed in an optical cement fluid (Norland NOA-65) and placed in a 25 μm layer between glass slides were aligned by a lateral electrical field of 100 V (60 Hz) across a 2 mm gap between parallel metal shim electrodes, as shown in Figure 7-1. These pictures, from a microscope looking through the glass cell, are for the initial cell before voltage was applied (left picture), the cell with fluid monomer while voltage was applied (center picture), and the cell after ultraviolet curing to form a solid polymer layer (right picture). An overall view of this cell is shown in Figure 7-2, which also has another microscope picture showing the curved alignment pattern of the microtubule in the inhomogeneous region at the edge of the electrodes. Under these conditions the microtubules were aligned mostly perpendicular to the electrode surface and into strings containing filament-like groups about 200 to 800 μm long. In this cell, these patterns did not change very much when the field was removed, nor when the optical cement fluid UV-cured to a solid.

A freely suspended dispersion of metal particles would be expected to form aggregates in the presence of a non-uniform external electric field E (or magnetic field B) due to the resultant attractive force F acting on a dipole moment p in the present of the field gradient dE/dx (where x is the displacement along maximum field gradient), as indicated in Eq. (10). Thus, some

$$F = - p \ (dE/dx) \tag{10}$$

filamentation effects might be expected in the inhomogeneous field region shown in Figure 7-2. However, although the overall field region shown in Figure 7-1 is more uniform filamentation also occurred. The metalized microtubules themselves may contribute to local field inhomogeneity which cause this effect. Such field induced clustering is detrimental to the reversible operation of active composite media consisting of metalized microtubule suspensions This effect could probably be reduced by decreasing the size of the microtubules so that the random particle Brownian motion is strong enough to disrupt the aggregating force, or by coating the surface of the microtubules with a thick layer of dielectric (e.g., polymeric gel) to induce some repulsive force between the particles.

LATERAL FIELD ALIGNMENT OF Cu-COATED μTs IN OPTICAL CEMENT
TRANSVERSE VIEWS OF GLASS CELL, 25 μm THICK

| NO VOLTAGE (FLUID) | 100V, 60 Hz (FLUID) | UV CURED WITH FIELD OFF (SOLID) |
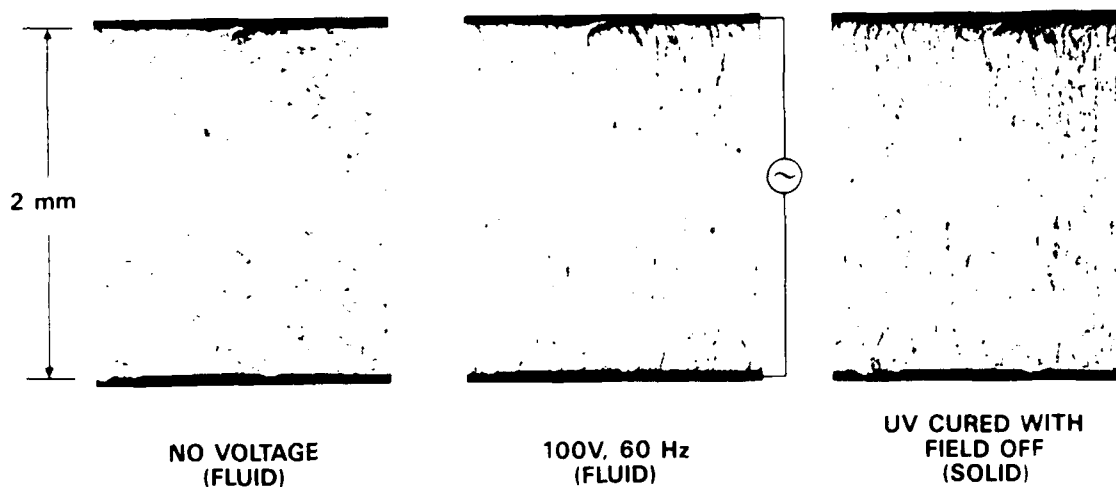
Figure 7-1   E-field alignment and filamentation in a monomer fluid and its polymer.

GLASS CELL WITH 25 μm
THICK METAL ELECTRODES.
MICROTUBULES IN OPTICAL CEMENT

ALIGNED WITH 100V (60 Hz).
UV CURED JUST AFTER
REMOVAL OF FIELD
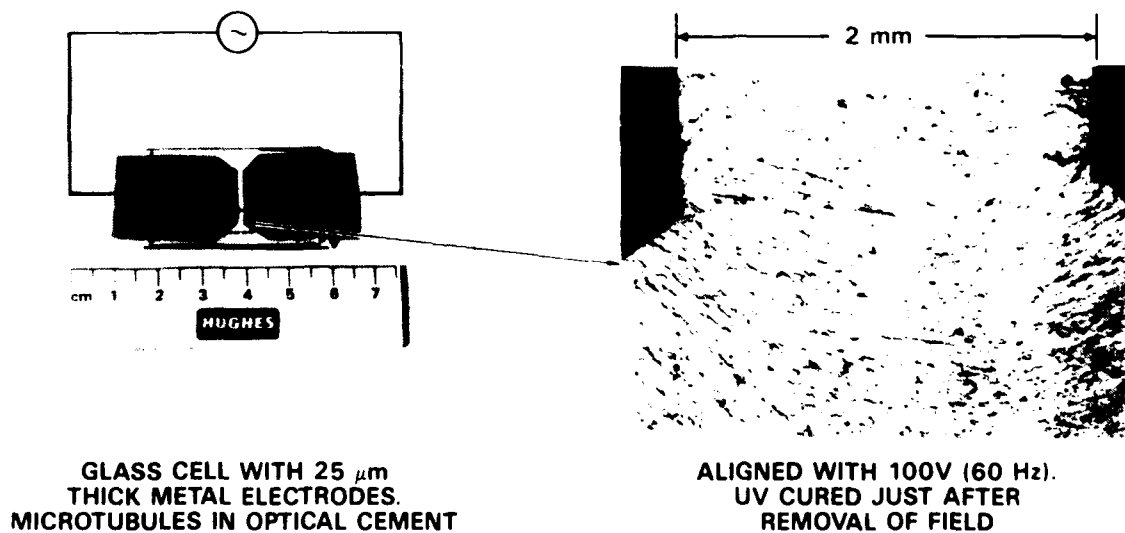
Figure 7-2 Lateral E-field cell for Cu-coated microtubules, and alignment patterns in an in homogeneous field region.

28

The formation of the field induced fibril aggregates might be of practical value as an anisotropic conductive film (*e.g.*, for use in microelectronic circuit packaging) if the electric conductivity was high along the filamentation direction, and the fibrils were aligned in a transverse, surface-perdendicular, direction through a thin polymer film. Our attempts to make such films are described below in Section 12.3, where we found no electrical conductivity along the fibril aggregates in the films prepared, indicating that the microtubules were not in direct physical contact with each other, but were instead separated by coatings of polymer. The alignment of microtubules or microtubule fibrils on surfaces in a perpendicular direction was also of interest for other device concepts, such as a basis for acoustic signal detectors. However, we found that although it was easy to obtain such transverse alignment in a monomer fluid between parallel plate conductors, it was difficult to maintain this alignment when the fluid was polymerized. This problem is illustrated in Figure 7-3 for Cu-coated microtubules (0.1 % by weight) dispersed in the optical cement Norland NOA-68 and placed in a 127 μm thick cell glass between indium tin oxide (ITO) conductive electrodes. One of the ITO electrodes was scribed, so that the applied field (20 V, 400 Hz) was only on the lower part of the pictures in Figure 7-3. In the field area before polymerization the microtubules appear mainly as dots, indicating their surface-perpendicular alignment. However upon polymerization (by UV curing) these microtubules became strongly tilted, due to flow effects as the fluid was converted to a solid polymer film. Extremely slow polymerizations were required to minimize this flow distortion of the microtubule field alignment.

We studied various types of electrical, magnetic, and acoustical field effects on microtubules in thin cells, and a common factor observed was a very limited reversibility of these effects. This appeared to be due both to filamentation, clustering, and surface sticking effects of the microtubules from the dispersions. Figures 7-4 and 7-5 show microscope pictures viewing an inner surface of planar cells made with one interdigitated ITO electrode (100 μm wide lines and spaces), an ITO counter electrode, and a 127 μm thickness of 1% permalloy-coated microtubules in Norland NOA-61 monomer. In Figure 7-4, alternate stripes of the interdigitated electrodes were activated with 30 V (60 Hz) versus the counter electrode. The pictures show largely surface-perpendicular alignment of the microtubules above the activated stripes, and lateral (surface-parallel) alignment at the edges between the activated and unactivated (floating) stripes. The lateral field effect is more pronounced in Figure 7-5, which was taken after the sequence of first activating at 30 V (60 Hz) alternate stripes versus the counter electrode (other stripes floating), and then activating between the interdigitated stripes (counter electrode floating). In each of these cells, the microtubules were nearly all fixed in position after a few minutes of operation, so that little change occurred on continued changes in the activation patterns.

BEFORE
POLYMERIZATION

AFTER
POLYMERIZATION

FIELD
ON
AREA

|◀─ |◀── 100 μm
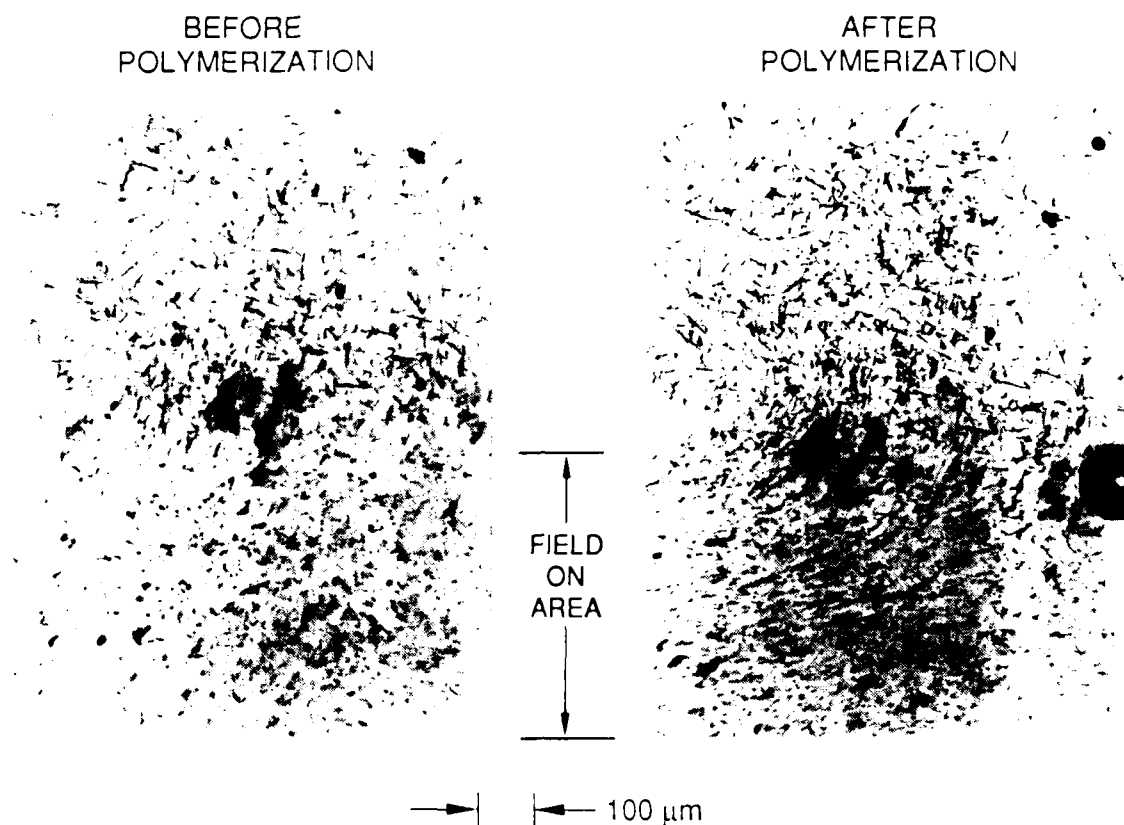
Figure 7-3.   Transverse E-field alignment of microtubules and polymerization effects.

|◀─ |◀── 100 μm |◀─ |◀── 100 μm
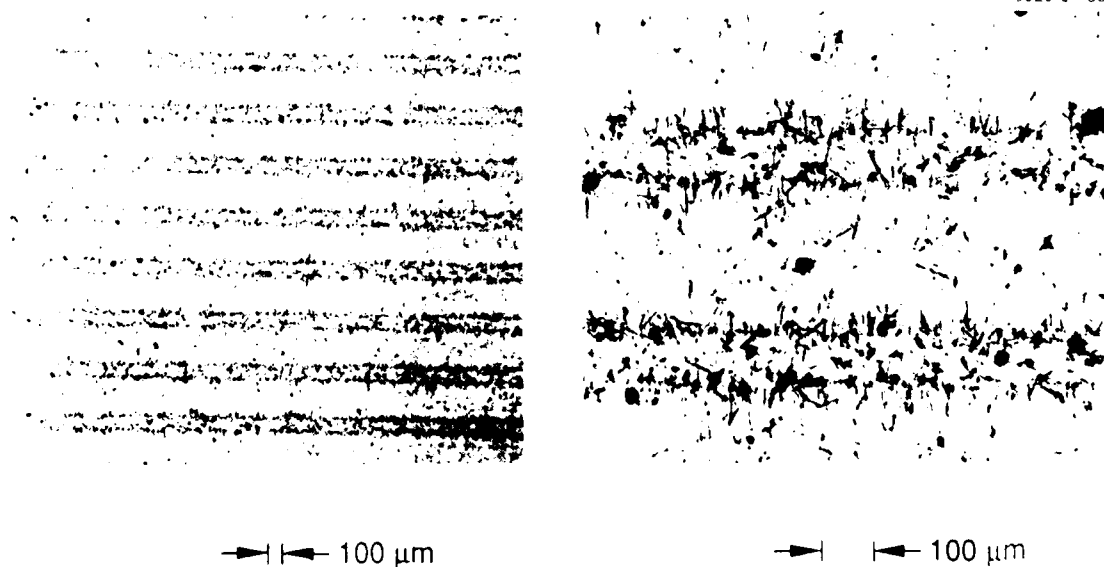
Figure 7-4. E-field alignment of permalloy-coated microtubules activated with interdigitated
electrodes versus a counter electrode.
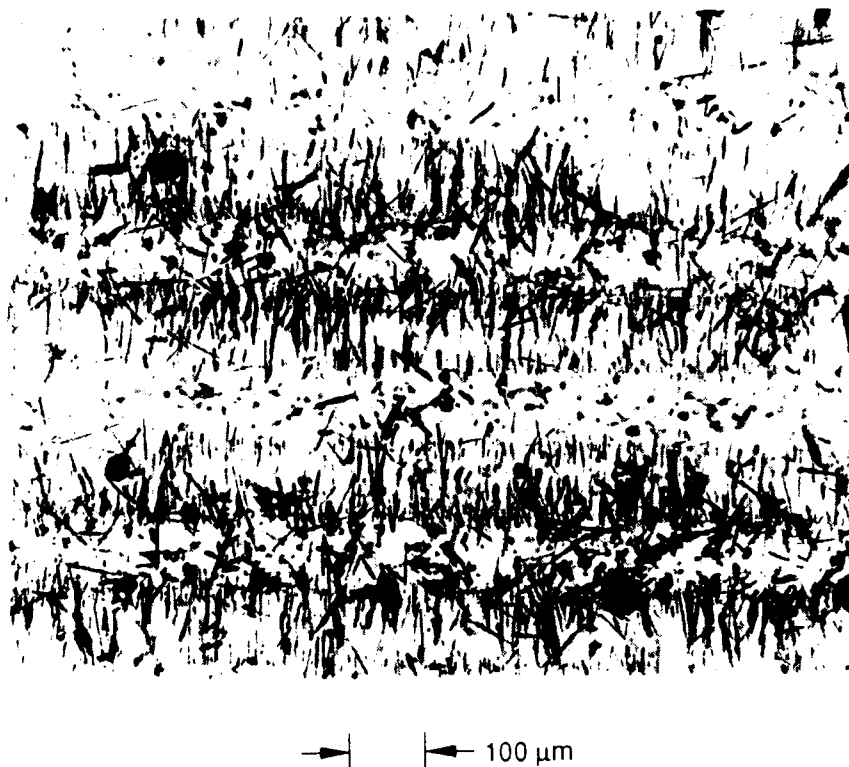
Figure 7-5. E-Field alignment of microtubules using an applied field sequence from
interdigitated electrodes.

A realignment effect on microtubules by an acoustical pulse is shown in Figure 7-6. This
planar cell contained Cu-coated microtubules dispersed in an epoxy fluid layer (254 µm thick)
between ITO electrodes. The microscope pictures from left to right show the sequence of
microtubule alignment which was initially random, then transverse from 2 seconds of 100 V
(60 Hz), then distorted to lateral by an acoustical pulse (left to right) applied to the edge of the
cell layer, and then back to transverse by another 2 s of applied voltage. These effects were
partially reversible, but on continued cycling (>10 times) most of the microtubules became fixed
in position and were no longer changed significantly by the acoustical pulse.

31

INITIAL | E-FIELD | ACOUSTIC | E-FIELD
RANDOM | VERTICAL | PULSE | VERTICAL
ALIGNMENT | ALIGNMENT | APPLIED | ALIGNMENT
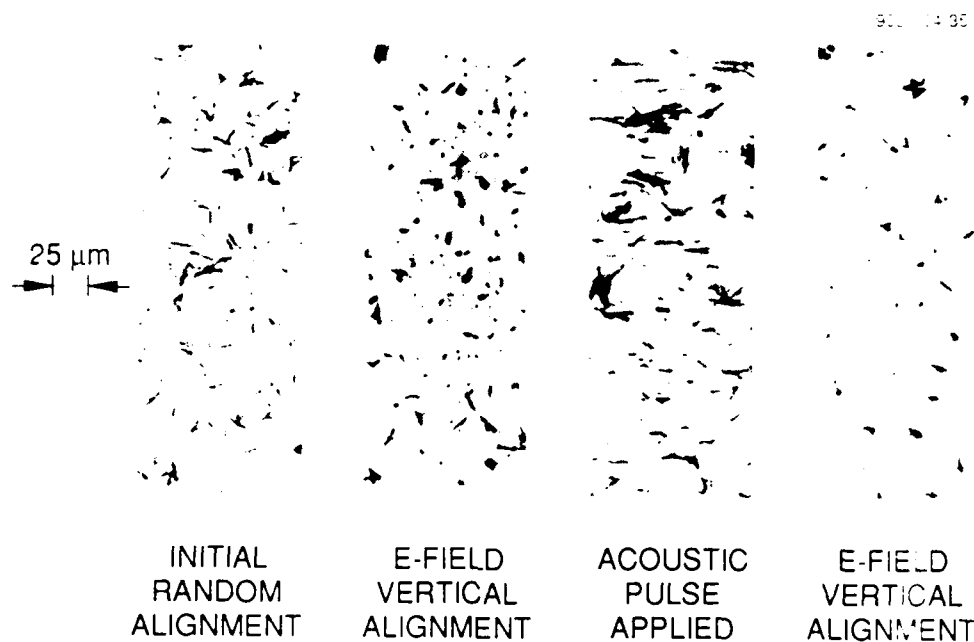
Figure 7-6.   Acoustic pulse modulation of microtubule alignment.

The E-field modulation of optical transmission of microtubule dispersions in thin cells was also studied. Figure 7-7 shows visible range spectrophotometer transmissions versus air for a 127-μm-thick cell of 1% permalloy-coated microtubules in Optistick 2060 monomer (between ITO electrodes), as compared to a similar cell with only the monomer. The two lower curves show the effect of an applied field on the transmission, which at 500 nm changed from 49 %T for randomly aligned microtubules to 63 %T for transverse field alignment in the direction of light propagation. The transmission losses include reflections from the cell as well as both absorption and scattering by the microtubules. The reversibility of the applied field effect was limited, but

this was partially due to the long time period for the microtubules to return to a random alignment distribution in the monomer fluid after field activation. In another cell, orthogonal magnetic and electrical fields were applied to switch the microtubule alignment back and forth as shown by the transmission data in Figure 7-8. This cell had a more dilute dispersion of 0.5 % permalloy-coated microtubules in Fluka 76234 paraffin wax oil and a larger thickness of 1 mm between ITO electrodes. (The microtubules had an average length of about 40 μm.) The transmission changes show the effects of a constant lateral magnetic field (0.8 kG) and a periodic transverse electric field (3.5 kV/cm). Although this cell could be cycled many times, the transmission changes gradually decreased and the overall transmission increased due to clustering, which was indicated by the upward trend shown in the data. A similar cell of 750 μm thickness was cycled briefly between 19 %T and 37 %T when switching from a lateral H-field to a transverse E-field (140 V, 100 Hz).

9029-04-36
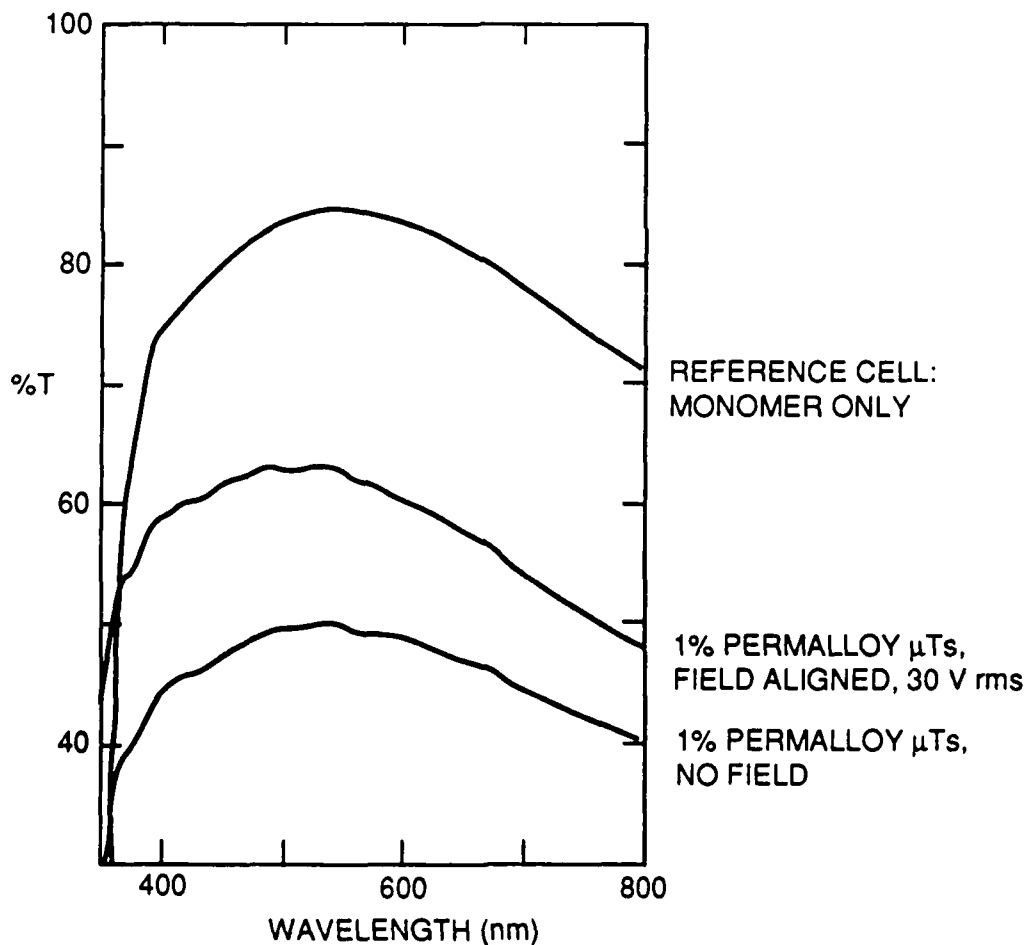
Figure 7-7.   Transmission change with E-field alignment of a microtubule dispersion.

33
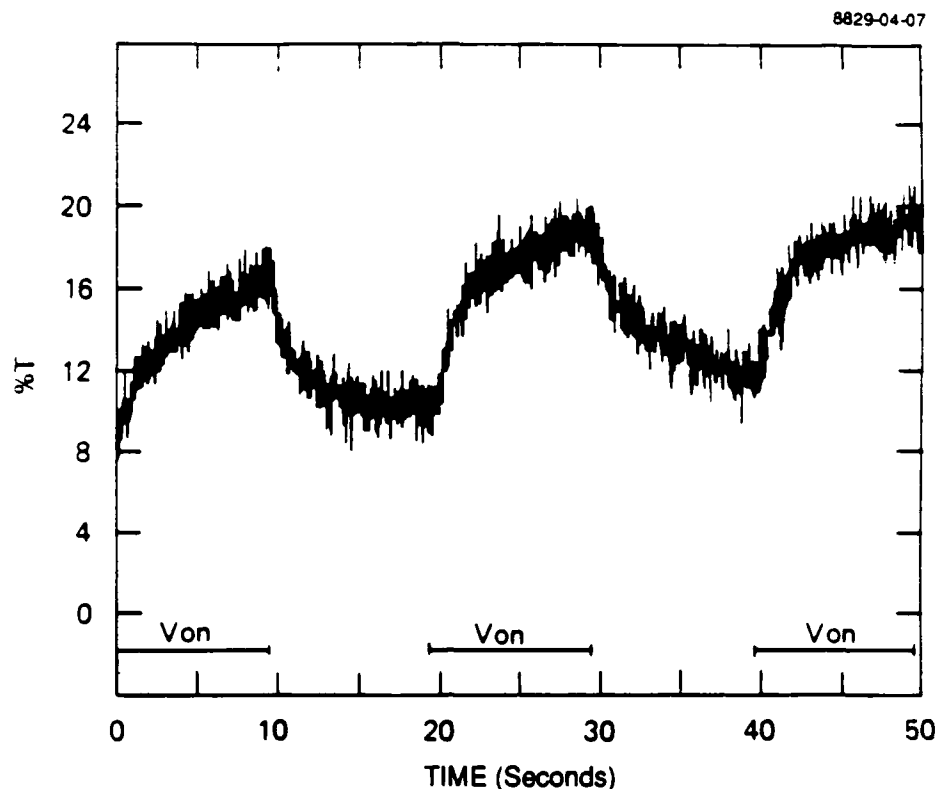
Figure 7-8. Transmission changes for a permalloy-coated microtubule dispersion in Fluka 76234 subjected to a lateral H-field and a periodic transverse E-field.

The effect of applied fields on the clustering on metalized microtubules was examined with a well-aged, untreated sample of permalloy-coated microtubules which no longer responded to a magnetic field (perhaps indication some oxidation and/or tiny cracks in the coating). These microtubules tended to cluster more quickly than later Ni-coated samples which had been treated with a silane or which had been coated in a plating bath containing PVP. Nevertheless, the clustering effects with this sample are documented in Figures 7-9 and 7-10. In the E-field aligned cell (Figure 7-9) a 1% microtubule dispersion was used in an epoxy fluid (127 μm thick) in a cell with ITO electrodes, one of which was scribed in the middle. The microscope pictures show substantial microtubule clustering in the lower part of the cell where 100 V (60 Hz) was applied for periods of 0.5 and 3 hours. Figure 7-10 shows the clustering effect for a 0.3% dispersion of this aged permalloy-coated sample in a 127-μm-thick epoxy fluid dispersion subjected to a 14 kG magnetic field for about 20 hours. Even though these microtubules were not aligned by the magnetic field, it did cause noticeable clustering.

100 µm

NO
VOLTAGE

VOLTAGE

NO VOLTAGE   100 V ON   100 V ON
FOR 0.5 HRS   FOR 3 HRS
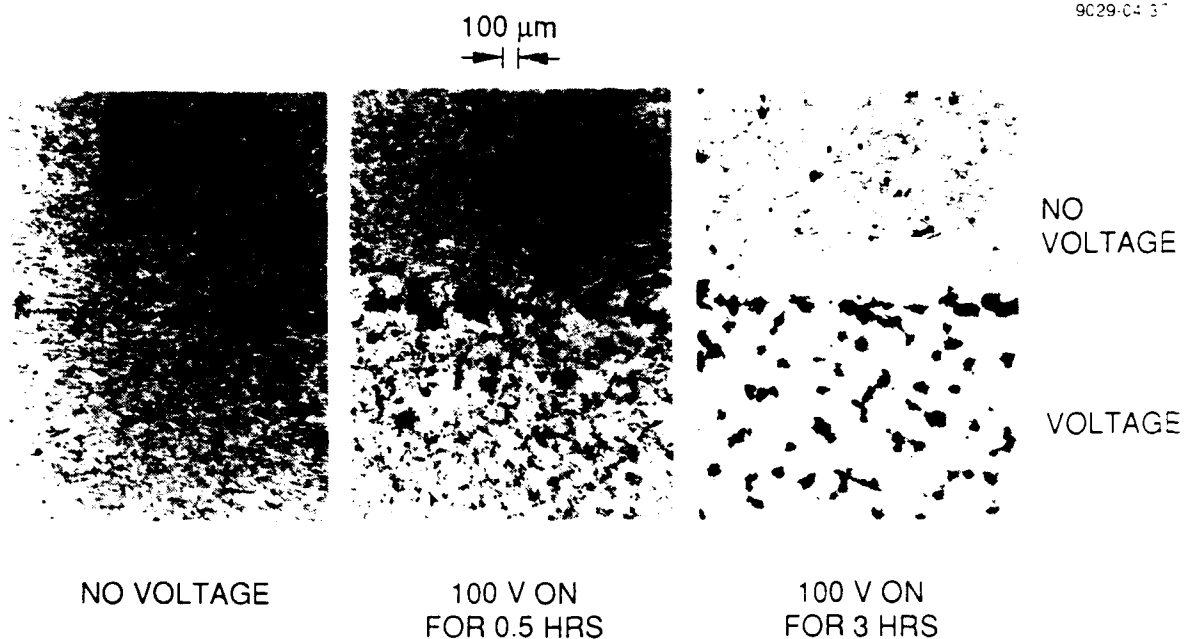
Figure 7-9.   E-field induced clustering of aged metalized microtubules.

BEFORE FIELD   FIELD ON OVERNIGHT

100 µm

Figure 7-10.   H-field induced clustering of aged metalized microtubules.

35

7.2   MICROTUBLES IN LIQUID CRYSTALS

Liquid crystals (LCs) were studied as possible hosts for the dispersion of metalized microtubules, mainly to investigate the possibility of using the liquid crystals to assist in controlling the alignment direction of the microtubules. Although the microtubule dimensions are enormous compared to the size of liquid crystal molecules, the collective interaction of groups of liquid crystal molecules normally extends over a range of about 0.1 μm even without surface and field interactions which can be used to order liquid crystals over distances larger than the length of microtubules. We also considered the possibility that if the liquid crystals were aligned surface-parallel on the microtubules themselves, then even a modest concentration of microtubules might act as a sort of internal alignment surface within the bulk of the liquid crystal. If this were the case, then we would expect cooperative interaction between liquid crystals and the microtubules. However, we found that, in fact, all the liquid crystals we studied aligned themselves *perpendicular to the surface of the metalized microtubules* (even those treated with silanes). This observation was clearest when we examined applied field effects under a polarizing microscope for microtubules in liquid crystals of positive dielectric anisotropy (*e.g.*, 0.01% of Cu-coated microtubules in BDH-E7 with 10 V of 10 kHz applied across a 50-μm-thick cell). Here the microtubules and the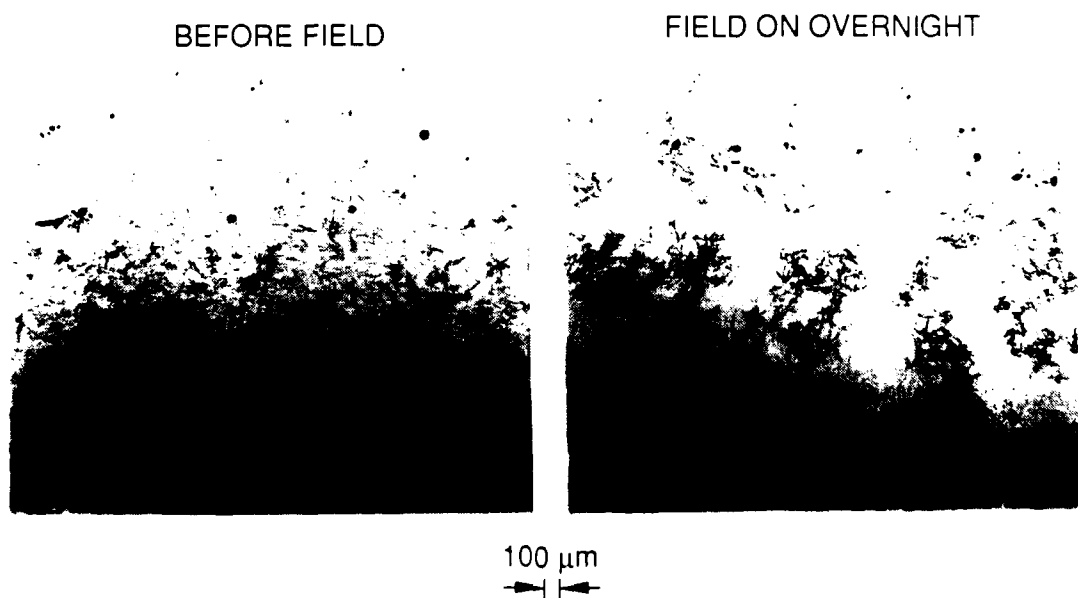 bulk of the liquid crystal were both strongly aligned in the field direction, perpendicular to the surfaces of the cell, but a "halo" of misaligned liquid crystal much larger than the microtubule diameter was observed around the end-on view of each microtubule. In any case, when this type of microtubule/LC dispersion was used in cells with surface-parallel liquid crystal alignment (*e.g.*, rubbed cell surfaces) the metalized microtubules did not follow the liquid crystal back to the surface-controlled alignment state when the field was turned off.

Because we had observed strong flow alignment effects of microtubules in various fluids, we attempted to use the turbulent flow of LCs in their dynamic scattering mode (DSM) to randomize microtubules previously field aligned. We first aligned the microtubules with a high frequency electrical field (no DSM), and then switched to the DSM with a low frequency field. The DSM caused the microtubules to move all around the cell, but due to their strong interaction with the field the microtubules stayed field aligned all the time. When the signal was removed, the DSM turbulence decayed much faster than the microtubule relaxation from the field alignment, so there was no net alignment change despite the dynamic flow effects.

Liquid crystal induced flow alignment effects were observed with oxidized microtubules which did not respond to applied E-fields. (Permalloy-coatings were oxidized with hydrogen peroxide.) These oxidized microtubules were studied in a crossover liquid crystal (ROTN-3421) in a 50-μm-hick cell between ITO electrodes overcoated with angle-deposited SiO_2. Although

birefringent domains were still observed around each tubule, and they disrupted the uniform surface alignment of the liquid crystal, some of the shorter microtubules were observed to follow the field-induced LC alignment directions: namely, surface-perpendicular at low frequency (100 Hz) and surface-parallel at high frequency (1 kHz). Table 7-1 shows some approximate response times for these effects.

TABLE 7-1. Alignment Response of Oxidized Permalloy-Coated Microtubules in a Crossover Liquid Crystal.

Signal Applied to Cell	LC Response (seconds)	μT Response (seconds)	Comments[a]
On (0 to 25 V, 100 Hz)	15	2	μTs aligned faster than LC[b]
Off (25 to 0 V, 100 Hz	10	25	LC aligned faster than μTs[c]
Frequency Switch at 25 V (from 100 Hz to 10 kHz)	4	7	LC aligned faster than μTs[d]

[a] Visually observed response times of a crossover LC and some shorter μTs. The changeable μTs aligned in the same direction as the LC, namely surface-perpendicular at low frequency and surface-parallel at high frequency.

[b] Presumably the μTs responded quickly to the initial flow realignment of the LC.

[c] The μTs followed the LC realignment to surface-parallel, induced by the cell surface

[d] The μTs followed the LC field realignment to surface-parallel.

Studies were made on the preparation of various mixtures of liquid crystals, LC-monomers, LC-polymers, and other polymerizable monomers to use in seeking improved electrical field alignment of microtubules. Small quantities of six different purified LC-monomers were prepared and purified, using methods which we had previously developed for the synthesis of these structures on another project. Four of these were alkylphenyl acryloyloxybenzoates and two were alkoxyphenyl acryloyloxybenzoates, as shown in Table 7-2. On the other project we had previously calculated five different combinations of these components, with the calculated compositions shown in Table 7-3. The two room-temperature nematic LC-monomer eutectic mixtures identified as HRL-LCM2 and HRL-LCM4 were prepared, and their measured clearpoints were in good agreement with the calculated values.

Photopolymerization of the LC-monomer mixtures gave high clearpoint LC-polymers. For example, the polymer from UV exposure of HRL-LCM4 doped with 5% diethoxyacetophenone (DEAP) had a clearpoint greater than the hot stage limit of 225 °C. Lower clearpoint polymers were obtained by UV polymerization of the LC-monomer mixtures dissolved in a nematic LC.

TABLE 7-2. Liquid Crystal Monomers and Their Properties.

9029-04-39

$$CH_2 = CH - COO - \langle 0 \rangle - COO - \langle 0 \rangle - R$$
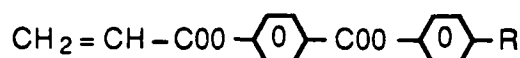
R	PURITY* (%)	MP °C	CLPT °C	ΔH cal
C_3H_7	93.6	56.9	64.2	5357
C_4H_9	98.0	48.3	40.9	7736
C_5H_{11}	91.5	47.2	64.5	3308
C_7H_{15}	97.8	44.5	64.1	7095
OC_2H_5	98.0	116.4	117.0	11314
OC_6H_{13}	94.2	60.3	101.7	7027

* ESTIMATED BY HPLC

TABLE 7-3. Eutectic Mixtures of Liquid Crystal Monomers.

9029-04-40

MIXTURES	LCM1	LCM2	LCM3	LCM4	LCM4A
MOLE RATIO OF COMPONENT:					
R = $-C_3H_7$	0.2534	0.2131	0.2186	0.1903	0.2131
$-C_4H_9$		0.1416		0.1203	0.1416
$-C_5H_{11}$	0.4990	0.4484	0.4556	0.4182	0.4484
$-C_7H_{15}$	0.2476	0.1968	0.2037	0.1695	0.1968
$-OC_6H_{13}$			0.1220	0.1017	
MELTING POINT, °C	9.4	4.4	5.1	1.2	4.4
CLEAR POINT, °C					
- CALCULATED	64.3	61.0	68.9	65.3	61.0
- MEASURED		61.5		66.2	

For example, a 1:3 mixture of LCM4/E7 showed a clearpoint of 147°C after polymerization. Some qualitative studies indicated that the field alignment of metalized microtubules during UV polymerization was maintained better in our LC-monomers than in isotropic optical cements. A dilute concentration (about 0.1%) of Cu-coated microtubules was studied in a 25:5:1 solution of LCM2/E7/DEAP. Polymerization with and without an applied field showed some visual transmission difference between two halves of a thin cell, where the LC-monomer and LC-polymer were field-aligned in the same direction as the microtubules.

SECTION 8

THICK CELL OPTICAL TRANSMISSION AND SCATTERING

Dilute dispersions of metalized microtubules in viscous polar fluids are much more stable suspensions than more concentrated dispersions in non-polar fluids. The lengths of the microtubules (typically 10 to 100 μm) are much longer than the wavelength of visible light, while their diameters (0.6 to 0.8 μm) are in the same range. Thus, visible light is strongly scattered (and also partially absorbed and reflected) by unaligned microtubules, while those aligned end on (in the direction of the light beam) cause much less attenuation of the light. We studied the light shuttering characteristics of metalized microtubules suspended in a glycerol/water host. The transmission intensities of a low power He-Ne laser beam (0.633 μm) was measured after it passed through a 1 cm cell of permalloy-coated microtubules (50 μm long) suspended in a mixture of glycerol and water (6:1 volume ratio, viscosity = 200 cP), with and without application of external magnetic field. The experimental set up is diagrammed in Figure 8-1. A pair of 0.2 kG electromagnets (which were strong enough to align all the microtubules in a reasonably short time) had 0.4 cm holes through their pole pieces. Field lines approximately parallel to the laser beam direction were used to align the microtubules. The transmission intensities through the composite medium in its random alignment state I_r is less than its aligned (parallel to laser beam) state I_a. The optical transmission intensities, I_a and I_r, of the aligned and randomly aligned suspensions (magnetic field on and off, respectively) were measured for concentration up to 0.16 wt.%, and a semi-log plot of transmission intensity as a function of concentration and alignment is shown in Figure 8-2.

The transmission intensity through the aligned microtubules is much higher than through those randomly aligned. The straight line graphs in Figure 8-2 indicate that the data is consistent with the Lambert-Beer relationship, Eq. (11), where σ is the scattering cross-section, c is the

$$I = I_0 e^{-\sigma c d} \tag{11}$$

concentration, and d is the optical path length. This indicated that there was no concentration induced aggregation at concentrations up to 0.16 wt.%. The contrast ratio, $C_r = I_a/I_r$, plotted as a function of the microtubule concentration is shown in Figure 8-3. This shows a rapid increase in the contrast ratio as concentration was increased, although of course the overall transmission of the cell decreased at higher concentrations. At a contrast ratio of 30:1, the transmission of the aligned state was 16%.
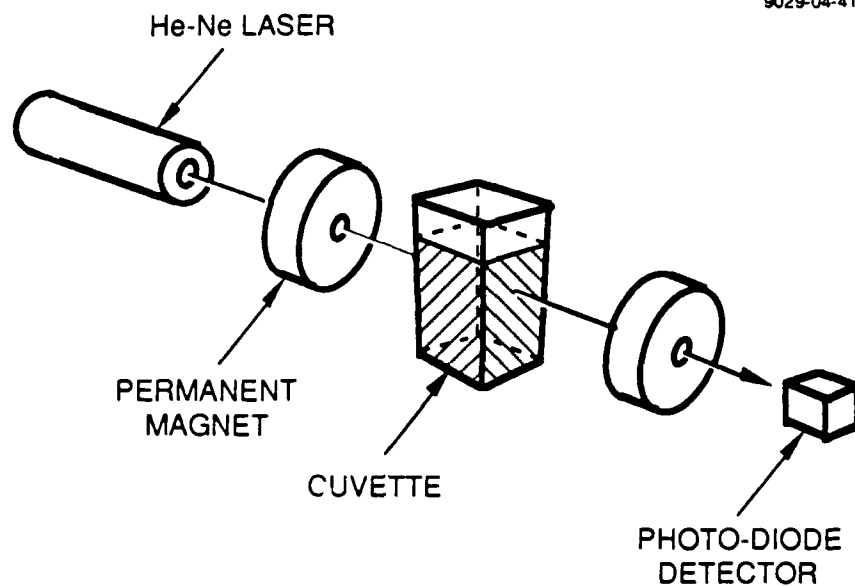
Figure 8-1.   Optical set up for transmission measurement of aligned microtubules.
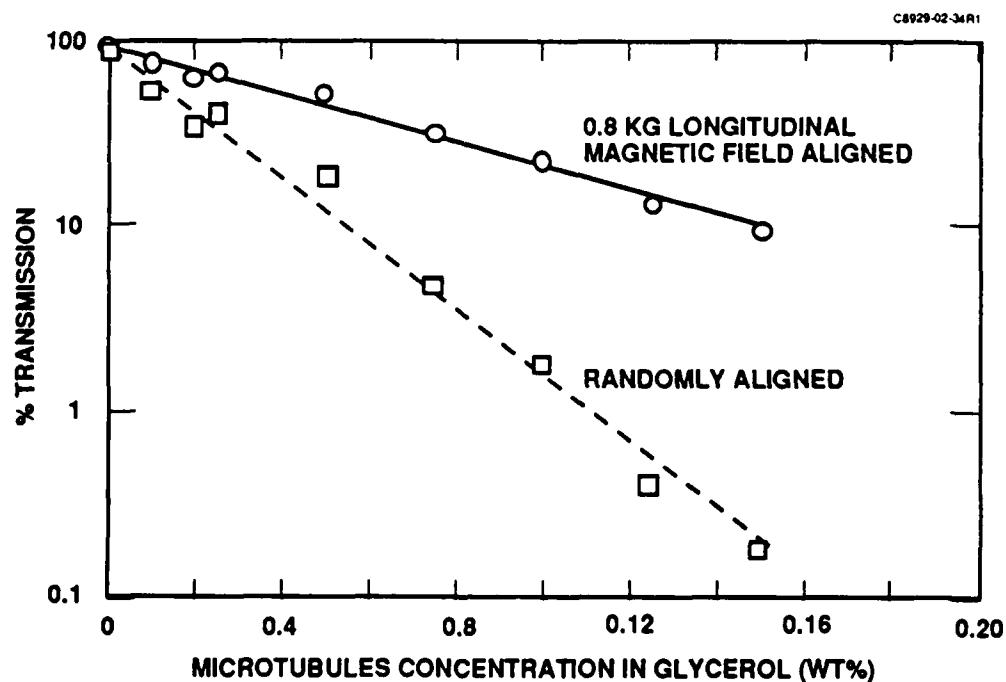
Figure 8-2. Effect of H-field alignment and concentration on transmission of 632.8 nm laser beam through a suspension of permalloy-coated microtubules.

41

C8929-02-33R1

CR = $\dfrac{I_A(\text{MAGNETIC FIELD ALIGNED})}{I_R(\text{RANDOMLY ALIGNED})}$

CONTRAST RATIO (CR)

MICROTUBULES CONCENTRATION IN GLYCEROL (WT%)
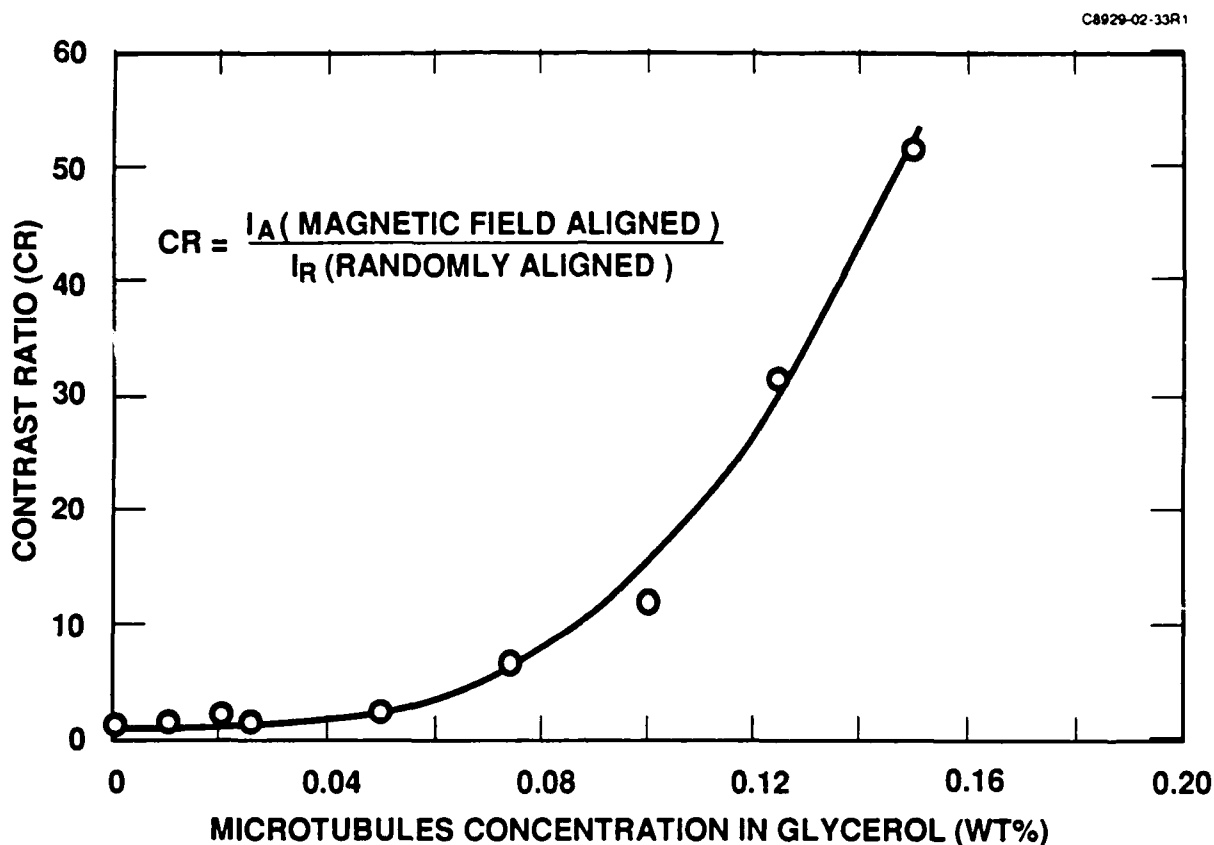
Figure 8-3. Contrast ratio for transmission of H-field aligned and unaligned microtubules as a function of concentration.

The effect of a E-field alignment on the pattern of laser light scattering was also studied for a dispersion of permalloy-coated microtubules (0.07 wt%) in paraffin oil wax (Fluka PW76234). The experimental set up is shown in Figure 8-4, where the cell was approximately the size of a 30 GHz waveguide. When a lateral field was applied, the microtubules were aligned in the field direction across (perpendicular to) the direction of the incident laser beam. The different scattering patterns with and without the field (400 V, 60 Hz) are shown in Figure 8-5. This experiment confirmed that the E-fields used in our microwave experiments (Sections 10 and 11) were adequate for alignment of the metalized microtubules in this fluid.
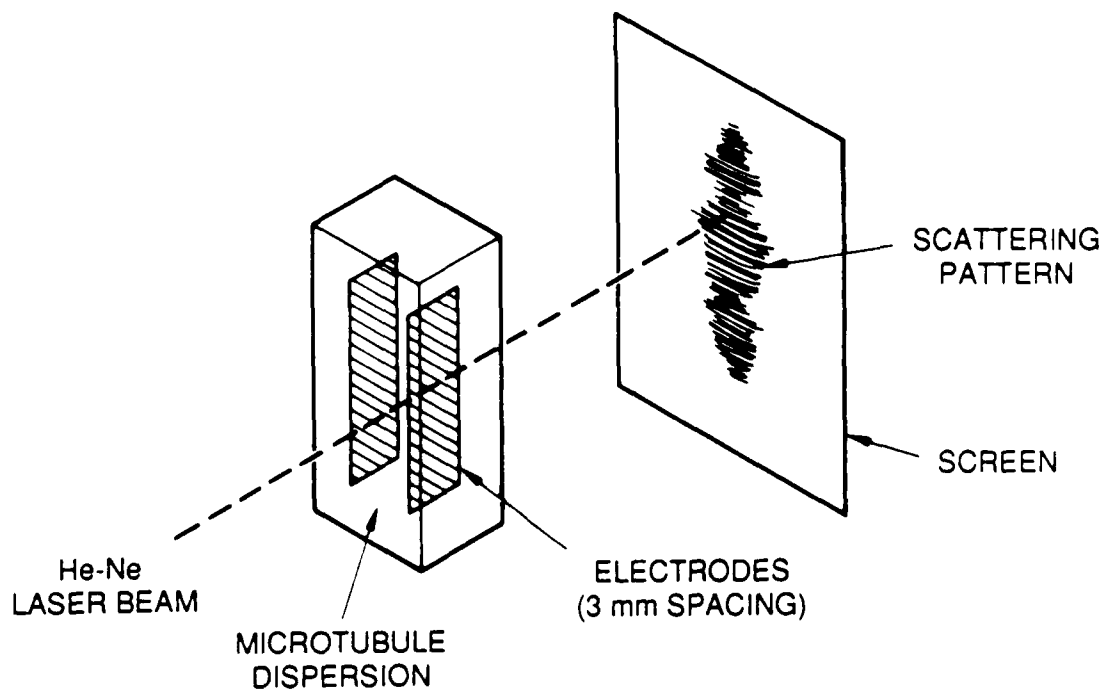
Figure 8-4.   Experimental set up for E-field modulation of light scattering patterns.

E = 0   **E = 400 V, 60 Hz**
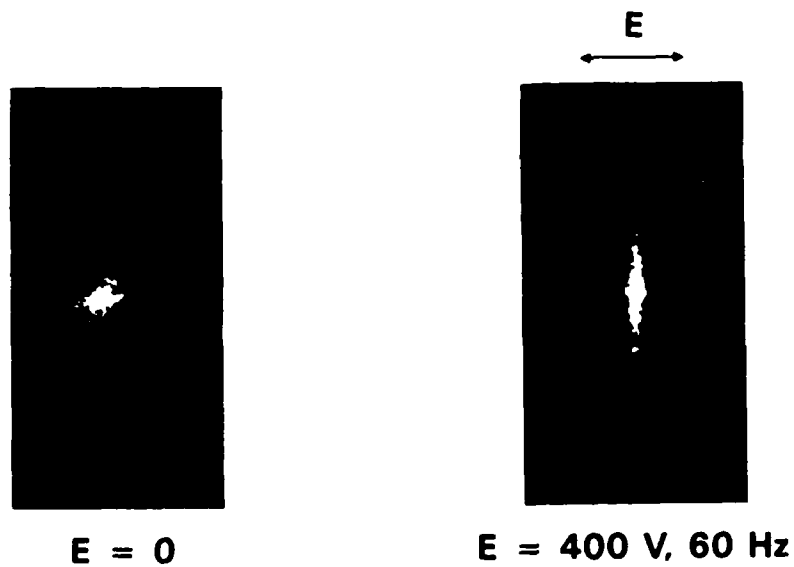
Figure 8-5.   Effect of E-field on scattering pattern of microtubule dispersion.

SECTION 9

LOW FREQUENCY DIELECTRIC CONSTANTS

Dielectric constants of a system of metallic particles dispersed in dielectric host medium are function of the concentration, geometrical shape, orientation ` nd conductivity of the metalic particles. The low frequency dielectric constants of aligned metalized microtubule composite media were measured by using a standard capacitor bridge. A samples of permalloy-coated microtubules (0.25 wt%) were suspended in liquid paraffin wax oil, whose dielectric constant is constant and independent of frequency at low frequency. These were used to fill the space in a cell between the electrodes of a calibrated parallel plate capacitor, which was rotated in a 2 kG magnetic field to align the microtubules either parallel or perpendicular to the small E-field used to measure the capacitance of the cell. The dielectric constants $\varepsilon_{//}$ and $\varepsilon_{\perp}$ (long axis of microtubules parallel and perpendicular to the small E-field between the capacitor plates, respectively) were measured from 100 to 10^4 Hz for two different samples with average microtubule lengths of 10 and 32 μm, respectively, as shown in Figure 9-1. As expected for aligned elongated electrically conducting particles, $\varepsilon_{//}$ is greater than $\varepsilon_{\perp}$ and the dielectric anisotropy $\Delta\varepsilon = \varepsilon_{//} - \varepsilon_{\perp}$ is large (in the range of about 0.1 to 0.5) and is larger for the longer microtubules, as shown in Figure 9-2, which shows the calculated maximum birefringence (Δn) which could be expected from these dispersions. As indicated in Figures 9-1 and 9-2, $\varepsilon_{//}$ and $\Delta\varepsilon$ decrease at increasing frequency, but we do not know the reason of the dispersion of $\varepsilon_{//}$ in this low frequency range.
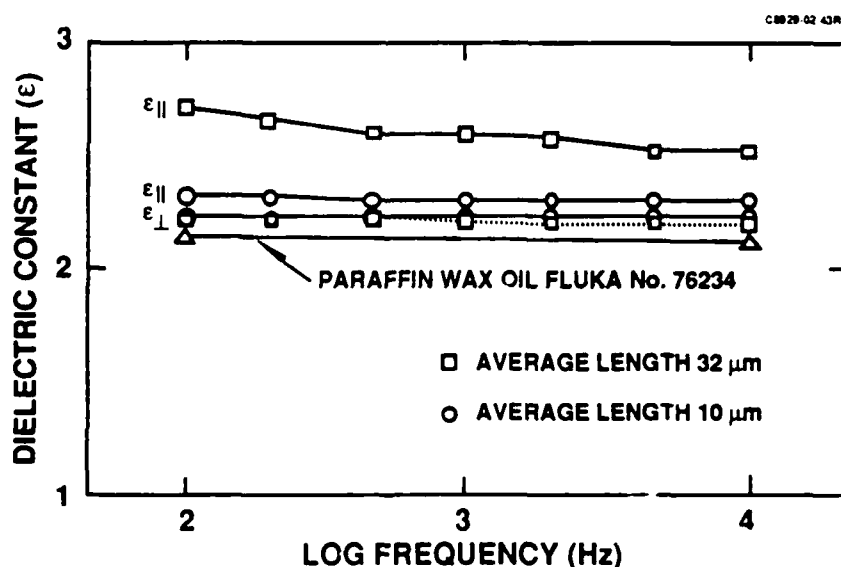

Figure 9-1.   Dielectric constants of permalloy-coated microtubule dispersions (0.25%).
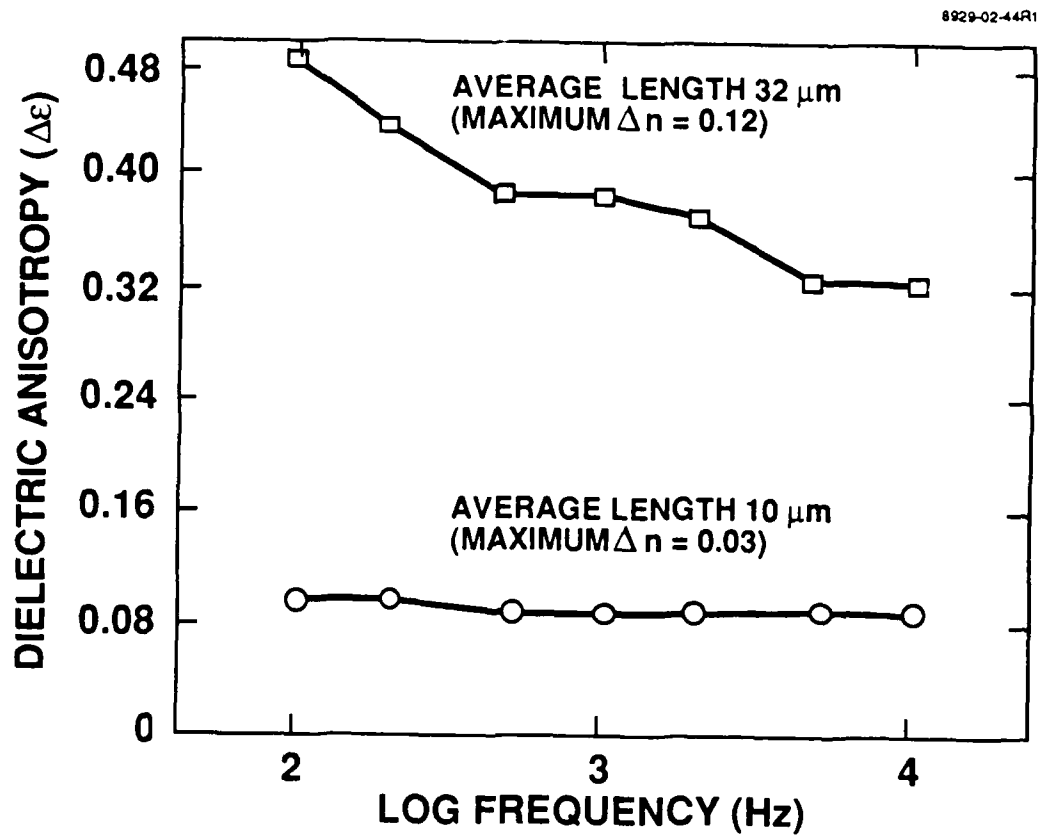
Figure 9-2.   Dielectric anisotropy of microtubule dispersions (0.25%) in Fluka 76234.

SECTION 10

MICROWAVE PHASE MODULATIONS: ISOTROPIC FLUID HOSTS

10.1   STUDIES AT 94 GHz

A 94 GHz microwave (more specifically, millimeter wave) phase bridge, shown schematically in Figure 10-1, was used to measure the phase retardation of the samples. The power from the Gunn oscillator passed through an isolator and an attenuator, and was split into two arms through a 10 dB directional coupler. One arm had a variable attenuator while the other had a 360° phase shifter and a sample cell. The power from the two arms was recombined through another 10 dB directional coupler and the output power was read by a diode detector. The 360° phase shifter and the attenuator were used to match the relative phase and power between the two branch to obtain a null output from the diode detector. The sample cell, consisting of a section of a vertical wave guide that was sealed at one end with transparent tape was placed in one branch of the apparatus. The experimental set up was sensitive to about ±2° of phase shift, but was not very sensitive for absorption loss measurements due to uncontrolled internal reflection of microwave in the waveguide and components. In these experiments, the metalized microtubules were suspended in Fluka PW76234 paraffin wax oil, which is a low loss isotropic fluid with a viscosity of 180 cP, and all of the anisotropic properties observed were due to the geometric shape and orientation of the microtubules. Magnetic fields were used to align the microtubules in the sample cell. A pair of horseshoe permanent magnets with long rectangular pole pieces provided an extended area of uniform aligning field perpendicular to the axis of the waveguide. A 10 cm long air core solenoid slipped over the waveguide was used to provide an aligning field along the axis of the waveguide. The magnetic field strengths at the sample cell area of the permanent magnet and the electromagnet were 2 kG and 0.2 kG, respectively, which appeared to be sufficient to completely align microtubules. These magnetic fields were used to obtain microtubule alignment in the three basic directions diagrammed in Figure 10-2, namely transverse to the microwave propagation direction and either parallel or perpendicular to the microwave electromagnetic field polarization, and longitudinal in the direction of the propagation.

The phase retardation of a randomly aligned (isotropic) composite fluid was measured using a known volume of a sample consisting of 0.22 wt.% permalloy-coated microtubules suspended in paraffin wax oil (Fluka PW76234) and placed in the sample cell waveguide. The corresponding phase retardations as the function of the column height (or optical path, d_{op}) of the sample are shown in Figure 10-3. The phase retardation P of a polarized electromagnetic wave

travelling through a medium with refractive index n and optical path length d_{op} is given by Eq. (12).:

$$P = 2\pi n d_{op}/\lambda. \tag{12}$$

The effective refractive index of the randomly aligned sample in Figure 10-3 was n = 1.58.
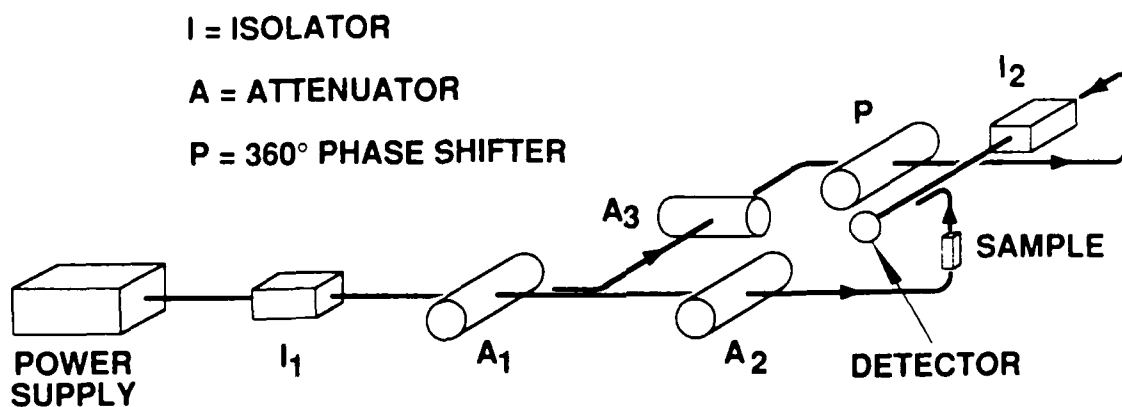

Figure 10-1.   Diagram of phase shift bridge for measurements at 94 GHz.
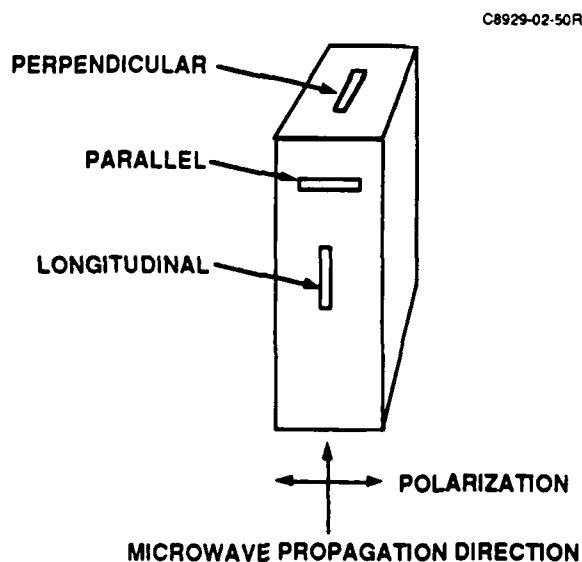
Figure 10-2.   Diagram labeling microtubule alignment directions in a waveguide.

47
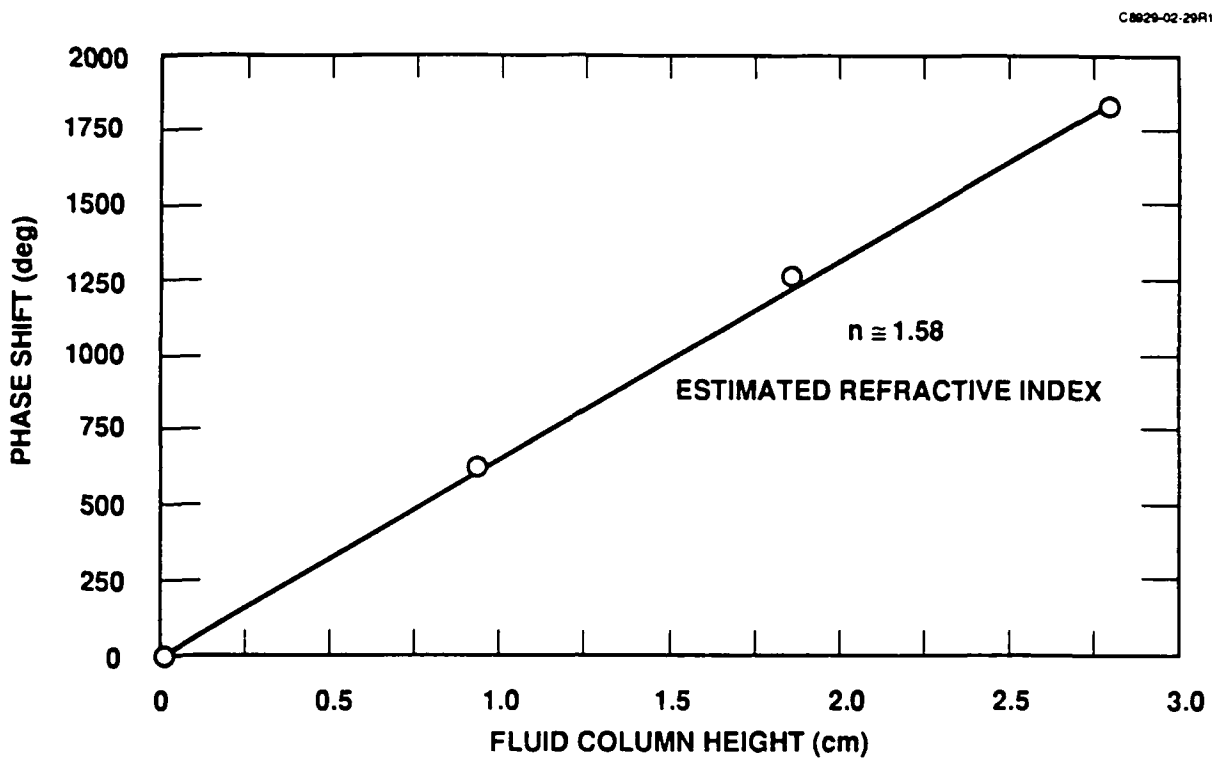
Figure 10-3. Refractive index determination of randomly aligned permalloy-coated microtubules (0.22 wt.% in Fluka PW76234) by phase shift measurements.

The external field modulated phase shift at 94 GHz was measured for a sample of 0.23 wt.% permalloy-coated microtubules (10 μm, average length) suspended in paraffin wax oil. The relative phase retardations of the sample column were measured as the microtubules were magnetically aligned parallel or perpendicular to the microwave field polarization (transverse-∥ and transverse-⊥, respectively), or along the microwave propagation direction in the waveguide (longitudinal). Figure 10-4 shows the relative phase shift in degree ($\Delta\theta$) as a function of column length for switching the alignment between three modes, namely: from transverse-⊥ to transverse-∥, from random to transverse-⊥, and from random to longitudinal. The relative phase shifts of random to longitudinal and random to transverse-⊥ were the same, within experimental error. This indicates that even though the permalloy-coated microtubules have ferromagnetic properties, they do not interact with the B-field vector of the microwave. The birefringence, calculated by Eq. (13) perpendicular to parallel alignment, was $\Delta n = 0.02$ for this sample.

$$\Delta n = n_e - n_o = \Delta\theta\lambda/2\pi d_{op} \tag{13}$$

48
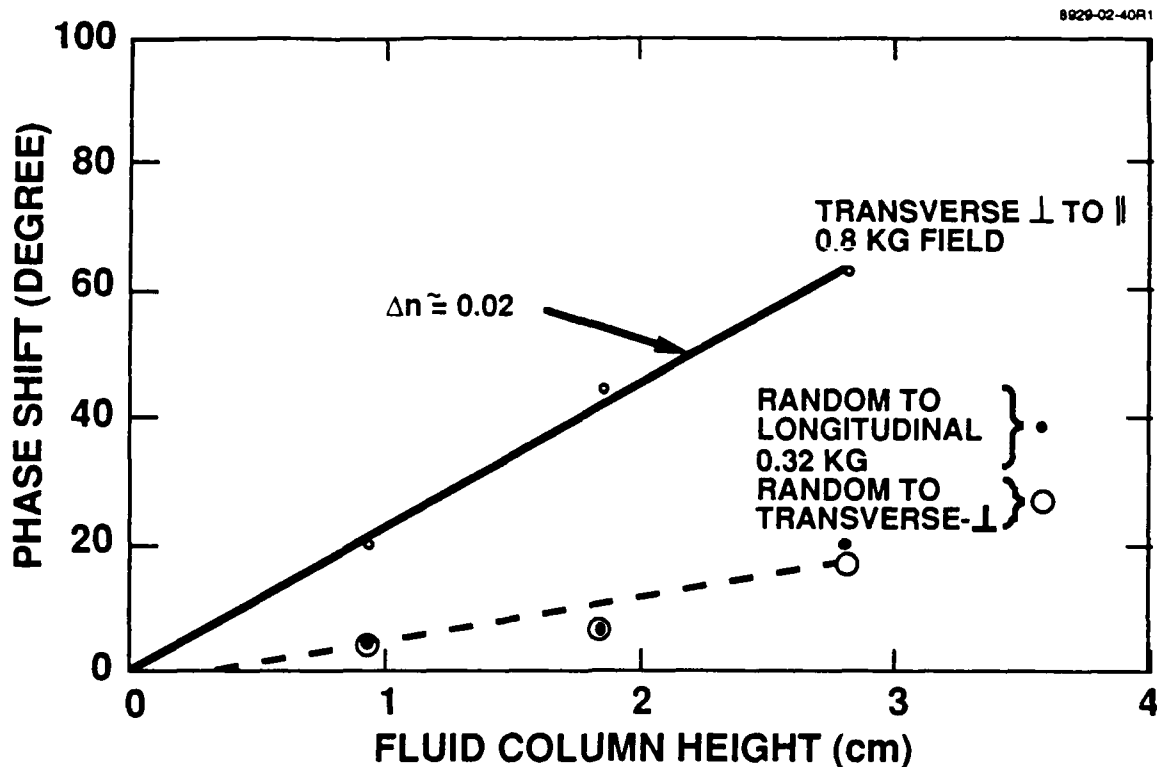
Figure 10-4. Phase shift changes at 94 GHz as a function of H-field alignment of permalloy-coated microtubules (0.23 wt.%).

The effect of the length of the microtubules on the phase retardation was also investigated. The metalized microtubules can be broken down into shorter lengths through violent mechanical agitations or sonication. To ensure consistency of data, a 0.4 wt.% sample of permalloy-coated microtubules with an average length of 40 μm was suspended in paraffin oil and divided into two portions: one portion was used without any further treatment, while the other portion was sonicated for half an hour. The average length of microtubules in this sonicated sample was 12 μm. The relative phase shift from transverse-$\perp$ to transverse-$/\!/$, modulated by external magnetic field, versus the microwave path length was measured at 94 GHz and is shown in Figure 10-5. The birefringence Δn of these samples was calculated to be 0.044 and 0.024 for the 40 and 12 μm microtubules, respectively. Figure 10-5 also shows results from the same base samples diluted to one-half their initial concentration with added Fluka PW76234, and these showed about half the birefringence, with Δn values of 0.024 and 0.011 for 0.2% concentrations of the 40 and 12 μm microtubules, respectively. Based on the above data of Δn versus length the empirical dependence of Δn on the particle length L was approximately $\Delta n = L^{0.5}$. If these microtubules are approximated as a metal prolate, it can be shown that the polarizability along its

49

semi-major axis (a) is approximately, $\alpha_a = a^3$, and the birefringence would be given by equation 14, in which Δn would have an a^3 dependence.

$$\Delta n = 2\pi n_0 N a_3 \qquad (14)$$
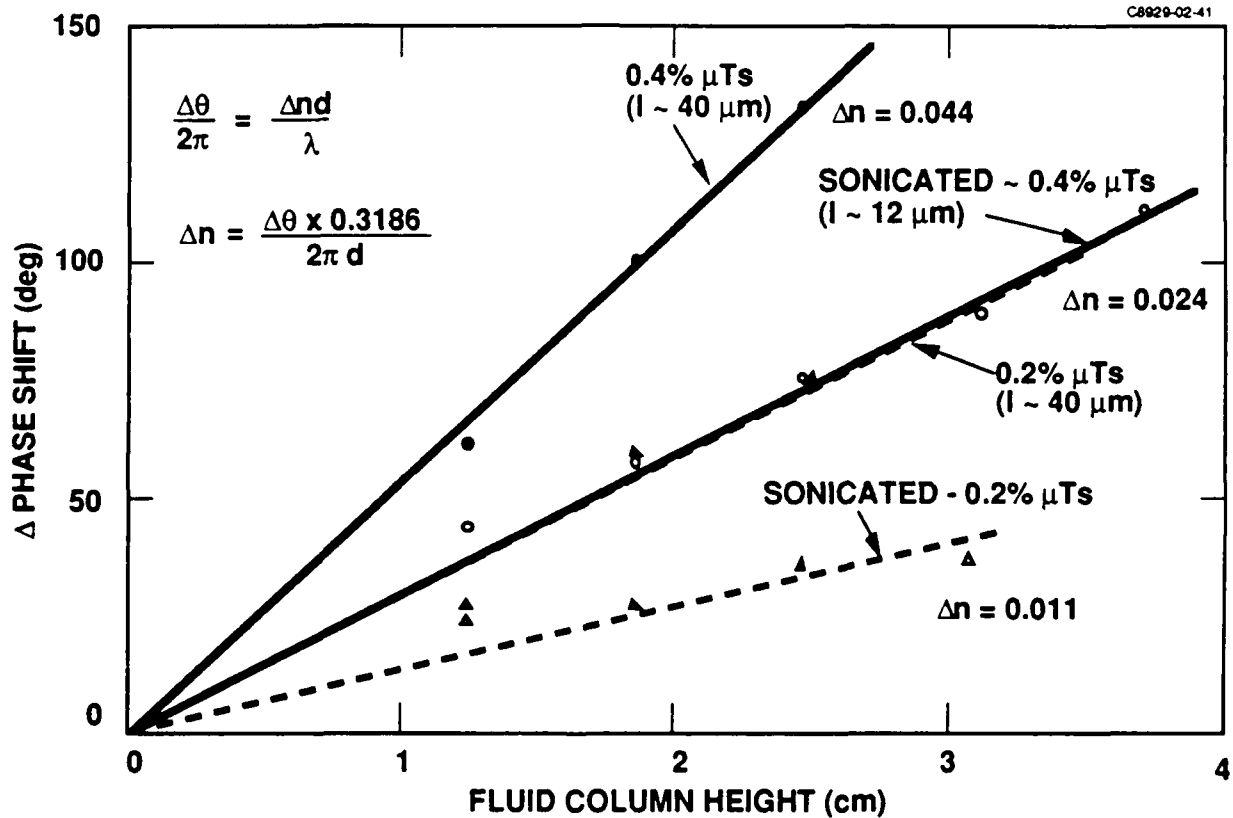

Figure 10-5.   Microtubule length and concentration effects on 94 GHz phase shift.

Both experiment and theory show that Δn increases as a function of particle length, but the power dependence is very much lower in case of the experimental data. This may be related to the distribution of particle sizes in the microtubule samples, or it may indicate that the metal coatings

50

are not continuous in the longer microtubules, or that the solid prolate approximation is not very appropriate for these hollow, cylindrical, double-walled microtubules.

10. 2 STUDIES AT 30 GHz

The microwave bridge apparatus for phase shift studies at 30 GHz is diagrammed in Figure 10-6, and it was very similar to the set up used at 94 GHz. A major difference is that we made a sample cell in which the microtubules could be oriented with an applied electrical field. In order to apply an electric field parallel to the polarized E-field vector of the propagating microwave, two opposite faces of the sample cell waveguide were modified into electrodes. The electrodes were insulated electrically from the rest of the waveguide. Figure 10-7 shows a diagram of the modified sample cell waveguide. The empty modified sample cell waveguide has an estimated insertion loss of about 5 dB. A variable step up transformer was used to obtain a maximum of 950 V (60 Hz) which could be applied across the electrodes to align the long axis of the microtubules parallel to the propagating microwave E-field vector. For nearly all experiments, an applied voltage of about 700 V, corresponding to a field strength of about 2400 V/cm, was used. With this field it was possible to completely align the microtubules in about 5 seconds, and to have consistent phase shifts over many on/off cycles. Continuous on/off cycles (10 seconds periods) of the field for more than two minutes began to cause irreversible field induced clustering in the sample. Experiments also indicated that applied fields above 3500 V/cm rapidly induced aggregation of the microtubules in this sample cell waveguide. In this cell the length of the electrodes was 3.9 cm along the axis of the waveguide, hence the modulated microwave path length was also 3.9 cm with a completely filled cell. Electric field modulated phase shifts were measured at 30 GHz with using a base sample with 0.29 wt.% of nickel-coated microtubules (average length of 10 µm) suspended in paraffin wax oil. The cell was filled to a level above the electrodes and the relative phase shift was measured when switching between parallel and perpendicular alignments by the applied electrical or magnetic fields. A voltage of 700 volts applied across the electrodes oriented the microtubules parallel (to the microwave E-vector), while a 1 kG field from a permanent magnet pair was used to orient the microtubules to a transverse-perpendicular (to microwave E-vector) alignment. The base sample was diluted and the experiments repeated. The experimental data of relative phase shift, and the corresponding calculated birefringence at 30 GHz, were directly proportional to the concentration, as shown in Figure 10-8. Other experiments indicated that the birefringences induced by the electric or by magnetic fields are consistent to each other.
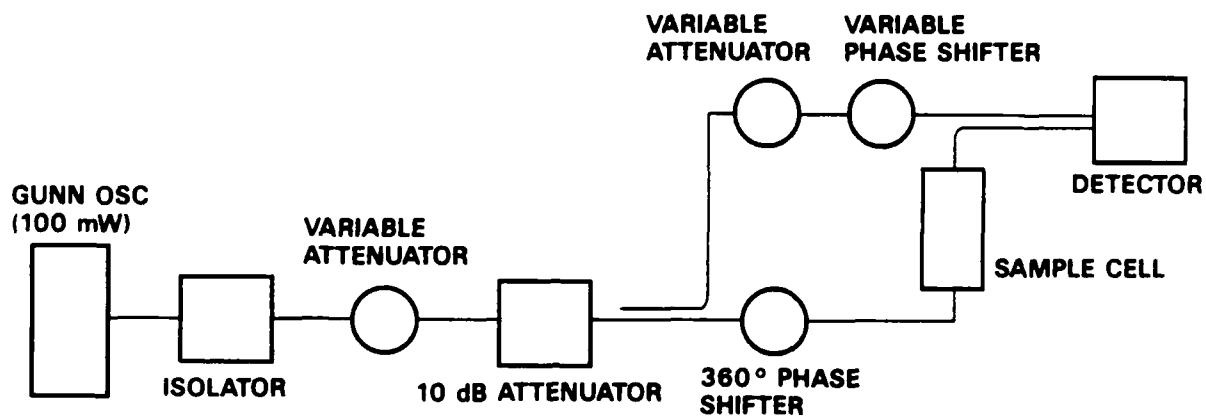
Figure 10-6. Experimental phase bridge set up for 30 GHz phase shift studies.

30 GHz WAVEGUIDE SECTION
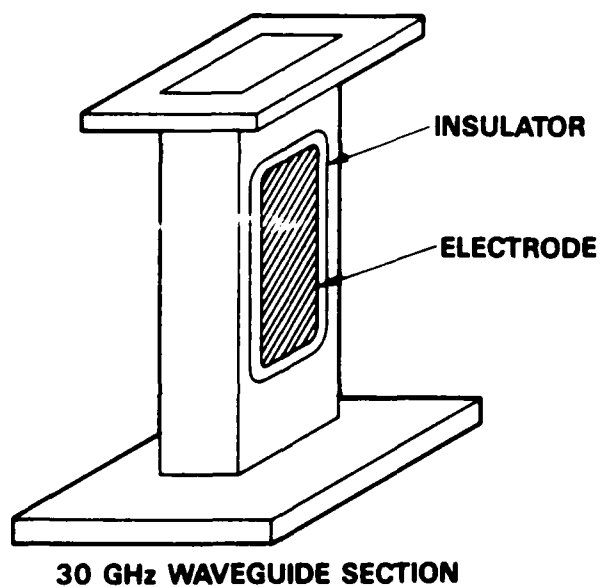
Figure 10-7. Modified waveguide cell with electrodes to orient microtubule dispersions.
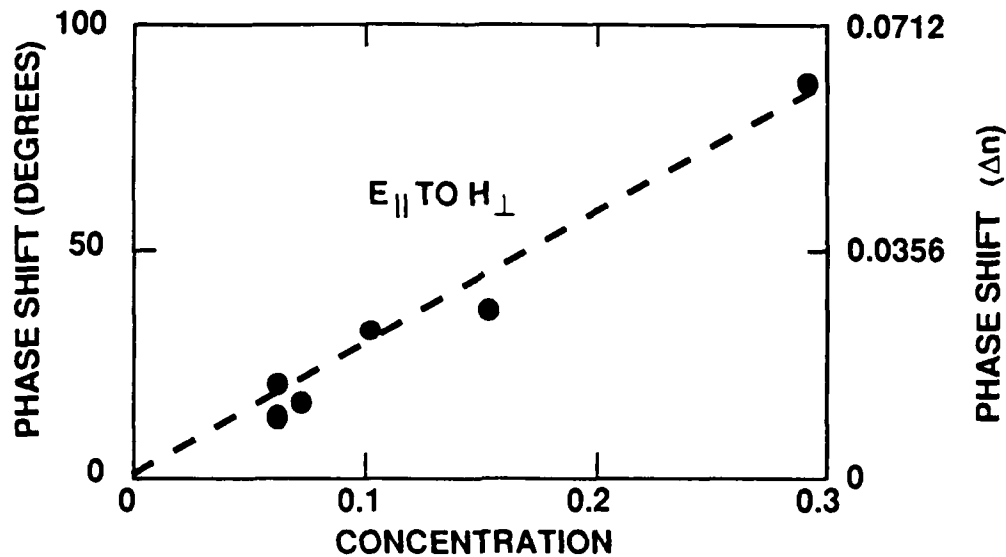
Figure 10-8. Phase shift and birefringence of Ni-coated microtubules in Fluka PW76234 at 30 GHz, by switching between orthogonal E- and H-fields.

10.3 MICROWAVE ABSORPTION LOSS

For most applications, the absorption loss of a composite dielectric medium should be small. The total insertion loss of a column of Ni-coated microtubules suspended in paraffin was oil was measured, as an indication of the loss suffered in an actual device caused by a column of active composite dielectric medium. The total insertion loss (reflection and absorption) of a column of 0.2 wt.% suspension of Ni-coated microtubules (20 µm average length) was less than 0.5 dB/cm when measured in the range of 16 to 26 GHz using a Wiltron scalar network analyzer. The total insertion loss of a similar column of the paraffin wax oil alone was 0.25 dB/cm. Thus the insertion loss of a 0.2 wt.% of the microtubules themselves was about 0.25 db/cm. This level of loss is considered acceptable for many applications.

53

SECTION 11

MICROWAVE PHASE MODULATIONS: ANISOTROPIC FLUID HOSTS

For most applications of active composites, it is important to have a large birefringence. The birefringence of an active composite medium consisting of suspended aluminium particles was reported[11] by previous investigators to be as high as $\Delta n = 0.08$. In the work described above in Section 10, it was shown that microtubule-based composites in isotropic fluids yield a birefringence of about $\Delta n = 0.05$. In theory (from equation 14 above), $\Delta n = 2\pi n_0 N a^3$ and Δn should be increased by increasing the concentration (N) or the particle length (2a). Attempts to increase the birefringence by increasing the concentration of microtubules often resulted in rapid aggregation effects. Experimentally, we found severe aggregation set in above 5 wt.% of metalized microtubules, even in very viscous isotropic hosts. Long length microtubules are difficult to prepare and are easily broken in handing. Also, we observed only an $a^{0.5}$ rather than an a^3 dependence of Δn on microtubule length.

We recently found that another way to increase the birefringence of a composite medium is to disperse metalized microtubules in a liquid crystal host. We had discovered, in the course of another research project, that liquid crystals had surprisingly high birefringence values (typically $\Delta n = 0.15$) in the millimeter wave region.[12] We found that the metalized microtubules dispersed well in liquid crystals and that this host reduced the field induced aggregation of the particles. We used the modified sample cell with electrodes, Figure 10-7, in the 30 GHz microwave phase bridge. Samples of Ni-coated microtubules in a liquid crystal (ROTN-404, viscosity of 120 cP) were aligned parallel to the microwave E-field vector by the application of 300 V (60 Hz) at the electrodes, and were aligned perpendicular to the microwave E-field vector by a pair of 3 kG permanent magnets. Figure 11-1 shows the birefringence phase shifts versus optical path lengths of two samples: (1) a pure liquid crystal, ROTN-404, and (2) a 0.2 wt.% dispersion of Ni-coated microtubules (10 μm average length) in the ROTN-404. From this experiment, the 30 GHz birefringences of the liquid crystal and the microtubule/liquid crystal composite were found to be 0.151 and 0.233 respectively. In this way, a high birefringence was obtained for a microtubule composite medium at a relatively low concentration of microtubules. In fact, the birefringence of this composite medium was higher than expected from the individual components. A 0.2 wt.% dispersion of the same microtubules in the isotropic fluid Fluka PW76234 had $\Delta n = 0.04$ (from the data in Figure 10-8). The sum of the birefringences of the liquid crystal ($\Delta n = 0.151$) and of 0.2 wt.% of microtubules in the isotropic fluid is 0.191, while a larger birefringence of $\Delta n = 0.233$ was measured for the liquid crystal composite with the same concentration of microtubules.
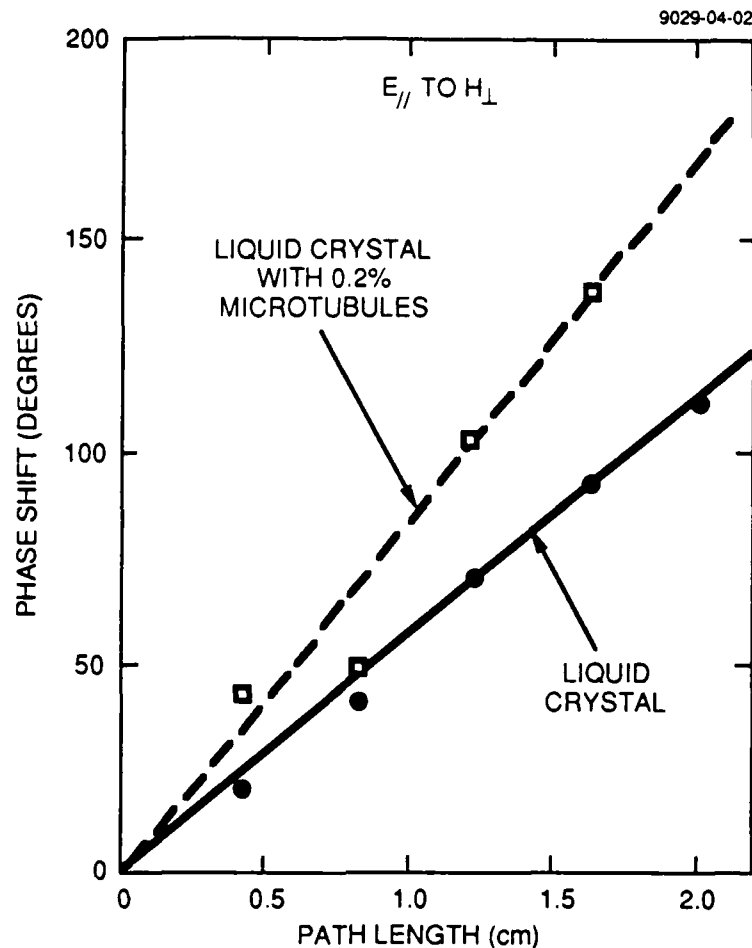
54

Figure 11-1. $E_{//}$ to $H_{\perp}$ phase shifts at 30 GHz of ROTN-404 and a dispersion of Ni-coated microtubules in ROTN-404.

Similar experiments were performed on these materials using H-field alignment in both directions (transverse-$//$ and transverse-$\perp$) to determine the phase shifts. Results as a function of path length are shown in Figure 11-2 for the liquid crystal alone and for three concentrations of the Ni-coated microtubules in this liquid crystal. A very high microwave birefringence of 0.28 was found for this composite with 0.6% microtubules. The experimental results as a function of microtubule concentration are shown in Figure 11-3 for the isotropic fluid composite as compared to the liquid crystal composite. The steeper slope of the latter plot indicates that the combination of microtubules and liquid crystals gives a somewhat enhanced birefringence. These studies on microtubule/liquid crystal composites are the basis for a patent application which has been filed.[13]
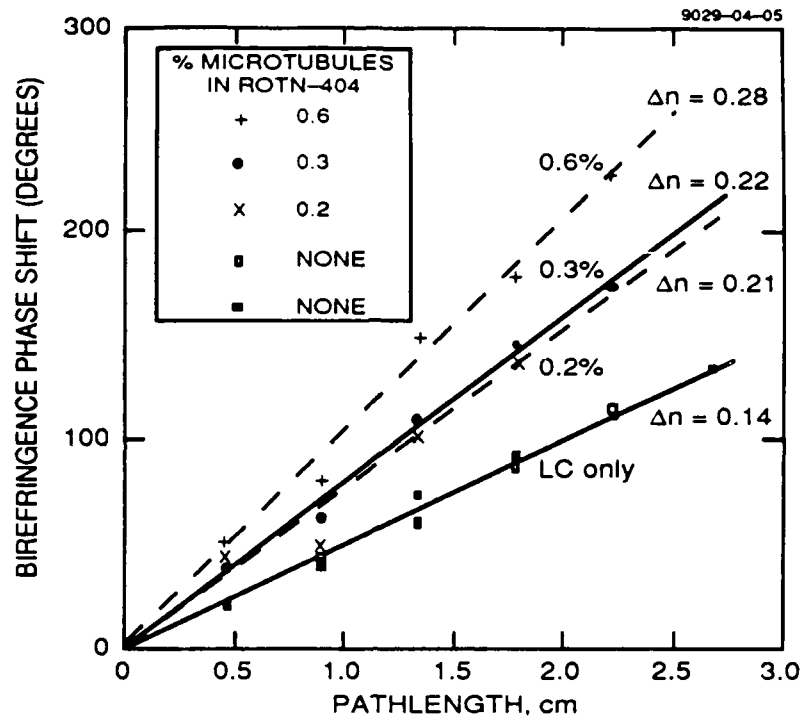
Figure 11-2.   Phase shift and birefringence at 30 GHz of microtubule/liquid crystal composites
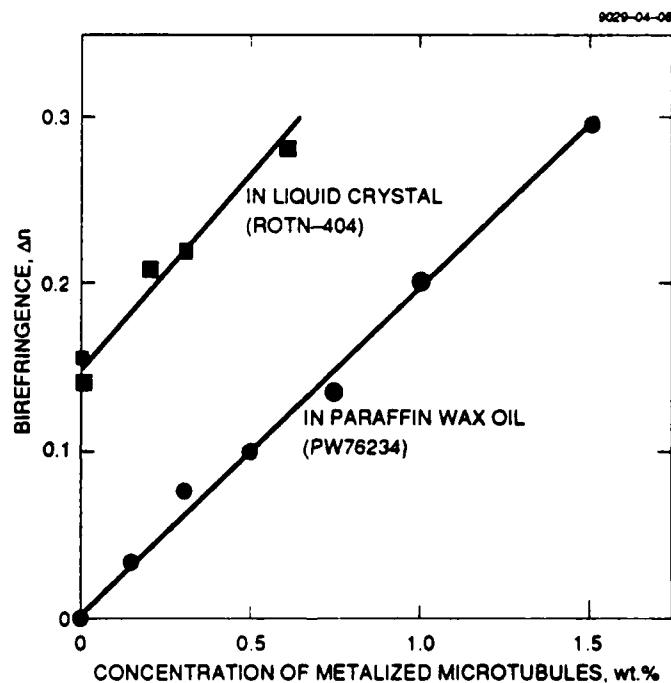of at various concentrations.

Figure 11-3.   Birefringence at 30 GHz of composites of Ni-coated microtubules as a function of
concentration.

SECTION 12

SOLID COMPOSITES WITH METALIZED MICROTUBULES

12.1 ALIGNED MICROTUBULES IN THIN FILMS

We found that we could make free-standing polymer films containing microtubules by UV-curing a dispersion in an optical cement (*e.g.*, ZLI-2060) between plates of Plexiglass. The cured film did not adhere to the Plexiglass and was easily separated. For example, a batch of permalloy-coated microtubules, which were strongly aligned by a magnetic field, was dispersed in ZLI-2060. A 127-μm-thick film of this between Plexiglass was uniformly aligned in a surface-parallel direction by a lateral H-field while it was UV cured. Good alignment directionality was retained in the resultant free-standing film, which showed strongly preferential scattering of a laser beam (632.8 nm) orthogonal to the microtubule alignment direction. Figure 12-1 shows a microscope picture of this free-standing film (which had some air bubbles on the surface) and the far field laser scattering pattern. This film did not show transmission polarization of light in the visible or IR region, because the concentration of microtubules was not sufficiently high to achieve spacing distances between parallel microtubules that were less than wavelength of the light.
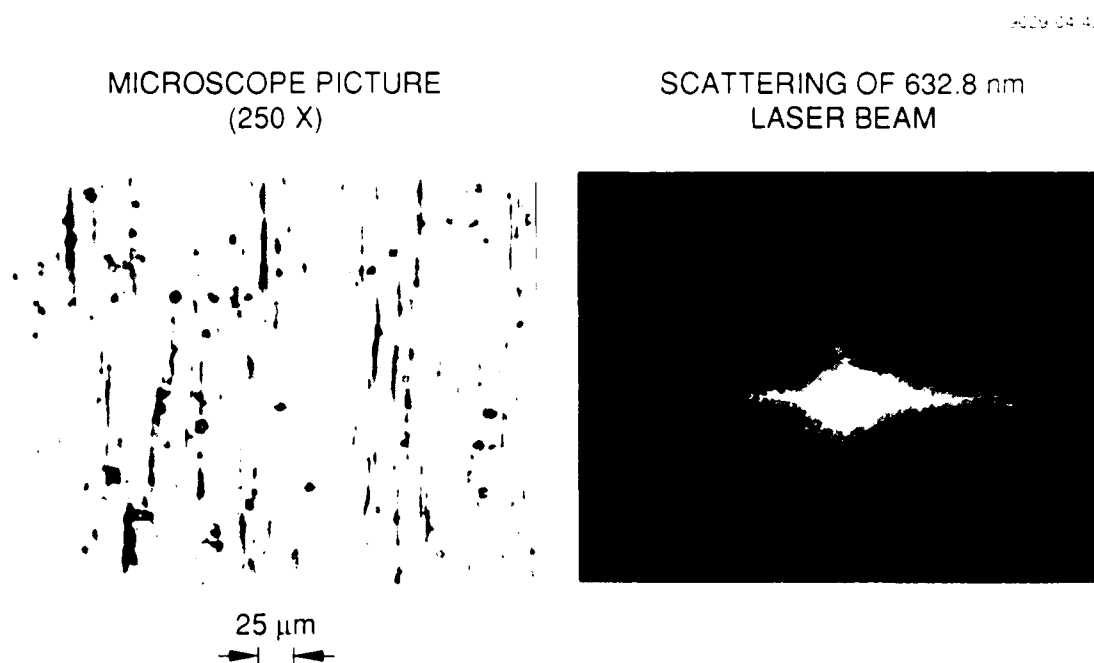
MICROSCOPE PICTURE
(250 X)

SCATTERING OF 632.8 nm
LASER BEAM

25 μm

Figure 12-1. Free-standing polymer composite film containing permalloy-coated microtubules uniformly H-field aligned parallel to the surface.

57

12.2 PATTERNED ALIGNMENT IN THICK FILMS FOR GRADIENT INDEX LENS

Lens-like alignment patterns were made in thick layer composites of Ni-coated microtubules in optical cements which were slowly UV-cured while under the influence of an inhomogeneous magnetic field. The technique consisted of curing the composite layer while it rested on top of a bar magnet, as diagrammed in Figure 12-2, in order to fix the magnetic field pattern as aligned microtubules in the solid polymer layer. The bar magnet used had a field strength of 0.6 kG, and a slow UV curing rate was used. For example, such a film 3x2.2x0.25 cm in size was made using 0.4 wt.% Ni-coated microtubules in Optistick 2060 with 5 minutes of UV curing.. To confirm the lens-like alignment of the microtubules, we examined the shape and intensity distribution of the scattered light from a transmitted laser beam (632.8 nm) as a function of the laser spot position across this composite structure. The results are shown in Figure 12-3, which shows pictures of the scattering pattern as well as the scattering intensity at various distances across the composite. The schematic diagram in the top of the figure indicates the type of microtubule alignment corresponding to the pictures at the indicated scattering intensity ratios. These results clearly indicated the expected lens-like variation in microtubule tilt direction across the width of the film.
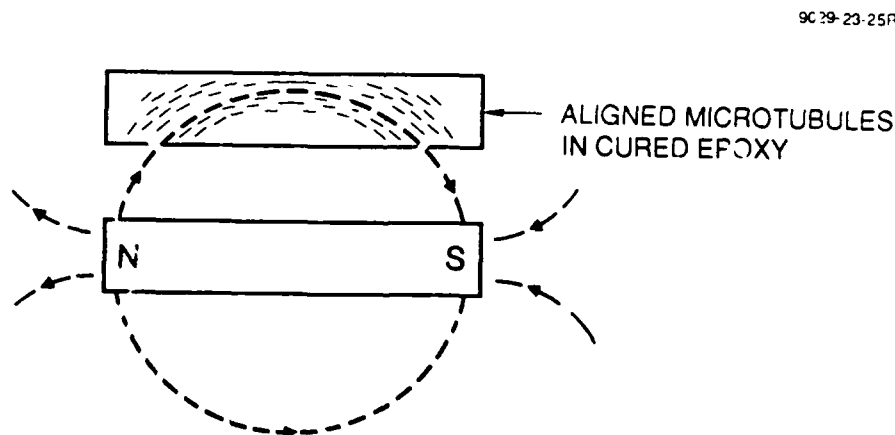
9C?9-23-25R1

Figure 12-2.   Method of forming a microtubule composite gradient index lens.
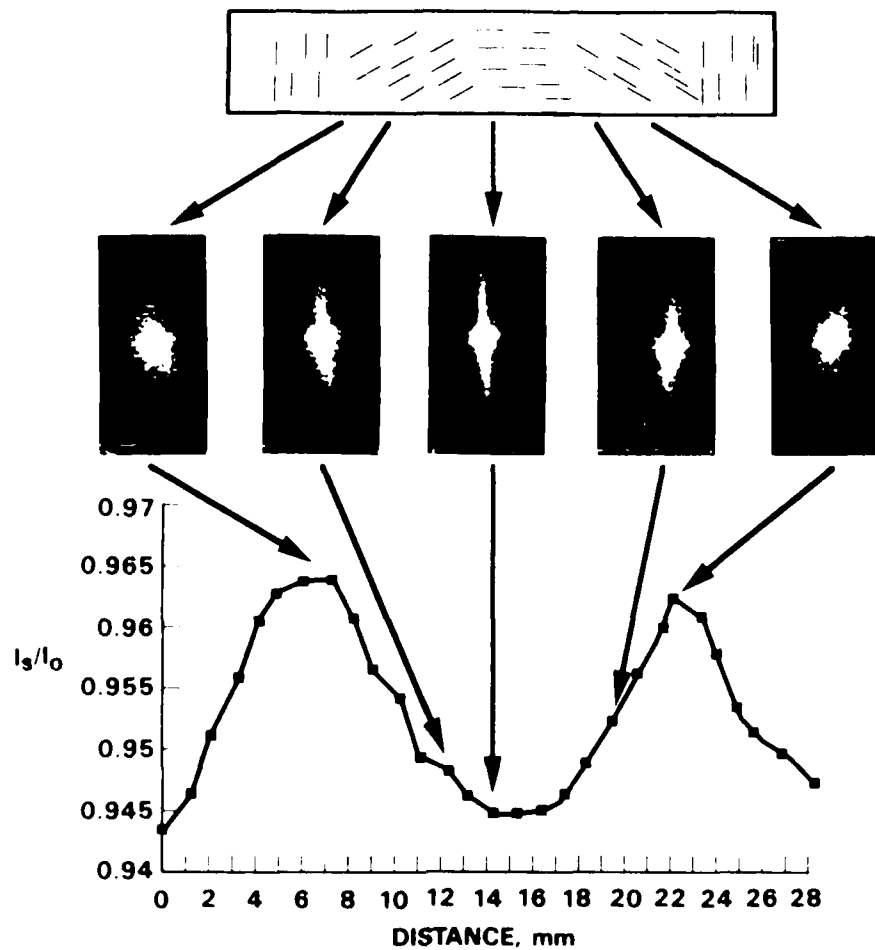
58

Figure 12-3.   Laser scattering by gradient index lens of microtubule alignment pattern.

A thicker (2 mm) composite gradient lens film of this type was made in the same manner with the same components, using 3 hr of low intensity UV curing. The effect of this lens on microwaves was examined with the experimental apparatus diagrammed in Figure 12-4. The lens was positioned in front of the transmitting microwave horn, and the distance (d) of the receiving horn was varied. The 94 GHz beam intensity picked up by the receiving horn is plotted as a function of the separation in Figure 12-5, which shows the difference between the absence and presence of the composite lens. The focusing effect of the lens appeared to be larger than its losses at horn separation distances of about 20 and 40 cm. (A very rough calculation indicated that this lens should probably have a focal length of about 63 cm.) Because the lens was only 2 mm thick, only a limited focusing effect was expected since the maximum phase shift difference from the edge to the middle of the lens would be about 5 to 10° for the concentration of microtubules used.
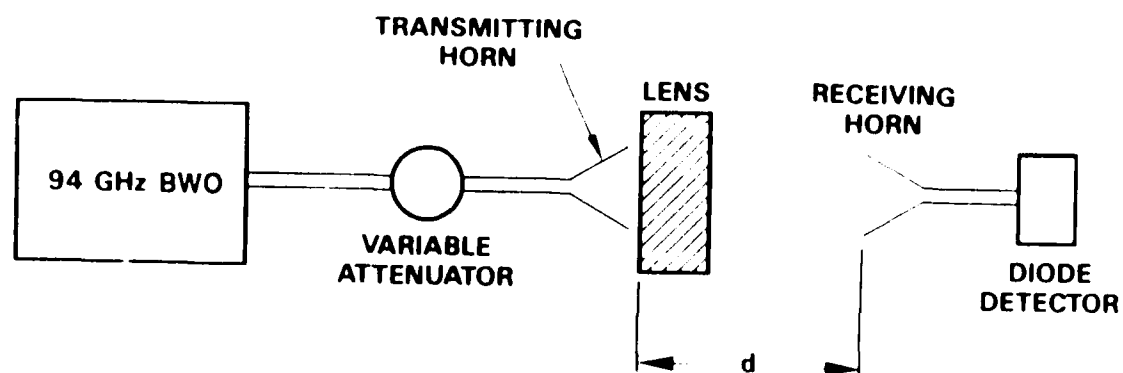
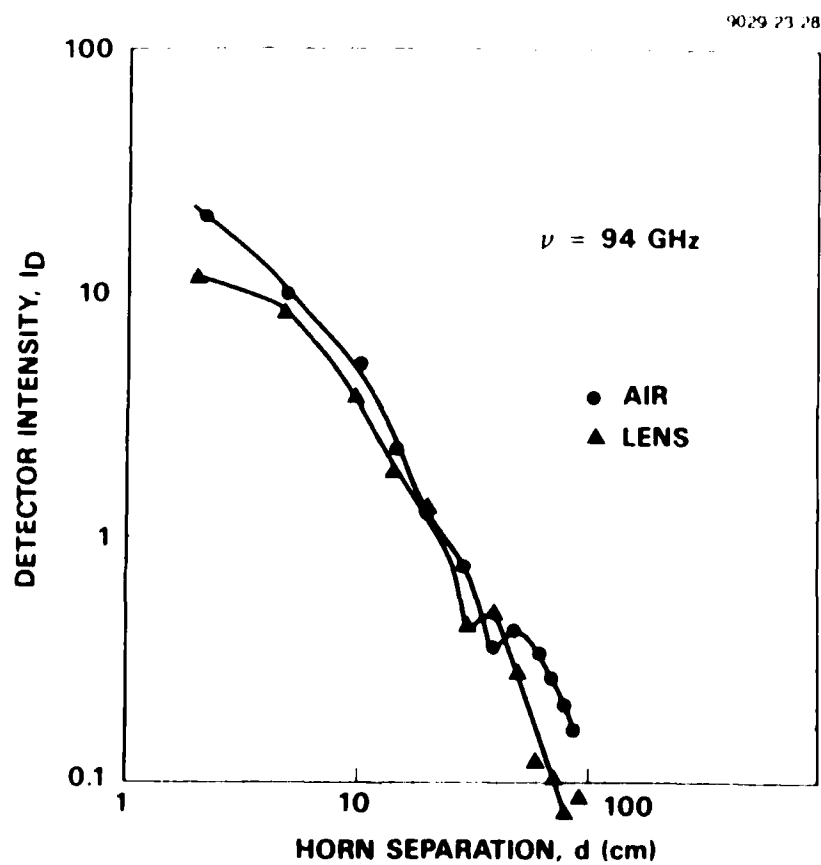Figure 12-4.   Diagram of experimental apparatus for microwave lens study.

Figure 12-5.   Microwave measurements on 2 mm thick gradient index lens.

12.3   STUDIES FOR ANISOTROPIC CONDUCTION IN THIN FILMS

As described above in Section 7.1, metalized microtubules in fluids were not only strongly oriented by applied electrical or magnetic fields, but also showed filamentation and clustering effects over a period of time which was a fairly short period at high fields and high concentrations. As a result of these observations, we investigated the concept of making anisotropic conductive polymer films based on obtaining surface-perpendicular filamentation of metalized microtubules through the depth of the films by applying transverse fields during polymerization or solidification. Most of our initial studies were made with Ni-coated microtubules UV-polymerized in either Norland NOA65 or in Merck Optistick 2060. Fabrication problems encountered when using electrical fields with about 50-μm-thick films included (1) flow misalignment of microtubules

during UV-curing as shown above in Figure 7-3, (2) incomplete curing when using microtubules higher concentrations of 2 to 3 weight percent, (3) burn spots from current arcing when using non-insulated electrodes, and (4) difficulties in separating free standing films. The problems of misalignment and incomplete curing were minimized by using slower polymerization rates (15 minute curing times) and lower microtubule concentrations in the 0.6-1.0% range. The problems of arcing and obtaining free-standing films were overcome by using Mylar sheets (254 μm thick) between the ITO-electrodes and the microtubule/monomer composite. (The Mylar acted as an insulator and as a release surface for the polymerized film.) For example, a good free-standing film was obtained in this manner using 1% microtubules in Optistick 2060 of about 50 μm nominal thickness, with 30 V applied (across across the Mylar sheets and microtubule composite) during UV curing with 10 mW/cm^2 (300 to 500 nm band, 100 W Hg-lamp.) Another example was a free-standing film made with 0.6 % microtubules in a composite about 130 μm thick, using the same conditions. We observed microtubule clustering in these films, but we did not observe good conduction through the films. From our subsequent work described below, we believe that this was because each microtubule in their clusters and at the surfaces was insulated by a thin coating of the host polymer.

Several additional experiments were carried out on films which were cured while a magnetic field was applied. In one of these experiments, diagrammed in Figure 12-6, the surface of the free-standing film (made with 0.6% Ni-coated microtubules aligned in Optistick 2060) was plasma etched to expose bare microtubules for electrical contract. SEM pictures of this surface are shown in Figure 12-7, in which the composite film was etched from 127 μm down to 104 μm thickness. Although these pictures show that the microtubules were clustered and were protruding vertically out of the surface of the film, there was not good conduction through the film.
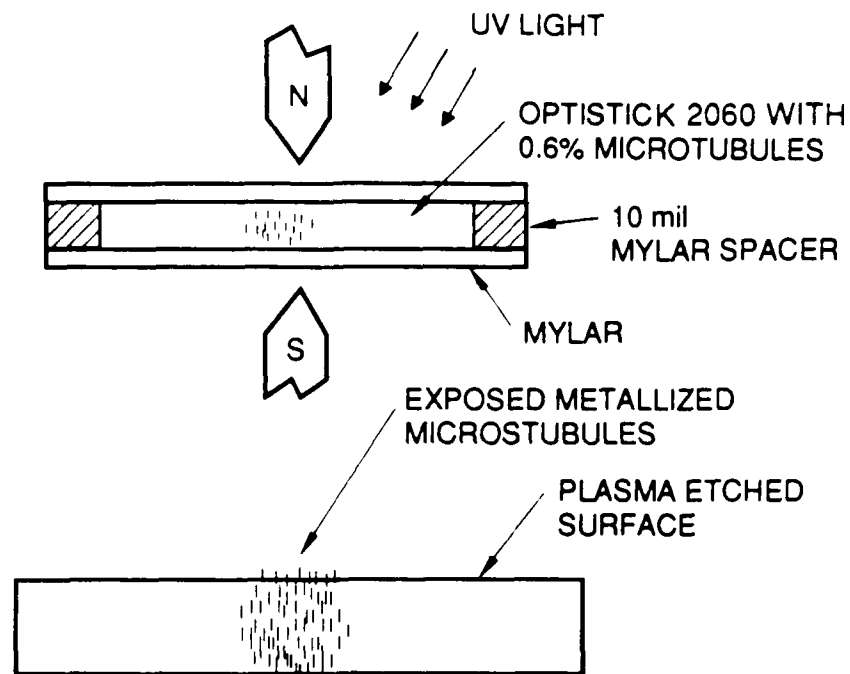
Figure 12-6. Diagram of H-field alignment of metalized microtubules in a free-standing film and subsequent plasma etching of the epoxy to expose the microtubules.
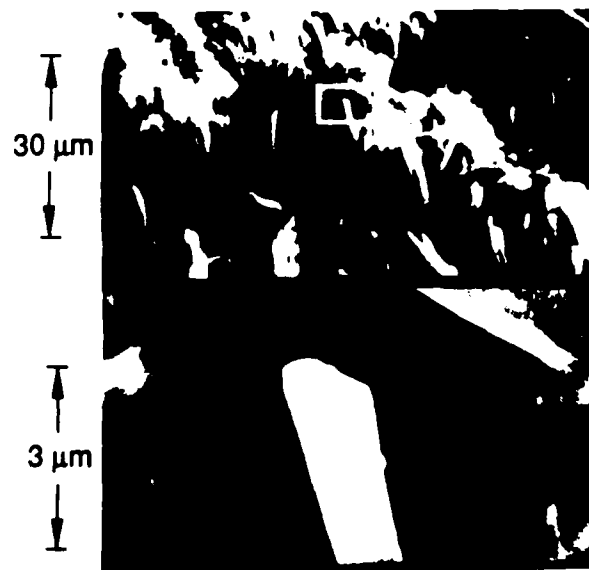
Figure 12-7. SEM pictures of surface-perpendicular metalized microtubules in an epoxy film after plasma etching.

In order to understand better what happened to aligned microtubules at a polymer surface, we performed the experiment diagrammed in Figure 12-8. Here a small block of poly(methyl methacrylate), PMMA, about 710 μm thick containing 0.8 % Ni-coated microtubules, was cast from a 20% solution of the polymer in methylene chloride by evaporation of the solvent while a transverse magnetic field was applied. The SEM pictures of the surface, also in Figure 12-8, showed individual microtubules protruding from the surface, but each was well covered by the polymer.

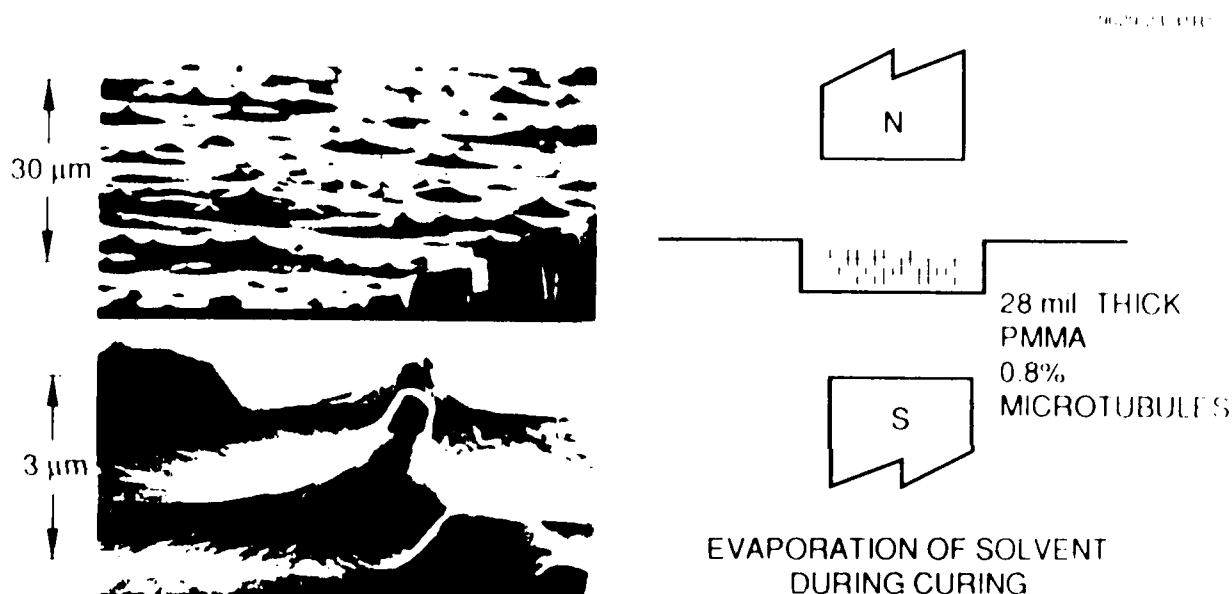
EVAPORATION OF SOLVENT
DURING CURING

Figure 12-8.   SEM picture of surface-perpendicular aligned metalized microtubules in a PMMA film made by solvent evaporation.

Finally, we did obtain anisotropic conduction through a thin free-standing (33 μm thick) composite film of magnetically aligned Ni-coated microtubules (2.2 wt.%, 10 μm average length, ranging from about 2-40 μm) formed in Norland NOA-65 by UV curing. There was conduction through the film, but not laterally along its surface. However, a radomly-aligned control film showed the same properties. This probably indicated that in both films some of the microtubules which were longer than 33 μm were transversely aligned and were exposed on each surface of the film. Because this effect appears to depend upon having a film thinner than some of the microtubules, which are available only in a distribution of lengths in a given batch, the resolution of this anisotropic conduction would not be expected to be as good as that obtainable by using uniform-size conductive spheres in films thinner than the diameter of the spheres.

SECTION 13

POTENTIAL MICROWAVE APPLICATIONS

13.1   SOLID COMPOSITES FOR MICROWAVE LENS AND WAVEPLATE DEVICES

We have shown that metalized microtubules, especially ones with ferromagnetic coatings, can be oriented in selected patterns in polymeric films which can have relatively low loss in the microwave-millimeter wave region. These oriented microtubule patterns can provide phase shift properties which are sensitive to the polarization direction of the microwaves. For example:

*   Waveplates:

Planar layer structures with uniform directional alignment of the microtubules can be made and used as a full waveplate or a quarter waveplate at selected microwave frequencies and polarizations.

*   Lenses:

Planar layer structures can be made as a gradient index lens, such as shown in the diagram in Figure 13-1, which can be used as a microwave lens which will focus one polarization and have little effect on an orthogonal one. Lenses are needed for applications such as for polarization splitting, to separate in-coming and out-going radar signals of different polarizations. This lens would focus an in-coming polarization to an off-axis position while not affecting an orthogonal out-going beam. These could be light weight devices would increase the efficiency of receiving in-coming signals by separating them from out-going signals, using a single unit transmitting/receiving antenna.

Both waveplates and lenses are particularly useful at high frequencies, such as 94 GHz and above, in systems which require transmission through atmosphere or in space, and to avoid the high loss incurred in waveguide transmission.
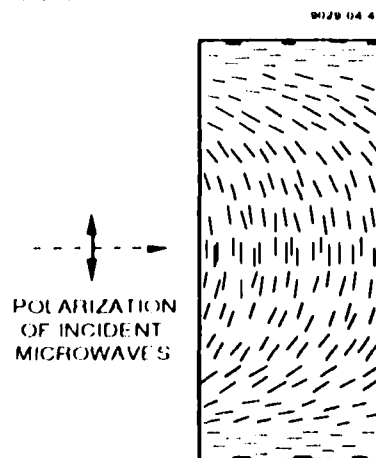

Figure 13-1.   Microwave gradient index lens configuration of microtubules aligned in a low loss polymer host.

13.2 DYNAMIC DEVICE CONFIGURATIONS AND APPLICATIONS

We have shown that applied fields (electric and magnetic) can be used to align dispersions of metalized microtubules, thereby inducing substantial phase shift changes in microwave devices. We have also shown that composite system dispersions of microtubules in liquid crystals have the highest reported birefringent values ever reported for fluids in the millimeter wave region, and that the phase shift of these composites can also be controlled with electric and magnetic fields. Based on our experience, some conceptual examples of dynamic operation of microtubule microwave devices are given in the following examples:

- Waveguide cross-field phase modulators:

Phase shifts can be modulated with an electric field applied across a waveguide cell containing a microtubule dispersion, as is shown above in Figure 10-7. It would also be useful to place these new phase shift materials in devices in which the media can be aligned in different directions by using two different orthogonal fields, as diagrammed in Figure 13-2. This is shown here as two different electric fields, but either or both of these fields could also be magnetic when the microtubules have ferromagnetic conductive coatings. (The magnetic field could be from permanent magnets or from electro-magnets.) The applied fields could be programmed to switch the phase shift back and forth, or to scan it back and forth, or to adjust it to a given value. Such devices could be the basic type element in electronically controlled phased array systems for microwave beam modulation or beam steering. When inexpensive microtubules are available in stable dispersions, such phase shifters could replace expensive ferrite or diode phase shifters with much less expensive devices, thereby making it economically feasible to incorporate radar systems in much larger numbers on widely deployed vehicles and weaponry where it might not otherwise be possible to do so.

- Waveguide flow aligned phase modulator:

Another device design which could utilize existing microtubule dispersions is a flow type waveguide phase shifter cell, as diagrammed in Figure 13-3. The flow through the cell would align the microtubules in the flow direction, longitudinal with respect to the microwave propagation direction. This flow alignment cell could be used with microtubules in isotropic fluids, and would also work well with the liquid crystal composites in which both the liquid crystal and the microtubules would be flow aligned. Such flow cell would have a minimum phase shift until it was increased by an applied electrical cross field that would reorient the microtubules (and liquid crystals of positive dielectric anisotropy) toward the direction of the applied field (which would be in the direction of the microwave polarization in the waveguide

65

cell). When the applied E-field is turned off, the flow would rapidly realign the microtubule system back to the longitudinal direction. Flow alignment for suspension composite media provide the advantages of both improved dispersion of particle suspensions, and of relaxation due to flow alignment forces.
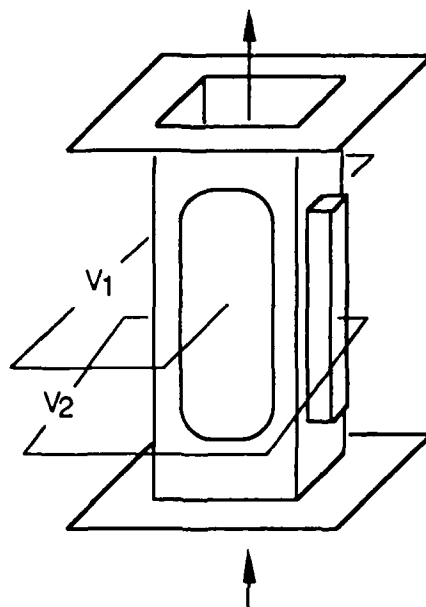
9029-04-44

Figure 13-2. Cross-field-switching phase-shift-modulator microwave waveguide cell.
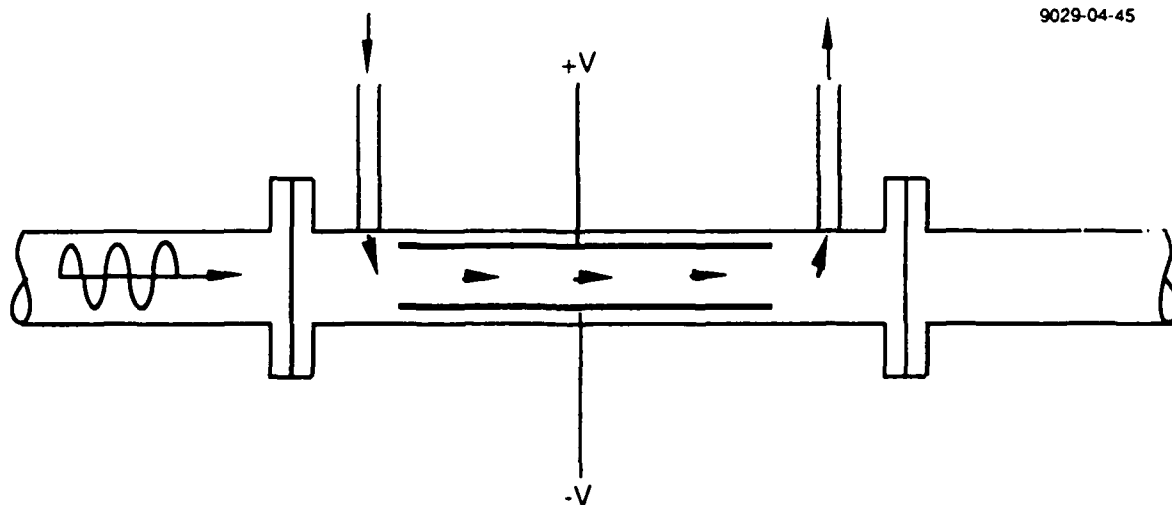
9029-04-45

Figure 13-3. Flow cell with field modulation in a microwave waveguide phase shifter.

66

- Traveling wave scanning slot array antenna:

One type of device configuration for utilizing the phase modulation effects obtained by field modulation of microtubule dispersions is a traveling wave scanning slot array antenna, as diagrammed in Figure 13-4 for an E-field modulated device. The microwave beam entering the cell from the left side of the cell shown in Figure 13-4(a) would have its polarization vector aligned vertically in the shorter dimension of the cell. The E-field, applied from the electrodes shown in Figure 13-4(b) cross-section, would be used to align the metalized microtubules parallel to the microwave polarization direction. If no other dynamic effects are used when the E-field is removed, the relaxation back to the initial state (random alignment) would be quite slow for microtubules dispersed in isotropic fluids. Small microtubules dispersed in liquid crystals would return more quickly to the initial surface-alignment state (*e.g.*, longitudinal alignment), if the cell walls are close enough together to control the bulk alignment of the composite. Such a slot array antenna could also be used in other configurations such as the E-field modulated flow cell (Figure 13-3), and also in a variation of the cross field cell (Figure 13-2) in which the slots were not blocked by the cross field electrode or magnet. Slot array antennas with microtubule phase shifters could be operated as both sending (beam sweep output) and receiving (beam direction receiver) devices. There is a great need for rugged, low cost millimeter wave antenna for operation a relatively low microwave power, and this type of traveling wave scanning slot array antenna could fulfill these requirements.
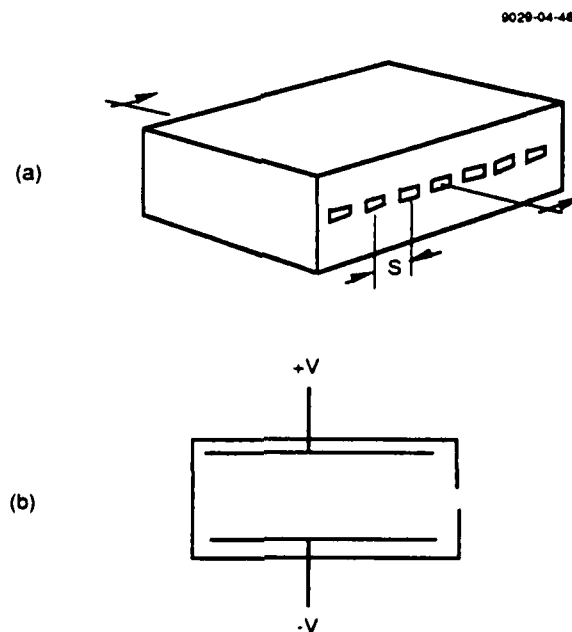

Figure 13-4.   E-field-modulated traveling wave slot array antenna.

67

• Large area phase modulator:

A layered electrode structure with electrodes more closely spaced than the walls of a waveguide, as illustrated in Figure 13-5, would permit operation of the microtubule dispersions at lower voltages, and would provide faster return of liquid crystal composites to a surface-parallel alignment off-state. This structure can be used in slot array antennas (replacing the electrodes shown in Figure 13-4b), in radome configurations as illustrated in Figure 13-6, or in beam steering devices as illustrated in Figure 13-7. The radome diagram in Figure 13-6(a) shows it unactivated, while in Figure 13-6(b) the radar beam is deflected by the phase modulator. For example, this could be used to keep a radar beam pointed in a specific direction by compensating for the rolling motion of a shipboard radar platform. The multiple electrode design in Figure 13-7 provides closely spaced electrodes which can be placed in front or inside the flare of a waveguide horn, where it could be activated for radar beam steering applications. The availability of such large area phase modulators could open a new area of millimeter wave optical device technology.
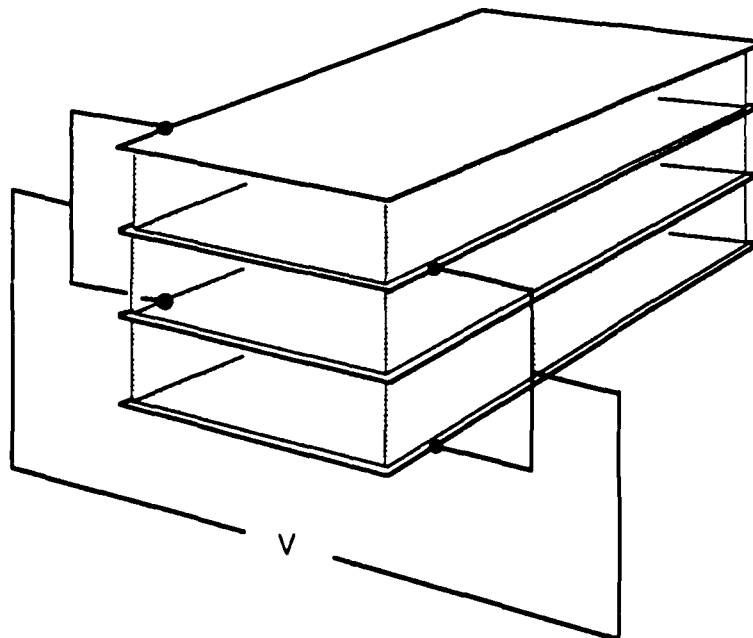
9029-04-47

Figure 13-5.   Multiple plate electrodes for a microwave modulator cell.
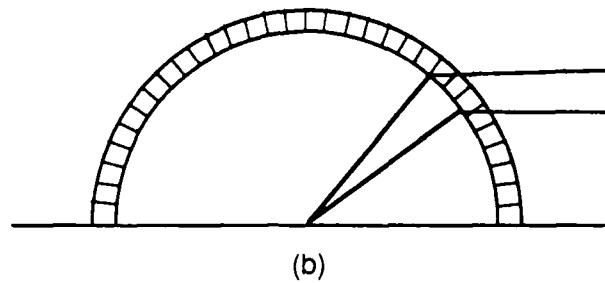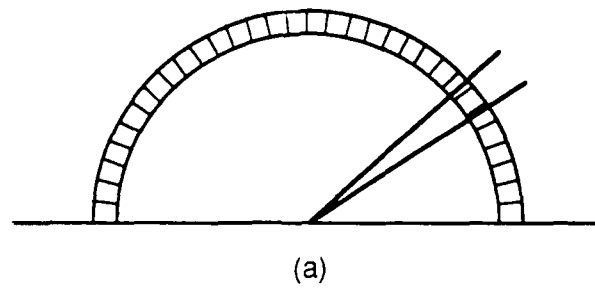
(a)

(b)

Figure 13-6.   Diagram of phase shift switchable radome.
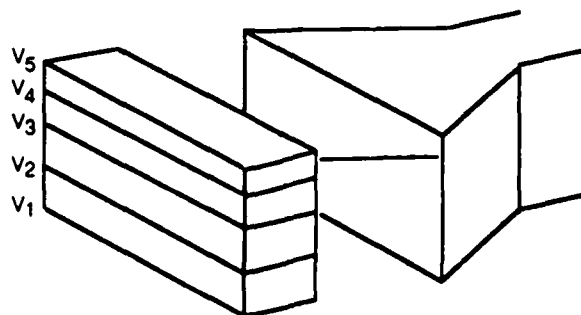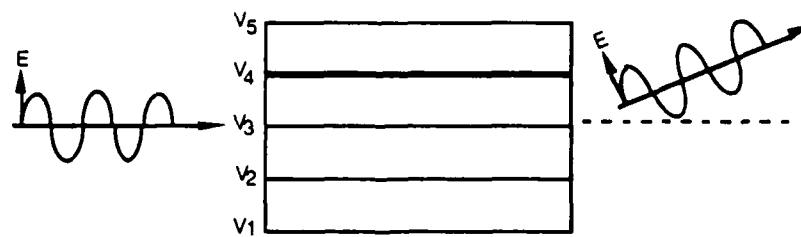
Figure 13-7.   Multi-electrode phase array beam steering radar device.

SECTION 14

DISCUSSION AND CONCLUSIONS

Our exploratory studies on potential applications of microtubules in the electro-optical arena showed that although the transmission and scattering of visible light could be modulated by applying fields to control the alignment direction of metalized microtubules in dispersions, their birefringence and phase shift effects in the microwave (millimeter wave) region were the most promising areas for new device development. Microtubules coated with permalloy or nickel were especially interesting because they could be aligned by application of either electric or magnetic fields. We observed much higher values of microwave birefringence ($\Delta n = 0.3$) with microtubule dispersions than the best ($\Delta n = 0.08$) which had been reported previously for "artificial dielectrics" of metallic particle suspensions. Particularly significant were our discoveries that metalized microtubules could be dispersed well in liquid crystals, with more stable suspensions than those in isotropic fluids of comparable viscosity, and that the microtubule/liquid-crystal composites showed high birefringence at relatively low microtubule concentrations. For example, $\Delta n = 0.3$ was obtained with only 0.6% microtubules in a liquid crystal, while 1.5% microtubules was required for the same birefringence in an isotropic paraffin oil. This is important because lower concentration microtubule dispersions are much more stable than those of higher concentrations.

We found that alignment switching of metalized microtubule dispersions between orthogonal field (magnetic or electric) directions induced substantial birefringent phase shift changes in the microwave (millimeter wave) region. For example, a 2.5 cm pathlength dispersion of 0.6% microtubules showed phase change switching of 188° at 94 GHz and 110° at 30 GHz in a paraffin oil, and 265° at 30 GHz in a liquid crystal. Thus, relatively short path lengths of microtubule dispersions can provide ample field-induced phase changes for radar phase shift modulators, traveling wave slot array antennas, and beam steering devices. However, metalized microtubules of the size presently available settle out of their dispersions (under a gravitational field) and also show irreversible filamentation and clustering effects under applied fields, unless mechanical agitation is applied. Use in space would avoid the settling problem, but not the field clustering problem. Thus, probably the only practical dynamic phase shift devices at present are flow cell types of modulators in which the media (preferably microtubules in liquid crystals) is pumped through a cell or slot antenna and is modulated by an applied electrical field. Nevertheless, such flow cell radar phase modulators should be much less expensive than the presently used ferrite phase shifters. The availability of smaller metalized microtubules (*e.g.* about 1 to 2 μm long and 0.1 μm in diameter) and improved organic coatings would probably

70

provide dispersions, especially in liquid crystals, which would be stabilized against both settling and field clustering effects, and which could be used a wide range of low cost radar phase shift modulators and scanning antennas.

We found that solid polymer layers and free-standing films could be made containing well-aligned patterns of metalized microtubules in the 0.5 to 1.0% range, using optical cement host dispersions that were slowly cured by ultraviolet exposure in the presence of an aligning magnetic field. We showed that this technique could be used to prepare a microwave gradient index lens for a 94 GHz radar beam. It appears feasible to align higher concentrations (*e.g.* 1 to 4%) of the presently available metalized microtubules in polymeric layers, using polymeric coatings on the metal and using hosts such as polymer solutions (solidified by solvent evaporation), thermoplastics, or prepolymers which are slowly cured thermally. Thus, a wide variety of inexpensive radar lenses and phase waveplates should be feasible for a various applications, such as the polarization splitting of in-coming and out-going radar signals.

REFERENCES

1. P. Yager and P.E. Schoen, "Formation of tubules by a polymerizable surfactant," *Mol. Cryst. Liq. Cryst.* , **106**, 371-381 (1984).

2. P. Yager, P.E. Schoen, C. Davies, R. Price, and A. Singr "Structure of lipid tubules from a polymerizable lecithin," *Biophvsical J.* , **48**, 899-906, (1985).

3. J.H. Georger, A. Singh, R.R. Price, J.M. Schnur, P. Yager, and P.E. Schoen, "Helical and tubular microstructures formed by polymerizable phosphatidylcholines," *J. Am. Chem. Soc.*, **109**, 6169-6175 (1987).

4. J.M. Schnur, R. Price, P. Schoen, P. Yager, J.M. Calvert, J. Georger, and A. Singh, "Lipid-based tubule microstructures,"*Thin Solid Films* , **152**, 181 (1987).

5. P.E. Schoen, J.M. Schnur, P. Yager, R. Price, and J.H. Georger, "Process for fabrication of lipid microstructures," *US Patent* 4,877,501 (Oct. 31, 1989)

6. R.R. Price, J.M. Calvert, J.H. Georger, P. Yager, P.E. Schoen, and J.M. Schnur, "Visualization of phospholipid microstructures at ambient temperatures in SEM using electroless plating,"*Elect. Micr. Soc. Am. Proceedings* (1989).

7. J.M. Schnur, P.E. Schoen, P. Yager, R. Price, J.M. Calvert, and J.H. Georger, "Metal clad lipid microstructures," *US Patent* 4,911,981 (March 27, 1990).

8. Private communication from NRL Bio/Molecular Engineering Branch .

9. L.J. Miller, "Means for inducing perpendicular alignment of a nematic liquid crystal on a coated substrate," *US Patent* 4,022,934 (May 10, 1977).

10. A.M. Lackner, J.D. Margerum, and L.J. Miller, "Process for inducing perpendicular alignment of liquid crystals," *US Patent* 4,464,134 (August 7, 1984).

11. H.T. Buscher, "Electrically controllable liquid artificial dielectric media," *IEEE Trans. Microwave Theories and Techniques* , **27**, 540-545 (1979).

12. K.C. Lim, *et al* , *Private Communication.*

13. K.C. Lim, J.D. Margerum, A.M. Lackner, and L.J. Miller, "Liquid crystal-based composite material having enhanced microwave birefringence," US Patent Application (August 1990).